MATHEMATICAL MODELING OF CANCER TREATMENTS AND THE ROLE OF THE IMMUNE SYSTEM RESPONSE TO TUMOR INVASION

A thesis submitted to the University of KwaZulu-Natal
for the degree of Doctor of Philosophy of Science
in the College of Agriculture, Engineering & Science

By
Joseph Malinzi
School of Mathematics, Statistics & Computer Science
November 2015

Contents

Abstract

Despite the success of traditional cancer treatments, a definite cure to several cancers does not exist. Further, the traditional cancer treatments are highly toxic and have a relatively low efficacy. Current research and clinical trials have indicated that virotherapy, a procedure which uses replication-competent viruses to kill cancer cells, is less toxic and highly effective. Some recent studies suggest that the success of combating cancer lies in the understanding of tumour-immune interactions. However, the interaction dynamics of recent cancer treatments with the tumour and immune system response are still poorly understood.

In this thesis we construct and analyse mathematical models in the form of ordinary and partial differential equations in order to explain tumour invasion dynamics and new forms of cancer treatment. We use these models to suggest possible measures needed in order to combat cancer. The thesis seeks to determine the most critical biological factors during tumour invasion, describe how the virus and immune system response influences the outcome of oncolytic virotherapy treatment, investigate how drug infusion methods determine the success of chemotherapy and virotherapy, and determine the efficacy of chemotherapy and virotherpy in depleting tumour cells from body tissue.

We present a travelling wave analysis of a tumour-immune interaction model with immunotherapy. Here we aim to investigate the existence of travelling wave solutions of the model equations with and without immunotherapy and calculate the

minimum wave speed with which tumour cells invade healthy tissue. This investigation highlights the properties which are most vital during tumour invasion. We use the geometric treatment of an apt-phase space to establish the intersection between stable and unstable manifolds. Numerical simulations are performed to support the analytical results. The analysis reveals that the main factors involved during tumour invasion include the tumour growth rate, resting immune cell growth rate, carrying capacity of the resting immune cells, resting cell supply, diffusion rate of the tumour cells, and the local kinetic interaction parameters. We also present a mathematical analysis of models that study tumour-immune-virus interactions using differential equations with spatial effects. The major aim is to investigate how virus and immune responses influence the outcome of oncolytic treatment. Stability analysis is carried out to determine the long term behaviour of the model solutions. Analytical traveling wave solutions are obtained using factorization of differential operators and numerical simulations are carried out using Runge-Kutta fourth order method and Crank-Nicholson methods. Our results show that the use of viruses as a means of cancer treatment can reduce the tumour cell concentration to a very low cancer dormant state or possibly eradicate all tumour cells in body tissue. The traveling wave solutions indicate an exponential increase and decrease in the immune cells density and tumour load in the long term respectively.

A mathematical model of chemovirotherapy, a recent experimental treatment which combines virotherapy and chemotherapy, is constructed and analyzed. The aim is to compare the efficacy of three drug infusion methods and predict the outcome of oncolytic virotherapy-drug combination. A comparison of the efficacy of using each treatment individually, that is, chemotherapy and virotherapy, is presented. Analytical solutions of the model are obtained where possible and stability analysis is presented. Numerical solutions are obtained using the Runge-Kutta fourth order method. This study shows that chemovirotherapy may have a

higher chance of reducing the tumour cell density in body tissue in a relatively short time. To the best of our knowledge, there has not been a mathematical study on the combination of both chemotherapy and virotherapy.

Lastly, the chemovirotherapy model is extended to include spatial distribution characteristics, thus developing a model which describes avascular tumour growth under chemovirotherapy in a two dimensional spatial domain. Numerical investigation of the model solutions is carried out using a multi domain monomial based collocation method and pdepe, a finite element based method in Matlab. This study affirmed that chemovirotherapy may possibly eradicate all tumour cells in body tissue.

Declaration

The work described in this thesis was carried out under the supervision of Prof. P. Sibanda and Dr. H. Mambili-Mamboundou in the School of Mathematics, Statistics, & Computer Science, University of KwaZulu-Natal (PMB), from September 2013 to November 2015. No portion of the work referred to in this dissertation has been submitted in support of an application for another degree or qualification of this or any other university or institution of learning. The thesis is my original work except where due reference and credit is given.

Sign: ....

Joseph Malinzi Date

Sign: ....

Prof. P. Sibanda Date

Sign: ....

Dr. H. Mambili-Mamboundou Date

List of publications

- J. Malinzi, P. Sibanda, and H. Mambili-Mamboundou. Response of immunotherapy to tumour-ticls interactions: a travelling wave analysis, *Abstract and Applied Analysis*. Vol. 2014. Article ID 137015, 10 pages, 2014. doi:10.1155/2014/137015

- J. Malinzi, P. Sibanda, and H. Mambili-Mamboundou. Analysis of virotherapy in solid tumor invasion, *Mathematical Biosciences* 263 (2015): 102-110

- J. Malinzi, P. Sibanda, and H. Mambili-Mamboundou. Enhancement of chemotherapy using oncolytic virotherapy: a mathematical analysis, *Mathematical Biosciences* (under review)

Acknowledgments

Working on my PhD thesis has been an exponentially wonderful experience. I have learned a great deal, met several people in different walks of life, achieved a lot, but also encountered several challenges. I seemed to be heading “nowhere" when I had just started this journey, but after extensive scrutiny of a number of articles and books, my interest became focused on the global health issue of cancer. My hope is that this piece of work will contribute to the quest for more effective cancer treatment, and possibly a cure.

The number of people who helped me throughout this remarkable journey is extensive and therefore I am unable to mention all of them. I am highly indebted to my research advisors, Prof. P. Sibanda and Dr. H. Mambili-Mamboundou, not only for their academic advice and support, but also for mentoring me into an independent researcher.

In no particular order, special mention goes to my amazing fiancée W. Nakiyingi, the African Institute for Mathematical Sciences (AIMS South Africa), Prof. K. Govinder, Prof. H. Mwambi, Prof. S.S Motsa, Dr. F. Chirove, Prof. J.Y.T. Mugisha, Prof. J. Kasozi, Dr. D.W. Ddumba, Dr. J.M. Kitayimbwa, Mr Y. Aungamuthu, Mrs R. Mcarthur, Ms C. Barnard, Ms J. Nassejje, Mr A. Bangirana, Mr D. Luyinda, Mr I. Kisawuzi, my siblings, the reviewers and examiners of the articles in this thesis and of course to my loving parents Mr & Mrs Basalirwa. In your individual capacities, you all contributed tremendously to this work and to helping me become the person I am right now.

I dedicate this thesis to all cancer patients in the world-do not give up the fight.

Chapter 1

Introduction

1.1 Background and motivation

Cancer, known medically as a malignant tumour, is currently the third leading cause of death in the world, after cardiovascular and infectious diseases (see Refs [1–3]). The National Vital Statistics Report [1] ranks neoplasms of the trachea, bronchus, and lung cancer as some of the most dangerous cancers and leading causes of death. The 2014 World Health Organization Cancer Report [4] states that 8.2 million people die each year from cancer, which is about 13% of all deaths worldwide.

Cancer begins when body tissue cells grow uncontrollably to form a solid tissue mass, known as a tumour, which later becomes invasive. Solid tumours are mainly caused by genetic disorders, tobacco and alcohol abuse, poor diet and physical inactivity, and radiation exposure among other carcinogens [5]. There are over one hundred distinct cancer types with diverse dynamics [6]. The particular cancer type is usually reflected by the tissue in which it arises, for example, gliomas arise from the nervous system; carcinomas result from epithelial cells, and meningiomas from the meninges.

A human body is made up of cells of different types. These cells are subjected to signals which determine their division, differentiation or death. If the cell multiplication is uncontrolled, for reasons mostly originating from altered Deoxyribonucleic acid (DNA) sequences, this may lead to the formation of a spherical cell mass. This mass can grow and expand, and can move to other body locations through a process called metastasis, thus becoming cancerous. A tumour develops through two stages; the avascular and vascular growth stages. The avascular stage is the first phase during which cells replicate uncontrollably. These cells, after contracting in one place, require oxygen and other essential nutrients for further growth. In the search for these nutrients they sprout out blood vessels to surrounding body tissue, thus moving to other body parts through two processes; angiogenesis and metastasis, which form the second stage of tumour growth [7]. During angiogenesis, tumour cells secrete biological signals known as tumour angiogenetic factors (TAF) which attract blood vessels towards the tumour to supply unlimited nutrients. Tumour cells can then move into the blood stream and settle in other body parts, a process known as metastasis. In this thesis and for all the models, we consider avascular solid tumours prior to angiogenesis.

A solid tumour consists of three layers: the necrotic core which contains cells deprived of nutrients, a quiescent layer which contains nascent cells, and a zone containing cells lying at the sheath of the tumour. The sheath of a tumour contains fast proliferating cells. Nascent cells lying in the quiescent layer may either die and move to the center of the tumour to form the necrotic core or may later be recruited into the proliferating zone [8]. A tumour may however remain dormant without metastasizing, possibly for an entire life time. This is supported by clinical evidence by Aguirre-Ghiso [9] and some mathematical models (see, for example, [10, 11] and the references cited therein). Current research attributes this dormancy to the interactions of immune cells with tumour cells (see [10, 11]).

Mambili-Mamboundou et al. [11] showed using a mathematical analysis that tumour infiltarating cytotoxic lymphocytes (TICLs) are capable of reducing tumour cell density to a very low and dormant state, but may not completely eliminate these cells.

Tumour cells have mechanisms through which they elude the immune system surveillance. These include: immune inactivation by tumour-derived cytokines; macrophage migration inhibitory factors (MIF) blocks T-cells activation and induces their death [12], immunosupression through amino acid depletion, accumulation of tumour regulation T cells (Tregs) [13], resistance to apoptosis, and immune inactivation by tumour derived cytokines [14]. It is therefore virtually impossible to mitigate tumour growth without any form of clinical therapy.

Cancer therapies are as diverse as cancer itself. The function of all cancer treatments however is to destroy cancer cells and should also distinguish between cancerous and healthy cells. Traditional cancer treatment methods include chemotherapy (see for example [15–20]) , surgical methods (see for example [21–24]), and radiation therapy (see for example [25–27]). Modern cancer therapies include imunotherapy (see for example [28–31]), use of anti-angiogenic drugs (see for example [32, 33]), and virotherapy (see for example [10, 34–37]). Here we give a review of chemotherapy, immunotherapy and virotherapy as they are the most relevant to the aims of this study.

Chemotherapy involves the use of drugs which are administered orally or intravenously to directly lyse cancer cells. These drugs target fast multiplying cells, thus utilizing the fact that cancer cells are fast replicating and hindering their ability to grow. Many of these drugs have the ability to interfere with the synthesis of molecules needed for DNA replication. They may accomplish this in several ways, for example, they can hinder the cell from completing the S phase

of the cell cycle. Some drugs like antitumour antibiotics, bind to the cell DNA to interfere with DNA replication and transcription. A class of drugs inhibits cell replication during mitosis. During this stage of cell growth chromosome separation requires spindle fibers which are made of microtubules; spindle inhibitors prevent the synthesis of microtubules [38, 39]. Because chemotherapeutic drugs lyse fast multiplying cells, they also kill certain cells that divide rapidly such as hair follicles, cells in the gastrointestinal tract, and bone marrow cells thus causing dangerous side effects which include severe hair loss, low white blood cell count, and gastrointestinal distress [38].

Immunotherapy involves boosting a body's immune system to mitigate cancer growth. There are three categories of immunotherapy: the use of immune boosting substances, use of monoclonal antibodies, and the use of vaccines. In the first category, non-specific immunotherapies for example, laboratory made interleukines and interferons are injected in a human body to boost the immune system thus lysing or slowing down the growth of cancer cells. Most non-specific immunotherapies are administered in combination with other treatments, for example, chemotherapy [40]. The second category involves monoclonal antibodies which are directed against a specific protein in cancer cells. Once a monoclonal antibody attaches to a cancer cell, it may allow for the immune system to destroy it or prevent it from rapidly growing. Some monoclonal antibodies direct drugs to the cancer cells, for example, Brentuximab vedotin (Adcetris), a cancer therapy for certain Hodgkin types and non-Hodgkin lymphoma [40]. Other monoclonal antibodies which are currently in use for cancer treatments include recombinant DNA-derived humanized IgG1 kappa monoclonal antibody (Alemtuzumab), Bevacizumab, Cetuximab, Ipilimumab, and Nivolumab. Several others are under clinical trials. The use of monoclonal antibodies can also be classified as a form of targeted therapy where they are used to target tumour cell specific genes, proteins, or the tissue environment that contributes to cancer growth [40]. In the third

category, vaccines are used to expose the immune system to antigens thus triggering the immune system to recorgnize and destroy the protein or related materials. There are two major types of vaccines: preventive vaccines which are given to a person with no cancer symptoms to prevent the person from developing a specific cancer type, for example, Gardasil and Cervarix are vaccines that prevent infection from human papillomavirus (HPV), and treatment vaccine which helps the body's immune system fight cancer by instructing it to recognize and lyse cancer cells [40]. Immunotherapy side effects include low blood pressure, rashes, and flu-like symptoms, such as fever. In this study we consider only the first category where a laboratory made protein, specifically interleukine2 (IL_2), is injected into a human body to stimulate the immune system thus boosting its response to the growth of cancer cells.

Virotherapy involves the conversion of certain viruses into cancer-fighting agents by engineering them to directly attack cancerous cells, while normal healthy cells remain undamaged. The idea of using viruses as a treatment for cancer began in the 1950s, when tissue culture and rodent cancer models were originally developed [41]. Oncolytic treatment involves the use of virus genomes which are altered to greatly enhance their anti-tumour specificity. This began with a study in which thymidine Kinase-negative HSV with attenuated neurovirulence was shown to be active in a murine glioblastoma model. Since then, the pace of clinical activities has accelerated considerably, with several trials using oncolytic viruses belonging to different virus families [10]. To date, several viruses have been developed, for example, adenovirus which has been approved in China [42], and Newcastle-disease virus (NDV) which are in phase three of clinical trials [43]. There is no recorded toxicity as a result of clinical use of oncolytic virotherapy to treat cancer [10, 34–37]). The virus characteristics that are most important in increasing the efficacy of virotherapy treatment are not well known despite the magnitude of research which has been done so far. In this thesis we will highlight

some of the most important virus characterisitcs which need to be optimized in order to mitigate cancer growth in body tissue.

Despite the success of existing cancer therapies, a definite cure to several cancers does not exist. This is because tumours possess mechanisms that suppress anti-tumour activity such as ligands that block natural killer cells and cytotoxic tumour infiltrating cell functions [44]. Thus tumour cells disguise themselves as normal body tissue cells, making it hard for them to be lysed. Moreover most of the traditional cancer treatments are highly toxic. This is as a result of their lysis characteristics, that is, killing fast multiplying cells, however certain normal body cells are also fast replicating. There is a dire need to therefore investigate the efficacy of new forms of cancer treatments that are less toxic, and determine tumour invasion characteristics that should be targeted in order to eradicate tumour cells from body tissue which could lead to a cancer cure.

1.2 A review of mathematical models

In this section we review mathematical models of tumour invasion dynamics and cancer therapy. We also point out some studies in cancer research that are of relevance in this thesis.

Mathematical modeling of tumours and their macro environment have been studied since the early 1980's (see for example [45]). Differential equations as tools of modeling have since been employed to draw very important deductions in cancer dynamics and therapy. The major results which have thus far been drawn from the analysis of these models, according to d'Onfrio et al. [46], include; the existence of a tumour free equilibrium, the possibility of a tumour growing to maximum size, the possibility of co-existence of a tumour, in small concentrations with immune cells (see for example [11]), limit cycles, where the tumour

and immune cell concentrations can keep alternating in a repetitive manner (see for example [47]), and a constant influx of immune cells in the tumour localization. Cancer treatment models, using differential equations have also since been developed and analyzed (see for example the models in [48]).

Mambili-Mamboundou et al. [11] presented a tumour-immune interaction model with immunotherapy to investigate cancer dormancy, a scenario where a tumour remains dormant for several years. Their model divided the cell population into concentrations of primed tumour infiltrating cytotoxic lymphocytes (TICLs), tumour cells , interleukine2, a cell complex, a chemokine , and resting cells. They assumed that the IL_2 does not bind with TICLs to form a cell complex but instead stimulates the immune system response against tumour cells through lymphocyte activation, growth, and differentiation. The model was an extension of Matzavinos et al. [47] with the inclusion of a class of resting cells and the assumption that the formation of the cell complexes occurs on a time scale of a few hours, while that of tumour cells as well as the influx of immune cells into the spleen occurs on a much slower time scale. They extended this model to incorporate space and thus studied the tumour-immune spatial temporal dynamics. The homogeneous model was analyzed through a stability analysis and numerical simulations and the heterogeneous model was simulated using the Crank-Nicholson scheme. Their analysis showed that immune cells are capable of keeping the tumour cell concentration at low levels and for a long period of time but may not totally eliminate them. The spatial model simulations showed oscillations in densities of both TICLs and the tumour with the tumour cell density having a small amplitude compared to the TICLs. The analysis also revealed that immunotherapy may reduce the tumour cell density inside the body tissue. Despite the fact that these results are helpful in explaining cancer dormancy, they did not explain the most important tumour invasion parameters. Furthermore, a dormant tumour may metastasize [49]. It is therefore important to investigate the

pertinent mechanisms, that is parameters in mathematics, through which tumour cells escape the immune system surveillance. Other studies of tumour dynamics and immunotherapy include the following research [45, 47, 50–54]. These studies give an indication of some important issues pertaining to cancer dynamics. Nevertheless, the dynamics of tumour-immune interactions are highly intricate and involve many parameters and therefore, there is a need for more studies to decode the mechanisms of tumour-immune interaction as this could potentially reveal another avenue of determining a cure for cancer.

Phino et al. [55] developed a mathematical model of chemotherapy for treatment of a tumour with the aim of investigating the efficacy of chemotherapy in eliminating cancer cells. In their analysis they showed the region of parameter space in which cancer cells can be eliminated. They also showed the outcome of the cell concentrations with varying infusion rates of the drug. Other chemotherapy mathematical models include [55–58]. Ursher [48] gave a comprehensive summary of mathematical models for chemotherapy. The analysis of all these models do not point to chemotherapy as a global cure for cancer. Therefore, there is a need to study new cancer treatment forms and combinations.

Tian [59] constructed and analyzed a basic mathematical model of virotherapy. He considered populations of uninfected tumour cells, infected tumour cells, and free viruses. His analysis showed that there are two threshold burst size values: below one of these values the tumour always grows to its maximum size, while above the other value, there exists one or three families of periodic solutions arising from Hopf bifurcations. His study confirmed that a tumour can be reduced to low undetectable cell counts when the burst size is large enough. Similar virotherapy mathematical models include [60–62].

Mathematical models to simulate cancer treatment combinations are few in number, despite the large number of theoretical and experimental studies. Dingli et al. [63] developed a mathematical model of cancer radiovirotherapy. They proved the existence of steady states related to a complete success, partial success, and therapy failure. They further evaluated the relevant therapeutic scenarios for the treatment combinations and identified important elements of optimization. Tao and Guo [64] described cancer radiovirotherapy using a free boundary problem for a non-linear system of PDEs. They proved global existence and uniqueness of the solutions to the boundary problem and constructed an explicit parameter condition corresponding to the success of this therapy. To the best of our knowledge, there has not been a mathematical study on the combination of both chemotherapy and virotherapy, yet experimental studies have shown that the oncolytic virotherapy (OV)-drugs combination may be a success in cancer treatment (see Reference [65]). Therefore treatment outcomes of chemovirotherapy need to be further investigated.

1.3 Classification of tumour dynamics models

There are several types of mathematical models, each requiring different techniques of analysis. In this section we present a basic classification of tumour dynamic models in mathematical biology, and appropriate to this thesis.

Mathematical tumour growth models may be categorized into microscopic and macroscopic models. Microscopic models are based on observations on a microscopic scale, for example, acidity, vascularization, and other internal cell dynamics [66]. These models mostly incorporate observable chemical reactions between tumour cells, the extra-cellular matrix and normal tissue cells, pressure, cell cohesion, and adhesion. The chemical reactions include the diffusion of nutrients and

oxygen into the tumour, mitosis, cell division, natural cell death, surface tension, cell cycles, and chemotaxis. Consequently, there are several parameters involved in such models and a large variety of mathematical techniques are a requirement to analyze them. Some examples of microscopic models include those given in [67–70] and the references therein.

Macroscopic models are based on observations on a macroscopic scale using, for example, diffusion tensor images (MR-DTI), computed topography (CT), and magnetic resonance images (MRI) [66]. The tumour dynamics observable factors on a macroscopic scale are limited and for this reason, macroscopic models are mathematically simple to analyze. The parameters that are most important in macroscopic modeling include diffusion and chemotaxis. Examples of macroscopic models can be found in the studies [11, 47, 50, 71, 72] and the references therein. Malinzi [71] gives a further classification of tumour growth models. In this thesis we consider modeling on a macroscopic level with diffusion and chemotaxis where necessary. We incorporate certain other salient features in tumour growth modeling such as apoptosis, natural cell growth, and local cell kinetic interactions.

The diffusion of cells, drugs, viruses, and other nutrients can be modeled using the Fisher-Kolmogorov equation (see [73]). This equation can be used to model the random movement of cells and nutrients in body tissue. The simplest macroscopic form of the Fisher-KPP can be written as

$$\frac{\partial U}{\partial t} = \frac{\partial}{\partial x}(D(x)\frac{\partial U}{\partial x}) + \rho U(1-U), \tag{1.1a}$$

$$\nabla \vec{n}_{\partial\Omega} = 0, \tag{1.1b}$$

where $U(x,t)$ is the cell density, $D(x)$ is a space dependent function that models the tumour diffusion coefficient. The function $\rho U(1-U)$ may be considered to be the tumour density natural growth function where ρ is the tumour proliferation

rate. Equation (1.1b) models the cell density at the boundaries of the tumour (no-flux boundary condition). x and t are space and time variables.

In the context of this thesis, chemotaxis is the movement of cells in response to a stimulus. The chemotaxis phenomenon can be simulated using the Patlak/Keler-Seigel equation (see [74]). It takes into account the density $U(x,t)$ of cells and the chemo-attractant $C(x,t)$

$$\frac{\partial U}{\partial t} = \frac{\partial^2 U}{\partial x^2} - \chi \frac{\partial}{\partial x}(U \frac{\partial C}{\partial x}), \quad t > 0, x \in \mathbb{R}^d, \tag{1.2}$$

where $C(x,t)$ is the chemical density, χ represents the chemotactic sensitivity function. The boundary conditions of Equation (1.2) depend on the assumptions made pertaining to the movement of cells at the boundary of the tumour.

The mathematical models we construct in this thesis are in the form of ordinary and partial differential equations. A differential equation relates a function with its derivatives. The function simulates observable quantities in real life.

1.4 Aims of the study

Despite the fact that several mathematical studies on cancer treatments have been conducted, more needs to be done in order to decode the complexities of the underlying processes in tumour invasion. Striving to determine a cure for cancer requires an investigation of processes such as the tumour invasion characteristics and understanding the mechanisms of interaction of the immune system with tumour cells. However, a full comprehension of tumour-immune interactions is still lacking (see Ref [71]).

In recent studies, virotherapy, a less toxic treatment, has been identified as a

possible cancer therapy (see [10, 41, 75]). This treatment type involves the use of laboratory made oncolytic viruses that infect, multiply, and directly lyse cancer cells with less toxicity [75]. The virus specific properties allow for biding, entry, and fast replication in the tumour [65]. Nevertheless, little is known about the virus characteristics that are most important for therapeutic purposes.

The major aim of this thesis is to investigate the efficacy of recent cancer treatments and explain the phenomenon of cancer dormancy. This thesis seeks to use analysis of mathematical models to achieve the following objectives: determine the most critical biological factors during tumour invasion, describe how the virus and immune system response influences the outcome of oncolytic virotherapy treatment, investigate how drug infusion methods determine the success of chemotherapy and virotherapy, and determine the efficacy of chemotherapy and virotherpy in depleting tumour cells from body tissue. Firstly, we seek to obtain an estimate of the strength with which a tumour invades immune cells, or the ability of tumour cells to resist attack by immune cells, and also identify the tumour invasion properties in the form of the main parameters that should be targeted to mitigate cancer growth in body tissue. Secondly, we seek to study how virus and immune responses influence the success of oncolytic treatment thus predicting the success of virotherapy as a cancer treatment in depleting tumour cells from body tissue. Thirdly, we construct a mathematical model to simulate chemovirotherapy, a cancer treatment that employs both chemotherapy and oncolytic virotherapy, use mathematical analysis to predict the efficacy of oncolytic virotherapy (OV)-drugs combination treatment, and compare the efficacy of using each treatment, namely, chemotherapy and virotherapy individually. Fourthly, we also aim to investigate how drug infusion methods determine the outcome of chemotherapy and virotherapy. Lastly, we develop a model of avascular solid tumour growth under chemovirotherapy treatment in a two dimensional spatial domain to study the spatial-temporal effects on chemovirotherapy treatment.

This study is likely to be of use to medical practitioners in a way that a more efficacious mode of cancer treatment will be pointed out. Further, this study is likely to identify the best infusion method for cancer drugs. An investigation into the tumour invasion characteristics which are most important during invasion may shade light in the development of effective cancer drugs. Lastly, alternative cancer treatments, other than chemotherapy, radiotherapy and surgery, will be suggested in this study.

1.5 Overview of the thesis

This thesis is divided into six chapters. In this chapter we have given background information and motivation for this research. We briefly discussed the biology of tumour formation and cancer therapy, reviewed some important mathematical models on tumour-immune modeling and cancer dynamics, and outlined some of the important methods which we employ in this thesis.

Chapter 2 describes a model for the analysis of a tumour-immune-immunotherapy interaction. An estimate of the strength with which a tumour invades immune cells is made, and we determine the parameters that are most pertinent in tumour invasion dynamics using a traveling wave analysis. Chapter 3 gives a study of the dynamics of tumour-immune-virus interactions. In Chapter 4 a chemovirotherapy model is developed and analyzed in order to investigate the effects of chemovirotherapy and the efficacy of chemotherapy and virotherapy treatments, and also to determine the infusion method that is most efficient in cancer treatment. Chapter 5 is an extension of the work presented in Chapter 4. The chemovirotherapy model is modified to incorporate space thus developing an avascular solid tumour growth model for chemovirotherapy treatment in a two dimensional spatial-temporal domain. Chapter 6 contains a general conclusion and discussion

of the findings in this thesis and suggestions for areas of further study.

Chapter 2

Response of immunotherapy to tumor-TICLs interactions: A travelling wave analysis

In this chapter we present a traveling wave analysis of a tumour-immune interaction model with immunotherapy. The mathematical model takes into account local kinetic interactions between cells, the random movement of cells and the chemotactic response of immune cells once a tumour cell interacts with a tumour infiltrating cytotoxic lymphocyte. The existence of traveling wave solutions is proved by establishing a heteroclinic connection between the stable and unstable manifolds in the apt-phase space. A minimum wave speed of the tumour solitons is estimated to measure the strength with which a tumour attacks immune cells or the strength with which immune cells resist being lysed by tumor cells. The expression of the minimum wave speed highlights the parameters which are most crucial during tumour invasion, thus indicating the tumour invasion characteristics which need to be targeted in order to mitigate tumour growth. Numerical simulations of the model are determined. Finally, implications of the model analysis are presented.

Hindawi Publishing Corporation
Abstract and Applied Analysis
Volume 2014, Article ID 137015, 10 pages
http://dx.doi.org/10.1155/2014/137015

Research Article

Response of Immunotherapy to Tumour-TICLs Interactions: A Travelling Wave Analysis

Joseph Malinzi, Precious Sibanda, and Hermane Mambili-Mamboundou

School of Mathematics, Statistics, and Computer Science, University of KwaZulu-Natal, Private Bag X01, Scottsville, Pietermaritzburg 3209, South Africa

Correspondence should be addressed to Joseph Malinzi; josephmalinzi@aims.ac.za

Received 19 March 2014; Revised 10 June 2014; Accepted 19 June 2014; Published 15 July 2014

Academic Editor: Igor Leite Freire

There are several cancers for which effective treatment has not yet been identified. Mathematical modelling can nevertheless point out to clinicians tumour invasion properties that should be targeted to mitigate these cancers. We present a travelling wave analysis of a tumour-immune interaction model with immunotherapy. We use the geometric treatment of an apt-phase space to establish the intersection between stable and unstable manifolds. We calculate the minimum wave speed and numerical simulations are performed to support the analytical results.

1. Introduction

In travelling wave analysis, the medium moves in the direction of propagation of the wave. Travelling wave analysis is important in tumour-immune interaction dynamics since if travelling waves exist, then we may estimate the potential with which the tumour cells invade healthy tissue [1]. Tumour-immune interaction studies have revealed a lot of information regarding cancer and cancer treatments [2–9] including cancer dormancy, when tumour cells remain in a quiescent state for a long period of time without metastasizing. Cancer dormancy has been attributed to tumour-immune interactions, particularly tumour infiltrating cytotoxic lymphocytes (TICLs) [2]. Travelling wave analysis could lead to an understanding of the analytical connection between model parameters and tumour invasion properties.

Most of the standard cell invasion models are related to the Fisher-Kolmogorov equation. The Fisher-Kolmogorov equation [10, 11] is the simplest macroscopic reaction-diffusion evolution equation for modelling cancer invasion just as seen in [12]. Many authors, for example, [12–14], have used the Fisher-Kolmogorov equation in modelling diffusive tumours and the evolution of cancer on a macroscopic scale. Several studies have shown that this equation exhibits travelling wave solutions and the minimum wave speed for these models has been estimated (see [15, 16]). The tumour-immune interaction model presented in this paper employs the Fisher-Kolmogorov equation to model the random movement of cells. The aim of this paper is to investigate the existence of travelling wave solutions in a tumour-immune interaction model with and without immunotherapy and to estimate the minimum wave speed with which tumour cells invade healthy tissue. In this way we obtain an estimate of the strength with which a tumour invades immune cells or the ability of tumour cells to resist invasion by immune cells and also identify the tumour invasion properties in the form of parameters that should be targeted to mitigate cancer in body tissue. The work presented in this paper complements the analysis done by Mambili-Mamboundou et al. [17]. They presented similar model equations, analyzed their equilibria, and found numerical solutions. The main objective in Mambili-Mamboundou et al.'s work [17] was to ascertain the cause of cancer dormancy and investigate the effect that immunotherapy has on the response of TICLs to solid tumour invasion.

2. The Model

The model considered here was derived by Mambili-Mamboundou et al. [17]. It subdivides the cell population

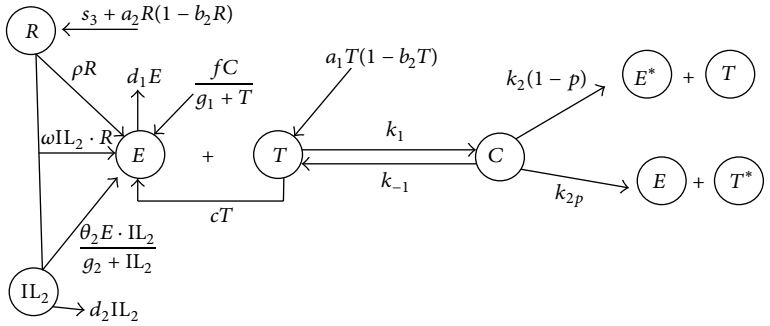

Figure 1: Schematic diagram of the local kinetic cell interactions [17].

into local concentrations of primed TICLs E, tumour cells T, interleukin 2 concentration IL_2, tumour-immune cell complex C, a chemokine α, and resting cells R. The class IL_2 represents a population of cultured immune cells that have antitumour reactivity with the tumour host. We assume that IL_2 does not necessarily bind with TICLs to form a cell complex but rather stimulates the TICLs to fight cancer through lymphocyte activation, growth, and differentiation. We also assume that IL_2 increases the rate of conversion of resting TICLs to primed TICLs (see [17, 18]). R is a class representing the population of TICLs which have not yet matured or been activated by antigens. During a tumour attack on immune cells or any other body tissue infection, naive or resting TICLs are primed by antigen presenting cells (APCs) in secondary lymphoid organs such as lymph nodes and spleen [19]. Figure 1 shows the cells' local kinetics.

Following the receptor-ligand kinetics theory in [20], when a tumour cell and an immune cell come into contact, it may lead to the formation of a tumour-immune complex at a binding rate k_1 which later can either lead to tumour cell death with probability p at a rate k_2p or lead to inactivation of TICLs at a rate $k_2(1 - p)$. In case of the latter, the tumour-immune complex is dissociated at a rate k_{-1}. k_2 is a parameter describing the detachment rate of TICLs from tumour cells, resulting in an irreversible programming of the tumour cells for lysis. Complex formation reduces both TICLs and tumour cell densities and increases the complex density by k_1ET. Similarly the TICLs and tumour cell densities, respectively, increase by $(k_{-1} + k_2p)C$ and $(k_{-1} + k_2(1 - p))C$, in case the tumour or immune cell dies. The binding of the primed TICLs to tumour cells leads to the production of a chemokine α. The chemokine gradient defines the migration of the TICLs towards the tumor by a process known as chemotaxis which is represented by $\chi\nabla \cdot (E\nabla\alpha)$ in the model, with χ being the chemotaxis constant. We assume that the rate of supply of immune cells into the region of tumour localization is ρR, where ρ is the supply rate. We consider the immune cells proliferation term to be $fC/(g_1 + T)$ and similarly the chemokine production term to be $fC/(g_3 + T)$, where f, g_1, and g_3 are constant parameters derived from experimental results. $fC/(g_1 + T)$ is a function that explains how tumour cells proliferate as a result of interaction with immune cells. We consider that all cell densities diffuse at constant rates. We thus consider the following system of parabolic nonlinear partial differential equations (Mambili-Mamboundou et al. [17]):

$$\begin{aligned}
\frac{\partial E}{\partial t} &= D_1\nabla^2E - \chi\nabla \cdot (E\nabla\alpha) + \rho R + \frac{fC}{g_1 + T} \\
&\quad - d_1E - k_1ET + (k_{-1} + k_2p)\,C \\
&\quad + \omega IL_2 \cdot R + \frac{\theta_2 E \cdot IL_2}{g_2 + IL_2} + eT, \\
\frac{\partial T}{\partial t} &= D_2\nabla^2T + a_1T\,(1 - b_1T) - k_1ET \\
&\quad + (k_{-1} + k_2\,(1 - p))\,C, \\
\frac{\partial C}{\partial t} &= k_1ET - (k_{-1} + k_2)\,C, \\
\frac{\partial \alpha}{\partial t} &= D_3\nabla^2\alpha + \frac{fC}{g_3 + T} - d_3\alpha, \\
\frac{\partial IL_2}{dt} &= D_4\nabla^2IL_2 + s_2 - d_2IL_2, \\
\frac{\partial R}{\partial t} &= D_5\nabla^2R + s_3 + a_2R\,(1 - b_2R) \\
&\quad - \omega IL_2 \cdot R - \rho R,
\end{aligned} \tag{1}$$

where D_i, $i = 1, 2, \ldots, 5$, are diffusion coefficients of primed TICLs, tumour, IL_2, α, and resting cell densities, respectively, and ω is the rate of stimulation of resting cells into activated TICLs as a result of injecting a patient with IL_2. The capacity of IL_2 to stimulate the production of antibodies is denoted by eT and $\theta_2E \cdot IL_2/(g_2 + IL_2)$ is a proliferation term also considered by Kirschener and Panetta [3]. It models the stimulation of TICLs by IL_2 and is of the Michaelis-Menten form (see [3]). $a_1T(1 - b_1T)$ and $a_2R(1 - b_2R)$ are logistic growth terms, respectively, modelling tumour and resting cells' growth, where a_i and b_i^{-1}, $i = 1, 2$, are, respectively, the growth rates and carrying capacities, s_2 is the IL_2 supply, and d_2, d_3 are, respectively, the deactivation rates of IL_2 and α. s_3, a_2, and b_2^{-1} are, respectively, the resting cells supply rate, growth rate, and carrying capacity.

We consider a one-dimensional spatial domain on the interval $[0, x_0]$ and assume that there are two regions in this interval, one fully occupied by tumour cells and the other fully occupied by TICLs (both activated and resting). We propose that the initial interval of tumour localization is $[0, L]$, where $L = 0.2x_0$ [2]. In our model, we do not include the Heaviside function since we consider a resting cell class. We further assume that these resting cells can be recruited into the activated cell class. The boundary and initial conditions therefore are

$$\begin{aligned}
&\mathbf{n}\cdot\nabla E = \mathbf{n}\cdot\nabla T = \mathbf{n}\cdot\nabla \mathrm{IL}_2 = \mathbf{n}\cdot\nabla R \\
&\quad = \mathbf{n}\cdot\nabla C = \mathbf{n}\cdot\nabla\alpha = 0 \quad \text{at } x = 0,\ x = x_0,
\end{aligned}$$

$$E(x,0) = \begin{cases} 0, & 0 \le x \le L, \\ E_0\left[1 - \exp\left(-1000(x-L)^2\right)\right], & L \le x \le x_0, \end{cases}$$

$$R(x,0) = \begin{cases} 0, & 0 \le x \le L, \\ R_0\left[1 - \exp\left(-1000(x-L)^2\right)\right], & L \le x \le x_0, \end{cases}$$

$$\mathrm{IL}_2(x,0) = \mathrm{IL}_{2_0}, \quad \forall x \in [0, x_0],$$

$$C(x,0) = C_0, \quad \forall x \in [0, x_0],$$

$$\alpha(x,0) = 0, \quad \forall x \in [0, x_0],$$

$$T(x,0) = \begin{cases} T_0\left[1 - \exp\left(-1000(x-L)^2\right)\right], & 0 \le x \le L, \\ 0, & L \le x \le x_0. \end{cases} \tag{2}$$

It has been shown that chemotaxis does not influence the existence of travelling wave solutions (see, e.g., [1]). We therefore do the travelling wave analysis without the effect of chemotaxis. Assuming that the formation of cellular conjugates occurs on a time scale of a few hours while that of tumour cells as well as the influx of immune cells into the spleen occurs on a much slower time scale, probably tens of hours, and nondimensionalizing the above system of (1) by taking E, T, IL_2, and R as fractions of their initial concentrations with $t_0 = x_0/D_1$ and $x_0 = 1$ cm give

$$\begin{aligned}
\frac{\partial E}{\partial t} &= \nabla^2 E + \overline{\phi_1} R + \frac{\overline{\theta_1} ET}{\eta_1 + T} - \psi E - \nu ET \\
&\quad + \overline{\omega_1}\mathrm{IL}_2 \cdot R + \frac{\overline{\theta_2} E \cdot \mathrm{IL}_2}{\eta_2 + \mathrm{IL}_2} + \overline{e}T, \\
\frac{\partial T}{\partial t} &= \phi\nabla^2 T + \beta_1 T\left(1 - \beta_2 T\right) - \overline{\mu_1} ET, \\
\frac{\partial \mathrm{IL}_2}{\partial t} &= \xi\nabla^2 \mathrm{IL}_2 + \sigma_2 - \overline{\mu_2}\mathrm{IL}_2, \\
\frac{\partial R}{\partial t} &= \zeta\nabla^2 R + \sigma_3 + \alpha_1 R\left(1 - \alpha_2 R\right) \\
&\quad - \overline{\omega_2}\mathrm{IL}_2 \cdot R - \overline{\phi_2} R,
\end{aligned} \tag{3}$$

where

$$\begin{aligned}
&\overline{\theta_1} = \theta_1 t_0, \quad \psi = d_1 t_0, \quad \overline{\theta_2} = \theta_2 t_0, \\
&\overline{e} = \frac{eT_0 t_0}{E_0}, \quad \overline{\omega_1} = \frac{\omega R_0 \mathrm{IL}_{2_0} t_0}{E_0}, \\
&\eta_1 = \frac{g}{T_0}, \quad \eta_2 = g_2 t_0, \quad \beta_1 = a_1 t_0, \\
&\beta_2 = b_1 T_0, \quad \overline{\mu_1} = mE_0 t_0, \\
&\sigma_3 = \frac{s_3 t_0}{R_0}, \quad \nu = lT_0 t_0, \quad \phi = D_2 t_0, \\
&\xi = D_4 t_0, \quad \overline{\eta_3} = g_3 t_0, \\
&\overline{\phi_1} = \frac{\rho R_0 t_0}{E_0}, \quad \sigma_2 = \frac{\sigma_2 t_0}{\mathrm{IL}_{2_0}}, \\
&\zeta = D_5 t_0, \quad \overline{\mu_2} = \mu_2 t_0, \\
&\overline{\omega_2} = \omega \mathrm{IL}_{2_0} t_0, \quad \alpha_1 = a_2 t_0, \\
&\alpha_2 = b_2 R_0, \quad \overline{\phi_2} = \rho t_0, \\
&l = Kk_2(1-p), \quad \overline{\theta_1} = fK, \\
&m = Kk_2 p, \quad K = \frac{k_1}{(k_{-1} + k_2)}.
\end{aligned} \tag{4}$$

The boundary and initial conditions are, respectively,

$$\begin{aligned}
&\frac{\partial E}{\partial x}(0,x) = \frac{\partial \mathrm{IL}_2}{\partial x}(0,t) = \frac{\partial R}{\partial t}(0,x) = \frac{\partial T}{\partial x}(0,t) = 0, \\
&\frac{\partial E}{\partial x}(1,t) = \frac{\partial R}{\partial x}(1,t) = \frac{\partial \mathrm{IL}_2}{\partial x}(1,t) = \frac{\partial T}{\partial x}(1,t) = 0, \\
&E(x,0) = \begin{cases} 0, & 0 \le x \le L, \\ \left[1 - \exp\left(-1000(x-L)^2\right)\right], & L \le x \le 1, \end{cases} \\
&R(x,0) = \begin{cases} 0, & 0 \le x \le L, \\ \left[1 - \exp\left(-1000(x-L)^2\right)\right], & L \le x \le 1, \end{cases} \\
&\mathrm{IL}_2(x,0) = \mathrm{IL}_{2_0}, \quad \forall x \in [0,1], \\
&T(x,0) = \begin{cases} \left[1 - \exp\left(-1000(x-L)^2\right)\right], & 0 \le x \le L, \\ 0, & L \le x \le 1. \end{cases}
\end{aligned} \tag{5}$$

3. Travelling Wave Solutions

In this section we investigate whether model (3) exhibits travelling wave solutions or not. We use the geometric treatment of an apt-phase space to establish the intersection between stable and unstable manifolds, a method also employed by Bellomo et al. [1] in investigating travelling wave solutions. The gist of this method is to establish the presence of a heteroclinic orbit joining two different equilibrium points in the phase space. We specify a travelling coordinate $z = x - ct$, where c the travelling wave speed is greater than zero ($c > 0$),

and let $\widetilde{E}(z) = E(x,t)$, $\widetilde{T}(z) = T(x,t)$, $\widetilde{\mathrm{IL}_2}(z) = \mathrm{IL}_2(x,t)$, and $\widetilde{R}(z) = R(x,t)$. For simplicity, we drop the tildes and the system (3) is transformed into

$$\begin{aligned}
-c\frac{dE}{dz} &= \frac{d^2E}{dz^2} + \overline{\phi_1}R + \frac{\overline{\theta_1}ET}{\eta_1 + T} - \psi E - \nu ET \\
&\quad + \overline{\omega_1}\mathrm{IL}_2 R + \frac{\overline{\theta_2}E\mathrm{IL}_2}{\eta_2 + \mathrm{IL}_2} + \overline{e}T, \\
-c\frac{dT}{dz} &= \phi\frac{d^2T}{dz^2} + \beta_1 T\left(1 - \beta_2 T\right) - \overline{\mu_1}ET, \\
-c\frac{d\mathrm{IL}_2}{dz} &= \xi\frac{d^2\mathrm{IL}_2}{dz^2} + \sigma_2 - \overline{\mu_2}\mathrm{IL}_2, \\
-c\frac{dR}{dz} &= \zeta\frac{d^2R}{dz^2} + \sigma_3 + \alpha_1 R\left(1 - \alpha_2 R\right) \\
&\quad - \overline{\omega_2}\mathrm{IL}_2 R - \overline{\phi_2}R.
\end{aligned} \tag{6}$$

For simple phase space analysis, we define variables

$$\begin{aligned}
E_1 &= \frac{dE}{dz}, \qquad T_1 = \frac{dT}{dz}, \\
\mathrm{IL}_{21} &= \frac{d\mathrm{IL}_2}{dz}, \qquad R_1 = \frac{dR}{dz},
\end{aligned} \tag{7}$$

and (6) are transformed into a system of autonomous first order differential equations as follows:

$$\frac{dX}{dz} = f(X), \quad \text{where } X = \begin{pmatrix} E_1 \\ E \\ T_1 \\ T \\ \mathrm{IL}_{21} \\ \mathrm{IL}_2 \\ R_1 \\ R \end{pmatrix} \in \mathbb{R}^8, \tag{8}$$

$f(X)$

$$= \begin{bmatrix} -cE_1 - \overline{\phi_1}R - \dfrac{\overline{\theta_1}ET}{\eta_1 + T} + \psi E + \nu ET - \overline{\omega_1}\mathrm{IL}_2 R - \dfrac{\overline{\theta_2}E\mathrm{IL}_2}{\eta_2 + \mathrm{IL}_2} - \overline{e}T \\ E_1 \\ \dfrac{1}{\phi}\left(-cT_1 - \beta_1\left(1 - \beta_2 T\right) + \mu_1 ET\right) \\ T_1 \\ \dfrac{1}{\xi}\left(-c\mathrm{IL}_{21} - \sigma_2 + \mu_2\mathrm{IL}_2\right) \\ \mathrm{IL}_{21} \\ \dfrac{1}{\zeta}\left(-cR_1 - \sigma_3 - \alpha_1 R\left(1 - \alpha_2 R\right) + \overline{\omega_2}\mathrm{IL}_2 R + \overline{\phi_2}R\right) \\ R_1 \end{bmatrix}, \tag{9}$$

with boundary conditions

$$\begin{aligned}
&\lim_{z\to-\infty}\left(E_1, E, T_1, T, \mathrm{IL}_{21}, \mathrm{IL}_2, R_1, R\right) \\
&\quad = X^0 = \left(0, E, 0, 0, 0, \mathrm{IL}_2, 0, R\right),
\end{aligned}$$

Table 1: Dimensional parameter values for model (1).

Parameter	Estimated value	Units	Source
a	0.18	day^{-1}	[2]
k_1	1.3×10^{-7}	$\mathrm{day\,cells}^{-1}\,\mathrm{cm}$	[2]
k_2	7.2	day^{-1}	[2]
d_1	0.0412	day^{-1}	[2]
g	2.02×10^7	$\mathrm{cells\,cm}^{-1}$	[2]
b	2.0×10^{-9}	$\mathrm{cells}^{-1}\,\mathrm{cm}$	[2]
k_{-1}	24	day^{-1}	[2]
p	0.9997	Dimensionless	[2]
f	0.2988×10^8	$\mathrm{day}^{-1}\,\mathrm{cells\,cm}^{-1}$	[2]
s	1.36×10^4	$\mathrm{day}^{-1}\,\mathrm{cells\,cm}^{-1}$	[2]
D_1	10^{-6}	$\mathrm{cm}^2\,\mathrm{day}^{-1}$	[2]
D_2	10^{-6}	$\mathrm{cm}^2\,\mathrm{day}^{-1}$	[2]
θ_2	0.1245	day^{-1}	[3]
e	$0 \le c \le 0.005$	day^{-1}	[3]
g_2	10^7	cm^3	[3]
d_2	10	day^{-1}	[18]
a_2	0.0245	day^{-1}	[18]
b_2	$\frac{1}{10^7}$	cell^{-1}	[18]
ρ	6.4×10^{-6}	$\mathrm{cells}^{-1}\,\mathrm{day}^{-1}$	[18]

$$\begin{aligned}
&\lim_{z\to+\infty}\left(E_1, E, T_1, T, \mathrm{IL}_{21}, \mathrm{IL}_2, R_1, R\right) \\
&\quad = X^1 = \left(0, E, 0, T, 0, \mathrm{IL}_2, 0, R\right),
\end{aligned} \tag{10}$$

where X^0 and X^1 correspond to the equilibrium points of the system (8).

The system (8) can be regarded as an eigenvalue problem because the wave velocity c is unknown. We take $c = 20$, a value that numerically gives rise to travelling wave solutions. We chose this value after simulating the system of (3). There are several other values of c that can give rise to travelling wave solutions. In the next section, we calculate a critical wave speed below which travelling wave solutions do not exist. We find a heteroclinic connection between X^0 and X^1, where, after substituting parameter values in Table 1,

$$X^0 \approx \begin{pmatrix} 0 \\ 0.0001 \\ 0 \\ 0 \\ 0 \\ 0.7968 \\ 0 \\ 0.001 \end{pmatrix}, \qquad X^1 \approx \begin{pmatrix} 0 \\ 5.8934 \\ 0 \\ 0.7986 \\ 0 \\ 0.7968 \\ 0 \\ 0.0002 \end{pmatrix}. \tag{11}$$

Here, X^0 and X^1 are equilibrium points of the system (8). Our interest is to establish the existence of an orbit $X_{\mathrm{con}}(z)$ that satisfies

$$\lim_{z\to-\infty} X_{\mathrm{con}}(z) = X^0, \qquad \lim_{z\to+\infty} X_{\mathrm{con}}(z) = X^1. \tag{12}$$

The existence of such an orbit would imply that travelling wave solutions do exist [1].

We consider the linearization

$$\frac{dX}{dz} = Df\left(X^0\right)X, \qquad \frac{dX}{dz} = Df\left(X^1\right)X, \tag{13}$$

of the vector field f at the equilibrium points X^0 and X^1, respectively. From the Jacobian

$$Df(x) = \begin{pmatrix} -c & A_1 & 0 & A_2 & 0 & A_3 & 0 & -I\omega_1 & -\phi_1 \\ 1 & 0 & 0 & 0 & 0 & 0 & 0 & & 0 \\ 0 & \frac{T\mu_1}{\phi} & -\frac{c}{\phi} & A_4 & 0 & 0 & 0 & & 0 \\ 0 & 0 & 1 & 0 & 0 & 0 & 0 & & 0 \\ 0 & 0 & 0 & 0 & -\frac{c}{\xi} & \mu_2 & 0 & & 0 \\ 0 & 0 & 0 & 0 & 1 & 0 & 0 & & 0 \\ 0 & 0 & 0 & 0 & 0 & \frac{\omega_2}{\xi} & -\frac{c}{\xi} & & A_5 \\ 0 & 0 & 0 & 0 & 0 & 0 & 1 & & 0 \end{pmatrix}, \tag{14}$$

where

$$\begin{aligned} A_1 &= T\nu - \frac{T\theta_1}{T+\eta_1} - \frac{I\theta_2}{I+\eta_2} + \psi, \\ A_2 &= E\overline{e} + E\nu - \frac{E\eta_1\theta_1}{(T+\eta_1)^2}, \\ A_3 &= \frac{E\eta_2\theta_2}{(I+\eta_2)^2}, \\ A_4 &= \frac{2T\beta_1\beta_2}{\phi} + \frac{E\mu_1}{\phi} - \frac{\beta_1}{\phi} - R\omega_1, \\ A_5 &= \frac{2R\alpha_1\alpha_2}{\xi} + \frac{I\omega_2+\phi_2}{\xi} - \frac{\alpha_1}{\xi}, \end{aligned} \tag{15}$$

we determine the spectrum of the matrices $Df(X^0)$ and $Df(X^1)$. For parameter values in Table 1, $Df(X^0)$ has eight real eigenvalues $(213.22, 27.11, 20, 15.68, -5.35 \times 10^{-9}, -7.11, -15.48, -193.22)$, four positive and four negative. The four positive eigenvalues imply the existence of a 4-dimensional unstable manifold $W^u(X^0)$. Similarly, $Df(X^1)$ has eight eigenvalues $(213.2, 27.11, 20, -15.68, -0.0002, -7.11, -15.48, -193.22)$, three positive and five negative, implying the existence of a 5-dimensional stable manifold $W^s(X^1)$. From this result, we note that

$$\dim\left(W^u\left(X^0\right)\right) + \dim\left(W^s\left(X^1\right)\right) = \dim\mathbb{R}^8 + 1. \tag{16}$$

Equation (16) suggests that $W^u(X^0)$ and $W^s(X^1)$ intersect transversally along a one-dimensional curve in the eight-dimensional phase space. This is because the solutions of the system (8) lie in eight dimensions (8D) but the summation of the dimension of the stable and unstable manifolds is nine (9D) just as shown in (16) (see [1, 21]). If this is the case, then this curve would define a generic heteroclinic connection [1]. This therefore confirms that the system (1) exhibits travelling wave solutions for certain parameter values.

4. Minimum Wave Speed

In the previous section, we established that (3) exhibits travelling wave solutions. In this section, we calculate the minimum wave speed for model (3) with ($\mathrm{IL}_2 \neq 0$) and without ($\mathrm{IL}_2 = 0$) treatment connecting the tumour-free equilibrium point to the cancer dormant equilibrium point. In this section we seek the minimum wave speed c. We apply the same technique used by Chahrazed [22] and Maidana and Yang [23] in determining c. This technique involves analyzing the phase space by characterizing the equilibrium points of the autonomous system. The minimum wave speed corresponds to a change in the eigenvalues of the travelling-wave differential equations at the equilibrium point ahead of the wave.

To calculate the minimum wave speed, we impose a condition that X^0, the tumour-free equilibrium point of (8), must not oscillate. In other words, the eigenvalues λ_i corresponding to this equilibrium point must have real values; that is, $\lambda_i \in \mathbb{R}$. We seek the travelling wave speed both with and without immunotherapy.

4.1. No Treatment Case. With $\mathrm{IL}_2 = 0$, the tumour-free equilibrium point of the system (8) is

$$\begin{aligned} X^0 &= \left(0, E^*, 0, 0, 0, R^*\right), \quad \text{where} \\ E^* &= \frac{\left(\alpha_1 - \phi_2 + \sqrt{4\alpha_1\alpha_2\sigma_3 + \left(\alpha_1-\phi_2\right)^2}\right)\phi}{2\alpha_1\alpha_2\psi}, \\ R^* &= \frac{\alpha_1 - \phi_2 + \sqrt{4\alpha_1\alpha_2\sigma_3 + \left(\alpha_1-\phi_2\right)^2}}{2\alpha_1\alpha_2}. \end{aligned} \tag{17}$$

For the equilibrium point X^0 to be biologically meaningful, E^* and R^* must be positive. E^* and R^* are positive provided that

$$\alpha_1 + \sqrt{4\alpha_1\alpha_2\sigma_3 + \left(\alpha_1-\phi_2\right)^2} \geq \phi_2. \tag{18}$$

The eigenvalues λ_i, $i = 1, 2, \ldots, 6$, corresponding to X^0 are

$$\lambda_1 = -\frac{1}{2}c + \frac{1}{2}\sqrt{c^2 + 4\psi}, \tag{19}$$

$$\lambda_2 = -\frac{1}{2}c - \frac{1}{2}\sqrt{c^2 + 4\psi}, \tag{20}$$

$$\lambda_3 = -\frac{c + \sqrt{c^2 + 4\left(\sqrt{4\alpha_1\alpha_2\sigma_3 + \left(\alpha_1-\phi_2\right)^2}\right)\xi}}{2\zeta}, \tag{21}$$

$$\lambda_4 = -\frac{c - \sqrt{c^2 + 4\left(\sqrt{4\alpha_1\alpha_2\sigma_3 + (\alpha_1 - \phi_2)^2}\right)\xi}}{2\zeta}, \tag{22}$$

$$\lambda_5 = -\Bigg(\alpha_1\alpha_2 c\psi + \sqrt{2\sqrt{\left(4\alpha_1\alpha_2\sigma_3 + (\alpha_1 - \phi_2)^2\right)}\alpha_1\alpha_2\mu_1\phi^2\psi - C + D}\Bigg) \times (2\alpha_1\alpha_2\phi\psi)^{-1}, \tag{23}$$

$$\lambda_6 = -\Bigg(\alpha_1\alpha_2 c\psi - \sqrt{2\sqrt{\left(4\alpha_1\alpha_2\sigma_3 + (\alpha_1 - \phi_2)^2\right)}\alpha_1\alpha_2\mu_1\phi^2\psi - C + D}\Bigg) \times (2\alpha_1\alpha_2\phi\psi)^{-1}, \tag{24}$$

where

$$C = \left(4\alpha_1^2\alpha_2^2\beta_1\phi - \alpha_1^2\alpha_2^2c^2\right)\psi^2, \qquad D = 2\left(\alpha_1^2\alpha_2\mu_1\phi^2 - \alpha_1\alpha_2\mu_1\phi^2\phi_2\right)\psi. \tag{25}$$

The first four eigenvalues (19)–(22) are real. Therefore (23) or (24) should determine the minimum wave speed which we obtain by setting

$$\sqrt{2\sqrt{\left(4\alpha_1\alpha_2\sigma_3 + (\alpha_1 - \phi_2)^2\right)}\alpha_1\alpha_2\mu_1\phi^2\psi - C + D} = 0, \tag{26}$$

since we require $\lambda_{5,6}$ to be real. Solving for c in (26) gives

$$c = \left(4\beta_1\phi + \frac{2\mu_1\phi^2\phi_2}{\alpha_1\alpha_2\psi} - \frac{2\mu_1\phi^2}{\alpha_2\psi} - \frac{2\sqrt{4\alpha_1\alpha_2\sigma_3 + \alpha_1^2 - 2\alpha_1\phi_2 + \phi_2^2}\mu_1\phi^2}{\alpha_1\alpha_2\psi}\right)^{1/2}. \tag{27}$$

Substituting parameter values from Table 1 into (27) gives $c \geq 4.176$. This indicates that the minimum wave speed $c_{\min}$ for the tumour-immune interaction model without immunotherapy is approximately 4.176.

4.2. Treatment Case. With $\mathrm{IL}_2 \neq 0$, the tumour-free equilibrium points of the system (8) are

$$X^0 = \left(0, \overline{E}, 0, 0, 0, \overline{\mathrm{IL}_2}, 0, \overline{R}\right), \quad \text{where}$$

$$\overline{E} = \frac{(\mu_2\phi_1 + \omega_1\sigma_2)(\eta_2\mu_2 + \sigma_2)\left(p_1 - p_2 + \sqrt{(A+P) - (B+Q)}\right)}{2\left(\eta_2\mu_2\psi + \psi\sigma_2 - \sigma_2\theta_2\right)\alpha_1\alpha_2\mu_2^2} \geq 0,$$

$$\overline{\mathrm{IL}_2} = \frac{\sigma_2}{\mu_2}, \qquad \overline{R} = \frac{p_1 - p_2 + \sqrt{(A+P) - (B+Q)}}{2\alpha_1\alpha_2\mu_2} \geq 0,$$

$$\text{provided} \quad (A+P) \geq (B+Q), \qquad (\eta_2\mu_2 + \sigma_2)\psi > \sigma_2\theta_2,$$

$$p_1 + \sqrt{(A+P) - (B+Q)} \geq p_2, \quad \text{where}$$

$$A = 4\alpha_1\alpha_2\mu_2^2\sigma_3 + \alpha_1^2\mu_2^2, \qquad B = 2\alpha_1\mu_2^2\phi_2,$$

$$P = \mu_2^2\phi_2^2 + \omega_2^2\sigma_2^2, \qquad Q = 2(\alpha_1\mu_2\omega_2 - \mu_2\omega_2\phi_2)\sigma_2,$$

$$p_1 = \alpha_1\mu_2, \qquad p_2 = \mu_2\phi_2 + \omega_2\sigma_2. \tag{28}$$

The eigenvalues λ_i, $i = 1, 2, \ldots, 8$, corresponding to X^0 (with immunotherapy) are

$$\lambda_1 = -\frac{c + \sqrt{4\mu_2\xi^2 + c^2}}{2\xi}, \tag{29}$$

$$\lambda_2 = -\frac{c - \sqrt{4\mu_2\xi^2 + c^2}}{2\xi}, \tag{30}$$

$$\lambda_3 = -\frac{c\mu_2 + \sqrt{c^2\mu_2^2 + 4\sqrt{(A+P) - (B+Q)}\mu_2\xi}}{2\mu_2\xi}, \tag{31}$$

$$\lambda_4 = -\frac{c\mu_2 - \sqrt{c^2\mu_2^2 + 4\sqrt{(A+P) - (B+Q)}\mu_2\xi}}{2\mu_2\xi}, \tag{32}$$

$$\lambda_5 = -\Big(c\eta_2\mu_2 + c\sigma_2 + \left((\eta_2\mu_2 + \sigma_2) \times \left(c^2\eta_2\mu_2 + 4\eta_2\mu_2\psi + \left(c^2 + 4\psi\right)\sigma_2 + 4\sigma_2\theta_2\right)\right)^{1/2}\Big) \times 2(\eta_2\mu_2 + \sigma_2)^{-1}, \tag{33}$$

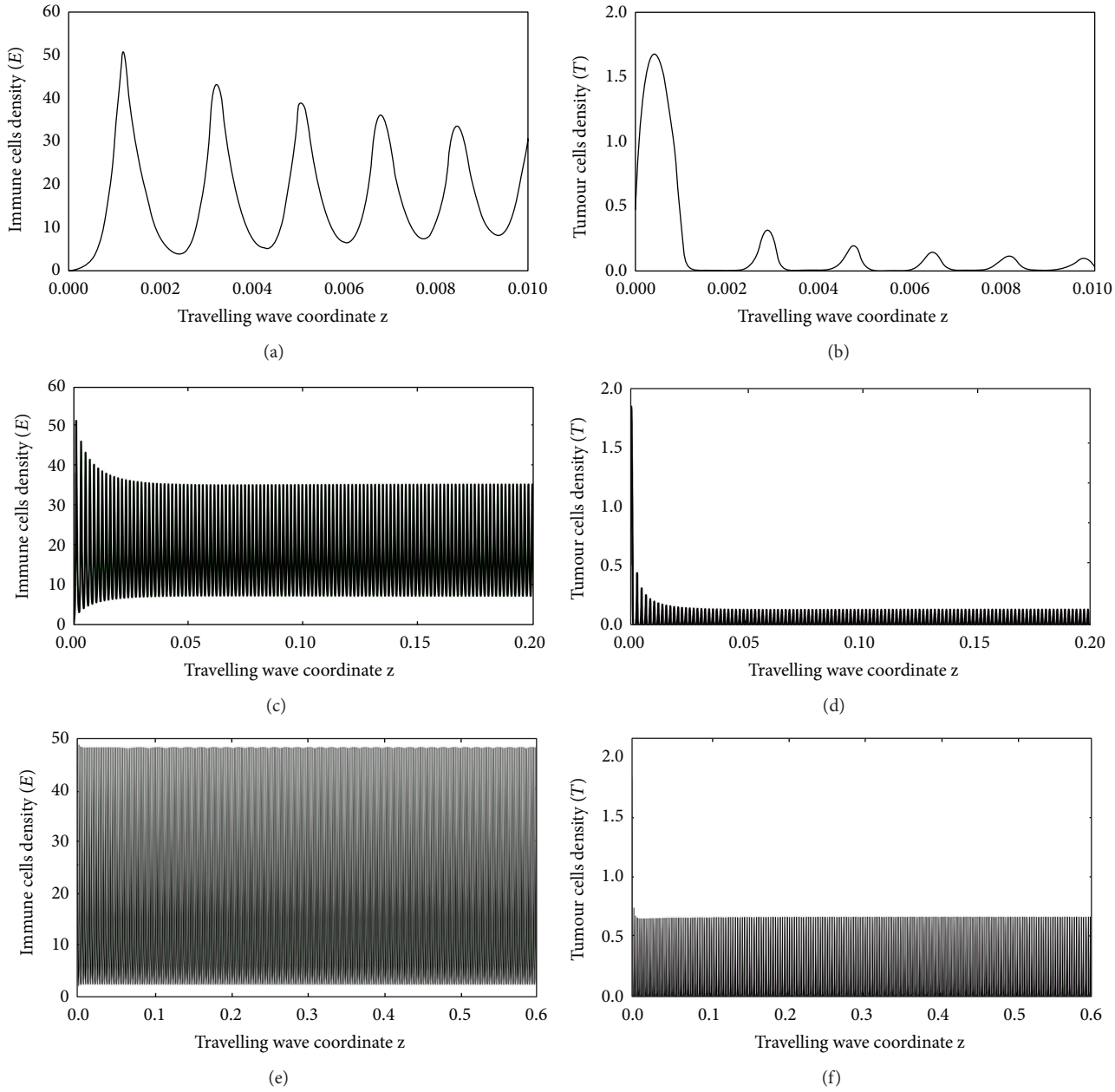

Figure 2: Travelling wave solutions of the system (3) for different travelling wave coordinates without treatment.

$$\begin{aligned}\lambda_6 &= -\Big(c\eta_2\mu_2 + c\sigma_2 \\ &\quad - \Big((\eta_2\mu_2 + \sigma_2) \\ &\quad \times \Big(c^2\eta_2\mu_2 + 4\eta_2\mu_2\psi + \Big(c^2 + 4\psi\Big)\sigma_2 + 4\sigma_2\theta_2\Big)\Big)^{1/2}\Big) \\ &\quad \times 2(\eta_2\mu_2 + \sigma_2)^{-1},\end{aligned} \tag{34}$$

$$\lambda_7 = -\frac{-\Gamma_1 + \sqrt{(A+P) - (B+Q) - C + D + \Gamma_2\alpha_1\alpha_2}}{2\left(\alpha_1\alpha_2\eta_2\mu_2^2\phi\psi + \alpha_1\alpha_2\mu_2\phi\psi\sigma_2 - \alpha_1\alpha_2\mu_2\phi\sigma_2\theta_2\right)}, \tag{35}$$

$$\lambda_8 = -\frac{-\Gamma_1 - \sqrt{(A+P) - (B+Q) - C + D + \Gamma_2\alpha_1\alpha_2}}{2\left(\alpha_1\alpha_2\eta_2\mu_2^2\phi\psi + \alpha_1\alpha_2\mu_2\phi\psi\sigma_2 - \alpha_1\alpha_2\mu_2\phi\sigma_2\theta_2\right)}, \tag{36}$$

where

$$\begin{aligned}\Gamma_1 &= -\alpha_1\alpha_2 c\eta_2\mu_2^2\psi + \alpha_1\alpha_2 c\mu_2\psi\sigma_2 - \alpha_1\alpha_2 c\mu_2\sigma_2\theta_2, \\ \Gamma_2 &= J\Big(4A + \alpha_1^2\mu_2^2 - 2\alpha_1\mu_2^2\phi_2 + \mu_2^2\phi_2^2 + \omega_2^2\sigma_2^2 \\ &\quad - 2\left(\alpha_1\mu_2\omega_2 - \mu_2\omega_2\phi_2\right)\sigma_2\Big)^{1/2},\end{aligned} \tag{37}$$

where $J = 2(\eta_2\mu_1\mu_2^2\phi\phi_1 + \mu_1\omega_1\phi\sigma_2^2 + (\eta_2\mu_1\mu_2\omega_1\phi + \mu_1\mu_2\phi\phi_1)\sigma_2)$.

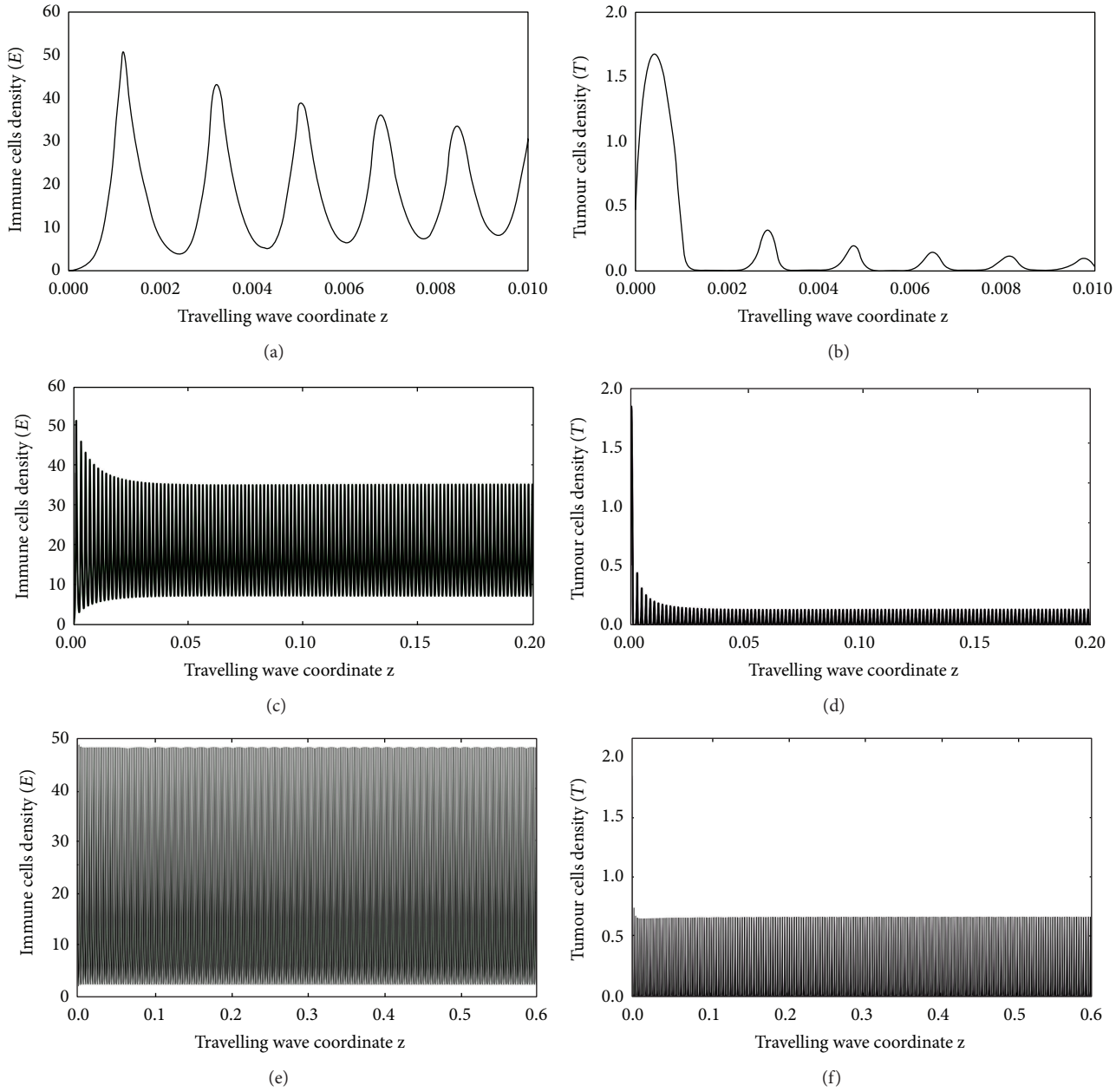

Figure 3: Travelling wave solutions of the system (3) for different travelling wave coordinates with immunotherapy.

The first six eigenvalues (29)–(34) are real provided that the conditions we have imposed for positivity of the tumour-free equilibrium point are fulfilled. Equation (35) or (36) should therefore determine the conditions for the existence of a minimum wave speed. We set $\Gamma_1 - \sqrt{(A+P)-(B+Q)-C+D+\Gamma_2\alpha_1\alpha_2} = 0$ and substituted parameter values in Table 1. The result gave the value $c \geq 4.176$ as in the case without treatment. This implies that the minimum wave speed for model (3) for both with and without treatment is the same. In other words, immunotherapy may possibly not influence the strength with which the tumour cells attack immune cells because the minimum wave speed with or without clinical treatment is the same. Fisher's equation exhibits travelling wave solutions for $c \geq 2$ [24]. The minimum wave velocity which we obtained is greater than two and therefore not a violation of the minimum wave speed for Fisher's equation.

5. Numerical Simulations

Using the parameter values in Table 1, we simulate model (3). These parameter values were obtained from data where the murine B cell lymphoma was used as an experimental model of tumour dormancy in mice [25]. The kinetic parameter values that were obtained in this experiment are shown

in Table 1. We assumed that R and IL_2 diffuse at the same rate as TICLs (i.e., $D_1 = D_4 = D_5 = 10^{-6}$) and used the diffusivity value 10^{-6} for immune cells by Matzavinos et al. [2]. We took the travelling wave speed to be $c = 20$ and implemented the simulations in python using a Runge-Kutta numerical method. The numerical simulations (see Figures 2 and 3) indicate that the system of (3) exhibits travelling wave solutions for certain parameter values. This supports the analytical results on the existence of travelling waves in Section 3. Figures 2 and 3, respectively, show the numerical travelling wave solutions for model (3) without and with clinical treatment, and for different travelling wave coordinates. They depict solutions that are periodic and oscillating around a stable equilibrium state. These solutions describe heterogeneous cell distributions with a relatively low tumour cell density. The travelling wave solutions indicate that tumour cells invade immune cells at a high potential. The minimum wave speed obtained in the previous section indicated that the model exhibits travelling wave solutions for $c \geq 4$. This is consistent with our numerical simulations for which we used $c = 20$.

6. Conclusions

Many biological and physical phenomena can be described by reaction-diffusion equations. However not many nonlinear reaction-diffusion equations are integrable. It is therefore imperative to find other quantitative methods for tackling such nonlinear systems. The objective of this study was to use a quantitative method to investigate travelling wave solutions of a tumour-immune interaction model and also identify the tumour invasion properties in the form of parameters that should be targeted to mitigate cancer by estimating the minimum wave speed. We investigated the existence of travelling wave solutions and estimated the minimum wave speed of the wave solutions by analyzing the model phase space. The existence of travelling wave solutions confirmed that a tumour attacks immune cells at full potential. The expression from which the minimum wave speed was calculated determined the parameters that need to be targeted to eradicate cancer in body tissue. We simulated model (3) and compared the results to analytical results. The numerical travelling wave solutions depicted periodic cell densities with a low tumor level, oscillating about a stable equilibrium state. These solutions depict cancer dormancy which has been observed in several cancers, for example, osteogenic sarcomas, basal-cell carcinoma, and breast cancers, and they also imply that the tumour cells attack the immune cells at their full potential.

Equation (27) highlights the main parameters ($\beta_1, \alpha_1, \alpha_2, \sigma_3, \phi, \phi_1, \mu_1$) involved in tumour invasion corresponding to tumour growth rate, resting TICLs' growth rate, carrying capacity of the resting TICLs, resting cells' supply, diffusion rate of the tumour cells, and the local kinetic interaction parameters (tumour cell death and inactivation of TICLs).

The results obtained in this paper are similar to those in Matzavinos and Chaplain [26]. In their work, they performed a travelling wave analysis of a model describing the growth of a tumour in the presence of an immune system response. Their results showed that indeed a tumor attacks immune cells at full potential since their model exhibited travelling wave solutions. In the future, we hope to consider diffusion in higher dimension due to the fact that body tissue geometry is highly intricate.

Conflict of Interests

The authors declare that there is no conflict of interests regarding the publication of this paper.

Authors' Contribution

Precious Sibanda and Hermane Mambili-Mamboundou are coauthors.

Acknowledgment

The authors are grateful for financial support from the University of KwaZulu-Natal.

References

[1] N. Bellomo, M. Chaplain, and E. De Angelis, *Selected Topics in Cancer Modelling : Genesis, Evolution, Immune Competition, and Therapy*, Birkhäuser, Boston, Mass, USA, 2000.

[2] A. Matzavinos, M. A. Chaplain, and V. A. Kuznetsov, "Mathematical modelling of spatio-temporal response of cytotoxic T-lymphocytes to a solid tumour," *Mathematical Medicine and Biology*, vol. 21, no. 1, pp. 1–34, 2004.

[3] D. Kirschener and J. C. Panetta, "Modeling immunotherapy of the tumor-immune interaction," *Journal of Mathematical Biology*, vol. 37, no. 3, pp. 235–252, 1998.

[4] A. d'Onofrio, "A general framework for modeling tumor-immune system competition and immunotherapy: mathematical analysis and biomedical inferences," *Physica D: Nonlinear Phenomena*, vol. 208, no. 3-4, pp. 220–235, 2005.

[5] N. V. Stepanova, "Course of the immune reaction during the development of a malignant tumour," *Biophysics*, vol. 24, no. 1, pp. 220–235, 1980.

[6] H. P. de Vladar and J. A. González, "Dynamic response of cancer under the influence of immunological activity and therapy," *Journal of Theoretical Biology*, vol. 227, no. 3, pp. 335–348, 2004.

[7] V. A. Kuznetsov, I. A. Makalkin, M. A. Taylor, and A. S. Perelson, "Nonlinear dynamics of immunogenic tumors: parameter estimation and global bifurcation analysis," *Bulletin of Mathematical Biology*, vol. 56, no. 2, pp. 295–321, 1994.

[8] L. G. de Pillis and A. Radunskaya, "A mathematical model of immune response to tumor invasion," *Computational Fluid and Solid Mechanics: Proceedings of the Second MIT Conference on Computational Fluid and Solid Mechanics*, vol. 56, pp. 1661–1668, 2003.

[9] A. Donofrio, "Tumor-immune system interaction: modeling the tumor-stimulated proliferation of effectors and immunotherapy," *Mathematical Models & Methods in Applied Sciences*, vol. 16, no. 8, pp. 1375–1401, 2006.

[10] P. Breuer, W. Huber, and F. Petruccione, "Fluctuation effects on wave propagation in a reaction-diffusion process," *Physica D: Nonlinear Phenomena*, vol. 73, no. 1, pp. 259–273, 1993.

[11] R. A. Fisher, "The, wave of advance of advantageous genes," *Annals of Eugenics*, vol. 7, no. 4, pp. 355–369, 1937.

[12] E. Konukoglu, O. Clatz, B. H. Menze et al., "Ayache Image guided personalization of reaction-diffusion type tumour growth models using modified anisotropic Eikonal equations," *Journal of Medical Imaging*, vol. 29, no. 1, pp. 78–95, 2010.

[13] K. Swanson, E. Alvord, and J. Murray, "Virtual brain tumours (gliomas) enhance the reality of medical imaging and highlight inadequacies of current therapy," *Journal of Cancer*, vol. 86, no. 1, pp. 14–18, 2002.

[14] G. Cruywagen, D. Woodward, P. Tracqui, G. Bartoo, J. Murray, and E. Alvord, "The modelling of diffusive tumours," *Journal of Biological Systems*, vol. 3, no. 1, pp. 937–945, 1995.

[15] W. Huang and Y. Wu, "Minimum wave speed for a diffusive competition model with time delay," *Journal of Applied Analysis and Computation*, vol. 1, no. 2, pp. 205–218, 2011.

[16] Q. Wang and X.-Q. Zhao, "Spreading speed and traveling waves for the diffusive logistic equation with a sedentary compartment," *Dynamics of Continuous, Discrete & Impulsive Systems*, vol. 13, no. 2, pp. 231–246, 2006.

[17] H. Mambili-Mamboundou, P. Sibanda, and J. Malinzi, "Effect of immunotherapy on the response of TICLs to solid tumour invasion," *Mathematical Biosciences*, vol. 249, pp. 52–59, 2014.

[18] F. S. Borges, K. C. Iarosz, H. P. Ren et al., "Model for tumour growth with treatment by continuous and pulsed chemotherapy," *Biosystems*, vol. 116, pp. 43–48, 2014.

[19] N. Zhang and M. J. Bevan, "CD8(+) T cells: foot soldiers of the immune system," *Immunity*, vol. 35, no. 2, pp. 161–168, 2011.

[20] D. A. Lauffenburger and J. J. Linderman, *Models for Binding, Trafficking, and Signalling*, Oxford University Press, New York, NY, USA, 1993.

[21] P. Ashwin, M. V. Bartuccelli, T. J. Bridges, and S. A. Gourley, "Travelling fronts for the KPP equation with spatio-temporal delay," *Zeitschrift für angewandte Mathematik und Physik ZAMP*, vol. 53, no. 1, pp. 103–122, 2002.

[22] L. Chahrazed, "Global stability and spatial spread of a nonlinear epidemic model," *European Scientific Journal*, vol. 9, no. 6, pp. 167–179, 2013.

[23] N. A. Maidana and H. M. Yang, "A spatial modelto describe foot and mouth disease dissemination," *Journal of Mathematics and Applied Computation*, vol. 12, no. 1, pp. 11–20, 2013.

[24] J. A. Sherratt, "On the transition from initial data to travelling waves in the Fisher-KPP equation," *Dynamics and Stability of Systems*, vol. 13, no. 2, pp. 167–174, 1998.

[25] H. Siu, E. S. Vitetta, R. D. May, and J. W. Uhr, "Tumour dormancy: regression of BCL tumour and induction of a dormant tumour state in mice chimeric at the major histocompatibility complex," *Journal of Immunology*, vol. 137, no. 1, pp. 1376–1382, 1986.

[26] A. Matzavinos and M. A. J. Chaplain, "Traveling-wave analysis of a model of the immune response to cancer," *Comptes Rendus Biologies*, vol. 327, no. 11, pp. 995–1008, 2004.

Chapter 3

Analysis of virotherapy in solid tumor invasion

In this chapter we study the dynamics of two tumour-immune-virus interaction models, that is, homogeneous and heterogeneous, with the aim of determining the efficacy of virotherapy and identifying the most important virus characteristics which are most pertinent during oncolytic virotherapy treatment. A stability analysis of time invariant solutions for the homogeneous model is presented. The heterogeneous model is analyzed by determining analytical traveling wave solutions using factorization of differential operators. Both models are numerically simulated and the solutions are compared to the analytical results.

Mathematical Biosciences 263 (2015) 102–110

Contents lists available at ScienceDirect

Mathematical Biosciences

journal homepage: www.elsevier.com/locate/mbs

Analysis of virotherapy in solid tumor invasion

Joseph Malinzi*, Precious Sibanda, Hermane Mambili-Mamboundou

University of KwaZulu Natal, School of Mathematics, Statistics, and Computer Science, Private Bag X01, Scottsville, Pietermaritzburg 3209, South Africa

ARTICLE INFO

Article history:
Received 23 July 2014
Revised 14 January 2015
Accepted 19 January 2015
Available online 25 February 2015

2000 MSC:
35Q92
92B05

Keywords:
Virotherapy
Tumor-virus-immune interactions
Oncolytic virus
Traveling wave analysis
Partial differential equations

ABSTRACT

Cancer treatment is an inexact science despite traditional cancer therapies. The traditional cancer treatments have high levels of toxicity and relatively low efficacy. Current research and clinical trials have indicated that virotherapy, a procedure which uses replication-competent viruses to kill cancer cells, has less toxicity and a high efficacy. However, the interaction dynamics of the tumor host, the virus, and the immune response is poorly understood due to its complexity. We present a mathematical analysis of models that study tumor-immune-virus interactions in the form of differential equations with spatial effects. A stability analysis is presented and we obtained analytical traveling wave solutions. Numerical simulations were obtained using fourth order Runge–Kutta and Crank–Nicholson methods. We show that the use of viruses as a cancer treatment can reduce the tumor cell concentration to a very low cancer dormant steady state or possibly deplete all tumor cells in body tissue. The traveling waves indicated an exponential increase and decrease in the cytotoxic-T-lymphocytes (CTLs) density and tumor load in the long term respectively.

1. Introduction

Cancer is one of the most dreadful and persistent killers. It is a group of diseases characterized by uncontrolled cell growth. In 2009, the risk of being diagnosed with cancer before the age of 85 was 1 in 2 for males and 1 in 3 for females [1]. The World Cancer Report, a publication of the World Health Organization shows that in 2012 the global incidence of cancer escalated to approximately 14 million new cases, a figure expected to further rise to an annual 19.3 million by 2025 [2].Cancer treatment is therefore still a major field of research.

Traditional cancer treatments include surgery, chemotherapy, and radiation therapy. These treatments however all involve a high level of toxicity and none of them has been found to be a definitive cure to any cancer [3]. Surgery, which involves the direct removal of the tumor, is not always a viable option and may lead to fatigue, loss of appetite and other infections. Radiation therapy involves the use of high ionizing radiation to kill the tumor cells. It may, depending on which part of the body is being treated, cause, among other side effects, severe hair loss. Chemotherapy involves the use of drugs that destroy cancer cells. Some common side effects of using drugs to treat cancer involve fatigue, nausea, vomiting, hair loss, mouth sores, and decreased blood cell count (see Ref. [2]). Modern therapies include immunotherapy and combinations of treatment types. Immunotherapy involves the use of genetically engineered cytokines which are used to boost the immune system. This however may not completely cure cancer in human body tissue (see Ref. [6]). It is therefore imperative to obtain a treatment with few side effects.

Oncolytic virotherapy uses replication-competent viruses to kill cancer cells. Specific viruses are turned into therapeutic agents to treat cancer. The idea of using viruses as a treatment for cancer began in the 1950s, when tissue culture and rodent cancer models were originally developed [4]. Today, oncolytic treatment involves the use of virus genomes which are engineered to enhance their anti-tumor specificity. This began with a study in which thymidine kinase-negative HSV with attenuated neurovirulence was shown to be active in a murine glioblastoma model. Since then, the pace of clinical activities has accelerated considerably, with several trials using oncolytic viruses belonging to different virus families [5]. To date, clinical trials have pointed out talimogene laherparepvec as a possible treatment for melanoma [5]. Clinical trials are ongoing using different viruses as cancer therapies. There is no recorded toxicity as a result of clinical use of oncolytic virotherapy to treat cancer [7].

There is however still a dire need to identify the virus characteristics that are most important for therapeutic purposes. Studies show that cancer cells exposed to viruses have quickly died compared to those that are not. Nevertheless, this cannot be entirely attributed to viral replication alone but also to cytotoxic-T-cells (CTLs) [8]. The responses detected as a result of a CTL meeting a tumor cell are a very important factor in tumor necrosis. Tumor-immune-virus

* Corresponding author. Tel.: +27 717990712.
E-mail addresses: josephmalinzi@aims.ac.za (J. Malinzi), SibandaP@ukzn.ac.za (P. Sibanda), Mambilimamboundou@ukzn.ac.za (H. Mambili-Mamboundou).

http://dx.doi.org/10.1016/j.mbs.2015.01.015
0025-5564/

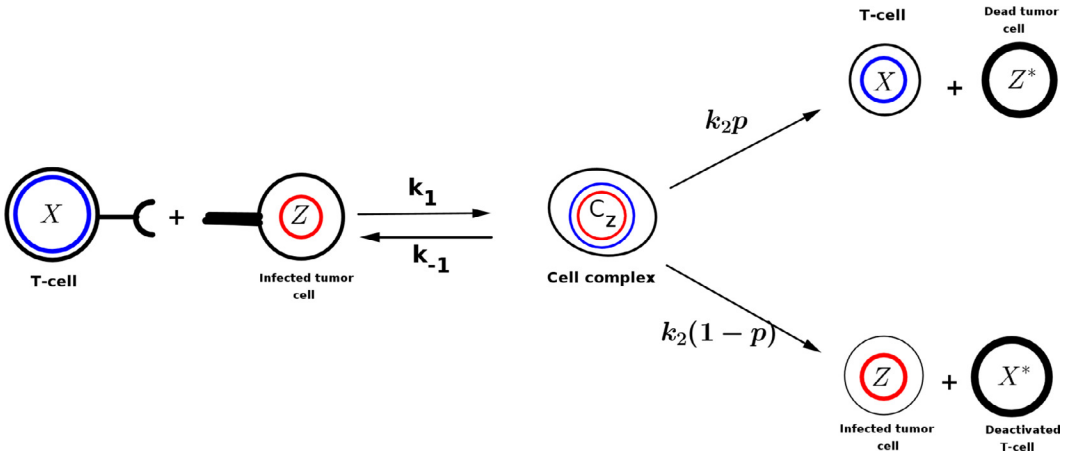

Fig. 1. Schematic diagram of the local kinetics between a CTL and an infected tumor cell.

interactions are highly complex and poorly understood. Therefore much effort is needed to understand the tumor-immune-virus dynamics. The aim of this study is to use mathematical models to understand how virus and immune responses influence the outcome of oncolytic treatment.

Earlier mathematical models that were developed described the evolution of a tumor under a viral injection [8–11]. A few models to include an immune response, for example [12,13], have also been constructed. Our model builds upon the model presented by Mukhopadhyay and Bhattachrrya [13] with inclusion of local kinetic interaction terms of tumor cells and CTLs, and a modified functional immune response to account for the saturation of immune cells in a tumor localization and the fact that only a portion of a tumor nodule comes into contact with CTLs (see Refs. [14–16]). Mukhopadhyay and Bhattachrrya [13] presented a deterministic model to study the dynamics of tumor-immune-virus interactions. They showed the importance of different host, viral, and immune system parameters in controlling the system dynamics. They extended their model to incorporate random noise. Our model captures important factors in the local kinetics and spatial distribution of the cells.

2. The homogeneous model

The model presented here subdivides the cell population into local densities of CTLs X, uninfected tumor cells Y, and the infected tumor cells Z, as a result of injecting tissue with an oncolytic virus. We consider the CTL supply into the tumor cell localization to be constant. When a single CTL comes into contact with a tumor cell, following the receptor-ligand kinetics theory in Ref. [18], it leads to the formation of a tumor–CTL complex which may either lead to tumor cell death or CTL deactivation. We consider only virus specific immune response just like in Ref. [13] and thereby not considering local kinetics between CTLs and uninfected tumor cells (see also Refs. [5,17]). When the infected tumor cells are destroyed, they release new infectious virus particles to destroy the remaining tumor. The virus also stimulates host anti-tumor CTL responses. The local kinetic interactions between a CTL and an infected tumor are schematically described in Fig. 1. With the above considerations, the system is described by the following nonlinear coupled system of ordinary differential equations;

$$\begin{aligned}
\frac{dX}{dt} &= s - d_1X + \frac{fC_z}{g_1+Z} - k_1XZ + (k_{-1}+k_2p)C_z,\\
\frac{dY}{dt} &= a_1Y(1-a_2Y) - \frac{\theta ZY}{g_2+Z},\\
\frac{dZ}{dt} &= b_1Z(1-b_2Z) + \frac{\theta ZY}{g_2+Z} - k_1XZ + (k_{-1}+k_2(1-p))C_z,
\end{aligned} \tag{1}$$

$$X(0) = X_0, \quad Y(0) = Y_0, \quad Z(0) = Z_0,$$

with the cell complex equation derived from the kinetics in Fig. 1 given by

$$\frac{dC_z}{dt} = k_1XZ - (k_{-1}+k_2)C_z, \tag{2}$$

where s is the CTL supply rate into the tumor localization, d_1 is the CTL death rate, $fC_z/(g_1+Z)$ is a response function of Michaelis-menten form [14] to model the increase in CTL proliferation in the tumor as a result of a single CTL meeting with an infected tumor cell, where f and g_1 are constant parameters derived from experimental results. k_1 is the binding rate of a CTL to an infected tumor cell to form a complex C_z, k_{-1} is a rate at which infected tumor cells get dissociated from CTLs resulting in an irreversible programming of the tumor cells for lysis. The probability with which infected tumor cells are killed through CTL-mediated mechanism once they form a cell complex is denoted by p and consequently k_2p is their rate of death. $k_2(1-p)$ is the inactivation rate of CTLs. $a_1Y(1-a_2Y)$ and $b_1Z(1-b_2Z)$ are logistic growth terms respectively modeling uninfected and infected tumor cells where a_1 and a_2^{-1}, are respectively the intrinsic growth rate and carrying capacity of the uninfected tumor cells, and b_1 and b_2^{-1} are respectively the intrinsic growth rate and carrying capacity of the infected tumor cells. The virus replication into the tumor is modeled by the function $\theta ZY/(g_2+Z)$ also of Michaelis-menten form [14], where θ is the virus replication rate. It is important to note that the dynamics of the lysed cell populations X^* and Z^* from the diagram of kinetics in Fig. 1 do not affect the rates of change of the cell concentrations X,Y, and Z. It is therefore sufficient to analyze the behavior given by Eqs. (1).

Biologically, the formation of complexes occurs on a time scale of a few hours while that of tumor cells and CTLs occurs on a much slower time scale, of tens of hours [19]. This implies that $\dot{C}_z \approx 0$. The system (1) is transformed to

$$\begin{aligned}
\frac{dX}{dt} &= s - d_1X + \frac{\rho_1XZ}{g_1+Z} - lXZ,\\
\frac{dY}{dt} &= a_1Y(1-a_2Y) - \frac{\theta ZY}{g_2+Z},\\
\frac{dZ}{dt} &= b_1Z(1-b_2Z) + \frac{\theta ZY}{g_2+Z} - mXZ,
\end{aligned} \tag{3}$$

where

$$l = Kk_2(1-p),\ \rho_1 = fK, \quad m = Kk_2p,\ K = \frac{k_1}{(k_{-1}+k_2)}.$$

The parameters in (3) have different units. It is therefore useful to nondimensionalize this system by setting $x = X/X_0$, $y = Y/Y_0$,

$z = Z/Z_0$ and $\bar{t} = t/t_0$. We choose the magnitudes of the concentrations to be $X_0 = 10^6$ and $Y_0 = Z_0 = 10^7$ since human body tissue can contain around 10^5–10^9 cells (see Ref. [20]). We scale the time relative to the rate of CTLs' deactivation, $t_0 = d_1^{-1}$. We drop the bar on the non-dimensionalized time $\bar{t}$ for notational simplicity and Eqs. (3) are expressed as

$$\begin{aligned}
\dot{x} &= \sigma - x + \frac{\gamma_1 xz}{\eta_1 + z} - \nu xz,\\
\dot{y} &= \alpha_1 y(1 - \alpha_2 y) - \frac{\theta_1 zy}{\eta_2 + z},\\
\dot{z} &= \beta_1 z(1 - \beta_2 z) + \frac{\theta_2 zy}{\eta_2 + z} - \mu xz,
\end{aligned} \tag{4}$$

where

$$\sigma = \frac{s}{X_0 d_1}, \quad \eta_1 = \frac{g_1}{Z_0}, \quad \gamma_1 = \frac{\rho}{d_1}, \quad \nu = \frac{lZ_0}{d_1}, \quad \alpha_1 = \frac{a_1}{d_1},$$
$$\alpha_2 = a_2 Y_0, \quad \theta_1 = \frac{\theta}{d_1}, \tag{5}$$

$$\eta_2 = \frac{g_2}{Z_0}, \quad \beta_1 = \frac{b_1}{d_1}, \quad \beta_2 = b_2 Z_0, \quad \theta_2 = \frac{\theta Y_0}{Z_0 d_1}, \quad \text{and} \quad \mu = \frac{m_1 X_0}{d_1}. \tag{6}$$

3. Asymptotics and stability analysis

We investigate the long term behavior of the solutions to (4) by calculating the system's asymptotic solutions. We do this by equating Eqs. (4) to zero. We investigate the stability of these steady states by linearizing the system (4) about each of the steady states to obtain

$$\frac{dX_i}{dt} = A_i \bar{X}_i \tag{7}$$

where A_i is the Jacobian matrix of (4) evaluated at the steady state $\bar{X}_i$. The model (4) has four biologically meaningful steady states;

- Tumor free state: $(x, y, z) = (\sigma, 0, 0)$. In this steady state both the infected and uninfected tumor cell concentrations are eliminated and a complete remission of cancer is possible. The eigenvalues of (7) evaluated at this state are;

  $\lambda_1 = \alpha_1, \quad \lambda_2 = -1, \quad \text{and} \quad \lambda_3 = \beta_1 - \mu\sigma.$

  The tumor free state is unstable, making it virtually impossible to achieve.
- Infected tumor free state: $(x, y, z) = (\sigma, 1/\alpha_2, 0)$ is a steady state where the CTLs manage to kill all the infected tumor cells although the whole tumor is not eliminated since some uninfected tumor cells remain. The eigenvalues of this state are;

  $$\lambda_1 = -\alpha_1, \quad \lambda_2 = -1 \quad \text{and} \quad \lambda_3 = \frac{\alpha_2\beta_1\eta_2 + \theta_2 - \alpha_2\eta_2\mu\sigma}{\alpha_2\eta_2}.$$

  It is locally asymptotically stable only if $\alpha_2\beta_1\eta_2 + \theta_2 \le \alpha_2\eta_2\mu\sigma$ otherwise it is unstable. The condition for stability does not trivially point out what needs to be clinically done in order to achieve this state. Nevertheless, it is evident from this condition that the properties which need to be checked are the intrinsic tumor growth rates, the virus replication rate, and local kinetic interaction parameters.
- Uninfected tumor free state: $(x, y, z) = (x^*, 0, z^*)$ with

  $$x^* = \frac{A - \Delta\beta_1}{2B\mu}, \quad z^* = \frac{\Delta\sqrt{\beta_1} - A}{2B\beta_1\beta_2}$$

  where

  $$A = \beta_1\beta_2\eta_1 + \beta_1\eta_1\nu - \beta_1\gamma_1, \quad B = 2(\eta_1\nu - \gamma_1)\mu, \quad \text{and}$$

  $$\Delta = (\beta_1\beta_2^2\eta_1^2 + \beta_1\eta_1^2\nu^2 - 2\beta_1\beta_2\eta_1\gamma_1 + \beta_1\gamma_1^2 + 2(\beta_1\beta_2\eta_1^2 - \beta_1\eta_1\gamma_1)\nu)\sigma - 4((\beta_2\eta_1^2\mu\nu - \beta_2\eta_1\gamma_1\mu)\sigma).$$

  Here the virus manages to infect all tumor cells. The eigenvalues of this state are;

  $\lambda_1 = \alpha_1, \quad \lambda_2 = -1, \quad \text{and} \quad \lambda_3 = f(A, B, \Delta).$

  This implies that the uninfected tumor free state is unstable rendering it impossible to achieve such a situation.
- Tumor dormancy state: $(x, y, z) = (x^{**}, y^{**}, z^{**})$, where (x^{**}, y^{**}, z^{**}) are the roots of the equations

  $$\begin{aligned}
  \sigma - x + \frac{\gamma_1 xz}{\eta_1 + z} - \nu xz &= 0,\\
  \alpha_1(1 - \alpha_2 y) - \frac{\theta_1 z}{\eta_2 + z} &= 0,\\
  \beta_1(1 - \beta_2 z) + \frac{\theta_2 y}{\eta_2 + z} - \mu x &= 0.
  \end{aligned} \tag{8}$$

  It is a difficult undertaking to calculate the roots to Eqs. (8) because they are coupled and nonlinear, also involving many terms. However, we substitute parameter values in Table 1 with $\theta = 4$ and the steady state solution is $(1.84, 0.004, 0.097)$ which is locally asymptotically stable since all its eigenvalues $(-1.88, -0.256 + 0.04i, -0.256 - 0.04i)$ have negative real parts. This biologically signifies that the virus is able to completely reduce the tumor to a low tumor concentration state which is dormant.

4. Homogeneous model simulations

We study the numerical solutions to the model equations (4) to substantiate our analytical findings in the previous sections. The fourth order Runge–Kutta method is used to integrate this system with the following set of non-dimensional parameter values;

$$\begin{aligned}
&\sigma = 1.650585, \quad \gamma_1 = 2.3261, \quad \eta_1 = 2.02, \quad \nu = 0.0073,\\
&\beta_1 = 2.4272, \quad \beta_2 = 2.0, \quad \mu = 0.1455, \quad \alpha_1 = 4.3689,\\
&\alpha_2 = 1.0, \quad \text{and} \quad \eta_2 = 2.02
\end{aligned} \tag{9}$$

with varying values of θ_1 and θ_2 within the range of θ, the virus replication rate. These values are obtained by substituting dimensional ones from Table 1 into the expressions in Eqs. (5) and (6). Our choice of the initial conditions is approximately the infected tumor free state with a fraction of some uninfected tumor cells and no infected tumor cells to necessitate virotherapy, i.e. $x(0) = 1.5$, $y(0) = 0.1$, and $z(0) = 0$. The range of θ is as a result of the underlying virus characteristics, for example, burst sizes. The local kinetic

Table 1
Dimensional parameter values for the model (1).

Parameter	Estimated value	Units	Source
k_1	1.3×10^{-7}	day cells^{-1} cm	[20]
k_2	7.2	day^{-1}	[20]
k_{-1}	24	day^{-1}	[20]
p	0.9997	dimensionless	[20]
f	0.2988×10^8	day^{-1} cells cm^{-1}	[20]
θ	$0.27 \le \theta \le 4$	day^{-1} cells cm^{-1}	[13]
g_1	2.02×10^7	cells cm^{-1}	[20]
g_2	10^7	cm^3	[13]
s	1.36×10^4	day^{-1} cells cm^{-1}	[20]
d	0.0412	day^{-1}	[20]
d_2	10	day^{-1}	[20]
a_1	0.18	day^{-1}	[20]
a_2	2.0×10^{-9}	cells^{-1} cm	[20]
b_1	0.1	day^{-1}	[13]
b_2	2.0×10^{-9}	cell^{-1}	[13]
ϕ_1	10^{-6}	cells day^{-1}	[20]
ϕ_4	10^{-4}	cells day^{-1}	[20]
χ	1.728×10^6	cm^2 day^{-1} moles^{-1}	[20]

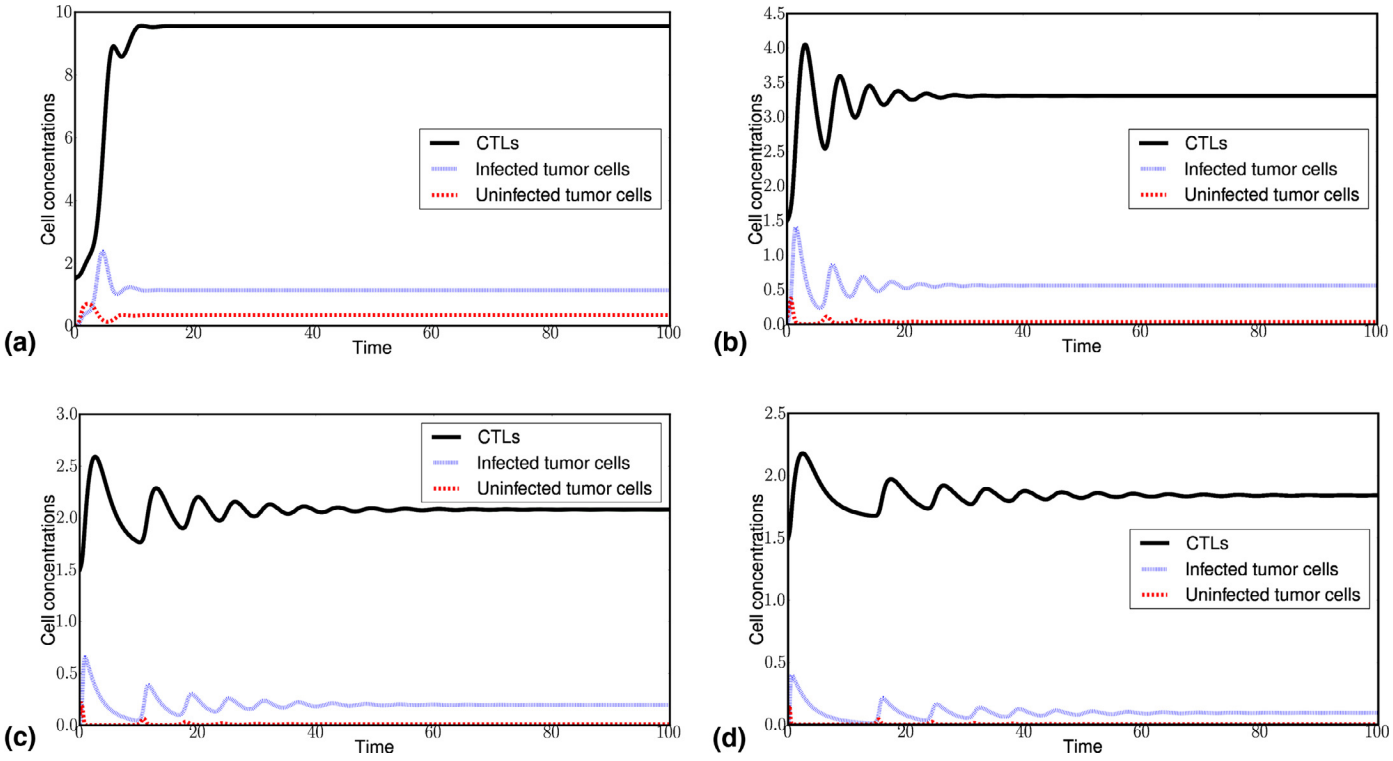

Fig. 2. Variation of cell concentrations with time for parameter values as in Eq. (9) and (a) $\theta = 0.33$, (b) $\theta = 0.8$, (c) $\theta = 2$, and (d) $\theta = 4$ respectively. Cell concentrations and time are nondimensional.

parameter values were obtained from data in which a murine B cell lymphoma was used as an experiment in modeling tumor dormancy in mice (see Refs. [20,21]). It is important to note that the kinetic parameter values are for tumor specific immune response and are the closest we could find in the literature for virus specific immune response.

Fig. 2 shows the variation of cell concentrations against non-dimensionalized time. It shows that as the virus replication rate is increased, both tumor cell concentrations decrease and converge to lower concentrations. Initially, there are oscillations in both CTL and tumor concentrations before they converge to the interior steady states (a) $(\bar{x}, \bar{y}, \bar{z}) \approx (9.52, 0.35, 1.16)$, (b) $(\bar{x}, \bar{y}, \bar{z}) \approx (3.3, 0.02, 0.57)$, (c) $(\bar{x}, \bar{y}, \bar{z}) \approx (2.07, 0.01, 0.2)$, and (d) $(\bar{x}, \bar{y}, \bar{z}) \approx (1.84, 0.004, 0.097)$. Fig. 2 clearly shows that it is possible to clear all infected tumor cells in body tissue for as long as the virus replication rate is high and all other parameters remaining constant. These numerical results concur with the stability analysis in the previous section. The stability analysis showed that the tumor free steady state and the uninfected tumor free states were unstable but the infected tumor free state was feasible to achieve under certain conditions involving the virus replication rate, tumor growth rate, and local kinetic interaction terms. It was also found out, using the same parameter values, that the interior tumor dormant state is locally asymptotically stable. Numerically, it is also found that the tumor load $(y + z)$ decreases with increasing values of θ, the replication rate of the virus. Fig. 3 shows a variation of the tumor load with time. We notice that the higher the virus replication rate is, the higher are the chances of curing cancer in body tissue. Furthermore, it depicts cancer dormancy, a phenomenon where all signs and symptoms of cancer have disappeared, although cancer may still be in body tissue. This can clearly be seen in Fig. 3 where the tumor load is reduced to a stable state with a small concentration of tumor cells. Fig. 4 shows a phase portrait of the tumor load $(y + z)$ against the CTLs concentration with $\theta = 0.8$. It shows the solution curves converging to the interior steady state.

5. The heterogeneous model

In this section we incorporate space in model (1). We do this by considering diffusion in order to capture the random motion of cells and derivation of nutrients and chemotaxis, the movement of CTLs toward a specific target following a chemokine gradient. We consider a one dimensional spatial domain to be the interval $[0, r_0]$ and assume that there are two regions in this interval. One fully occupied by the tumor load and the other fully occupied by CTLs. We denote the region initially occupied by the tumor load $[0, L]$. We consider the same denotation for the cell densities as considered in model 2 and the space variable is denoted by r. Therefore the cell density solutions are denoted by $X(t, r)$, $Y(t, r)$ and $Z(t, r)$. The chemokine concentration is denoted by α. We assume constant diffusivity for all the cell densities. With the above assumptions we have the following system of parabolic reaction-diffusion partial differential equations

$$\begin{aligned}
\frac{\partial X}{\partial t} &= \phi_1 \frac{\partial^2 X}{\partial r^2} - \chi \frac{\partial}{\partial r}\left(X \frac{\partial \alpha}{\partial r}\right) + sH(r) - d_1 X + \frac{\rho_1 XZ}{g_1 + Z} - lXZ,\\
\frac{\partial Y}{\partial t} &= \phi_2 \frac{\partial^2 Y}{\partial r^2} + a_1 Y(1 - a_2 Y) - \frac{\theta ZY}{g_2 + Z},\\
\frac{\partial Z}{\partial t} &= \phi_3 \frac{\partial^2 Z}{\partial r^2} + b_1 Z(1 - b_2 Z) + \frac{\theta ZY}{g_2 + Z} - mXZ,\\
\frac{\partial \alpha}{\partial t} &= \phi_4 \frac{\partial^2 \alpha}{\partial r^2} + \frac{\rho_2 XZ}{g_1 + Z} - d_2 \alpha,
\end{aligned} \tag{10}$$

where ϕ_1, ϕ_2, ϕ_3 and ϕ_4 are respectively diffusion constants for CTLs, uninfected tumor cells, infected tumor cells, and the chemokine concentration. χ is the chemotaxis constant. The response function $(\rho_2 XZ/(g_1 + Z))$ models the multiplication of chemokine concentration at the tumor location and d_2 is the deactivation rate of the

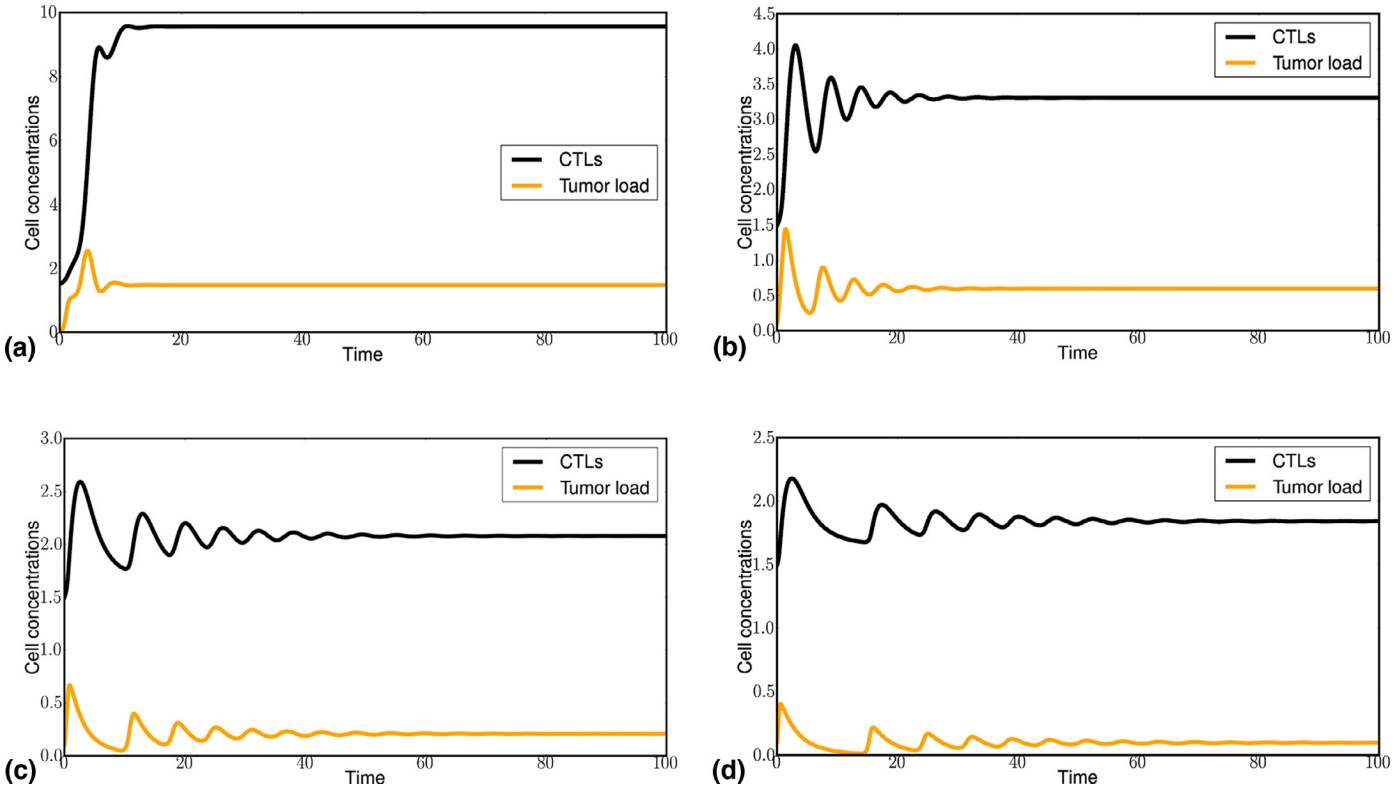

Fig. 3. Variation of tumor load $(y+z)$ and CTLs with time for (a) $\theta = 0.33$, (b) $\theta = 0.8$, (c) $\theta = 2$, and (d) $\theta = 4$ respectively. The other parameters used are in Eq. (9). Cell concentrations and time are nondimensional.

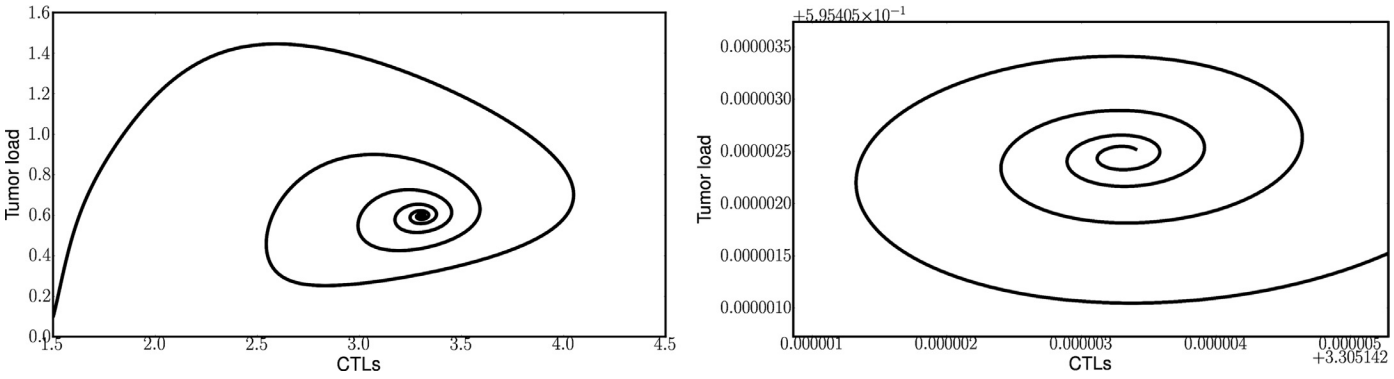

Fig. 4. Phase portrait showing the cell concentrations converging to the interior equilibrium point with parameter values as in Eq. (9) and $\theta = 0.8$. The right hand figure is a zoomed version.

chemokine α. The term $sH(r)$ models the supply of immune cells in the domain where CTLs lie.

$$H(r) = \begin{cases} 0 & \text{if } r - L \le 0, \\ 1 & \text{if } r - L > 0 \end{cases}$$

represents a heaviside function which divides the domain $[0, r_0]$ into two sections to differentiate tumor and immune cells localization and also incorporate space competition between the CTLs and tumor cells (see Ref. [20]). We consider initial and boundary conditions similar to those considered by Matzavinos et al. [20]. We consider that initially the uninfected tumor cells occupy a wider domain than the infected tumor cells with the assumption that virus multiplication will have just begun and thereby covering a smaller part of the body tissue. We assume that there is no cell movement at the boundaries of the domain, (see also Ref. [20]).

The initial and boundary conditions are

$$X(r,0) = \begin{cases} 0, & 0 \le r \le L \\ X_0[1 - \exp(-100(r-L)^2)], & L \le r \le r_0, \end{cases}$$

$$Y(r,0) = \begin{cases} Y_0[1 - \exp(-50(r-L)^2)], & 0 \le r \le L \\ 0, & L \le r \le r_0, \end{cases}$$

$$Z(r,0) = \begin{cases} Z_0[1 - \exp(-10(r-L)^2)], & 0 \le r \le L \\ 0, & L \le r \le r_0, \end{cases}$$

$$\alpha(x,0) = 0, \quad \forall\, x \in [0, r_0],$$

$$\mathbf{n}.\nabla X = \mathbf{n}.\nabla Y = \mathbf{n}.\nabla Z = \mathbf{n}.\nabla \alpha = 0 \text{ at } r = 0 \text{ and } r = r_0. \tag{11}$$

We non-dimensionalize the model (10) by taking X, Y and Z as fractions of their initial concentrations $(x = X/X_0, y = Y/Y_0, z = Z/Z_0)$

and the chemokine density through some reference concentration, that is $\bar{\alpha} = \alpha/\alpha_0$ where $\alpha_0 = 10^{-10}$ [20] with time $\tau = t/t_0$ where $t_0 = r_0/\phi_1$. We non-dimensionalize the space variable relative to the space under consideration, that is $\bar{r} = r/r_0$ where $r_0 = 1$. We assume $L = 0.2$ and for convenience, we drop the bar on r and α. The system (3) is transformed to

$$\begin{aligned}
\frac{\partial x}{\partial \tau} &= \frac{\partial^2 x}{\partial r^2} - \lambda \frac{\partial}{\partial r}\left(x\frac{\partial \alpha}{\partial r}\right) + \sigma H(r) - \psi x + \frac{\gamma_1 xz}{\eta_1 + z} - \nu xz,\\
\frac{\partial y}{\partial \tau} &= \bar{\phi}_2 \frac{\partial^2 y}{\partial r^2} + \alpha_1 y(1-\alpha_2 y) - \frac{\theta_1 zy}{\eta_2 + z},\\
\frac{\partial z}{\partial \tau} &= \bar{\phi}_3 \frac{\partial^2 z}{\partial r^2} + \beta_1 z(1-\beta_2 z) + \frac{\theta_2 zy}{\eta_2 + z} - \mu xz,\\
\frac{\partial \alpha}{\partial \tau} &= \bar{\phi}_4 \frac{\partial^2 \alpha}{\partial r^2} + \frac{\gamma_2 xz}{\eta_1 + z} - \delta\alpha,
\end{aligned} \tag{12}$$

where

$$\begin{aligned}
&\sigma = \frac{st_0}{X_0}, \quad \psi = d_1 t_0, \quad \eta_1 = \frac{g_1}{Z_0}, \quad \gamma_1 = \rho_1 t_0, \quad \nu = lT_0 t_0,\\
&\bar{\phi}_2 = \phi_2 t_0, \quad \alpha_1 = a_1 t_0, \quad \alpha_2 = a_2 Y_0, \quad \eta_2 = \frac{g_2}{Z_0}, \quad \theta_1 = \theta t_0,\\
&\bar{\phi}_3 = \phi_3 t_0, \quad \beta_1 = b_1 t_0, \quad \beta_2 = b_2 Z_0 \quad \lambda = \xi\alpha_0 t_0,\\
&\theta_2 = \frac{\theta Y_0 t_0}{Z_0}, \quad \text{and} \quad \mu = mX_0 t_0, \quad \gamma_2 = \frac{\rho_2 X_0}{\alpha_0 t_0}, \quad \delta = d_2 t_0.
\end{aligned}$$

The initial and boundary conditions become

$$\begin{aligned}
x(r,0) &= \begin{cases} 0, & 0 \le r \le 0.2 \\ X_0[1-\exp(-100(r-0.2)^2)], & 0.2 \le x \le 1, \end{cases}\\
y(r,0) &= \begin{cases} Y_0[1-\exp(-50(r-0.2)^2)], & 0 \le r \le 0.2 \\ 0, & L \le r \le 1, \end{cases}\\
z(r,0) &= \begin{cases} Z_0[1-\exp(-10(r-0.2)^2)], & 0 \le r \le 0.2 \\ 0, & 0.2 \le r \le 1, \end{cases}\\
&\alpha(x,0) = 0, \quad \forall\, x \in [0,1],\\
&\mathbf{n}.\nabla x = \mathbf{n}.\nabla y = \mathbf{n}.\nabla z = \mathbf{n}.\nabla\alpha = 0 \text{ at } r = 0 \text{ and } r = 1.
\end{aligned} \tag{13}$$

6. Traveling wave solutions

Finding analytical solutions to the system (12) is a difficult undertaking due to its nonlinearity and the many terms involved. Nevertheless, we can find a certain class of particular analytical solutions to this system. In this section we use factorization of differential operators, a method developed by Rosu and Corneju [22–24] to determine traveling wave solutions to the system (12). These solutions can be helpful in analyzing the tumor-immune-virus dynamics under investigation thus predicting the future cell densities. For the sake of mathematical simplicity we ignore the heaviside function and do not consider the effect of chemotaxis. This is a realistic assumption as it has been shown in Ref. [25] that chemotaxis and the heaviside function do not influence the formation of traveling wave components.

Factorization of differential operators provides an effective and efficient way to obtain particular solutions of Lienard type equations. It has been used in determining exact solutions of some types of differential equations (see Refs. [26–28]). The equations in system (12), without chemotaxis ($\alpha = 0$), can all be transformed to be of Lienard equation type

$$\frac{d^2U}{dx^2} + G(U)\frac{dU}{dx} + F(U) = 0. \tag{14}$$

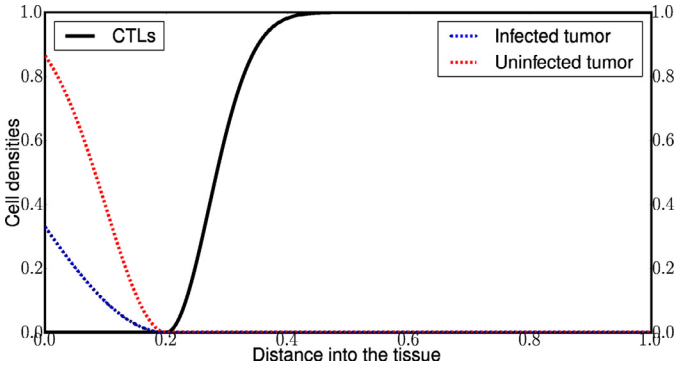

Fig. 5. Initial tumor and CTLs densities for the model (12) showing the tumor load on one side of the domain and the CTLs on the other.

We use the coordinate transformation $\xi = r - c\tau$ and by applying chain rule, the system (12) is transformed to

$$\begin{aligned}
&\frac{d^2x}{d\xi^2} + G_1(x,y,z)\frac{dx}{d\xi} + F_1(x,y,z) = 0,\\
&\frac{d^2y}{d\xi^2} + G_2(x,y,z)\frac{dx}{d\xi} + F_2(x,y,z) = 0,\\
&\frac{d^2z}{d\xi^2} + G_3(x,y,z)\frac{dx}{d\xi} + F_3(x,y,z) = 0,
\end{aligned} \tag{15}$$

where

$$\begin{aligned}
&G_1 = c, \quad F_1 = x\left(\frac{\sigma}{x} - \psi + \frac{\gamma_1 z}{\eta_1 + z} - \nu z\right),\\
&G_2 = \frac{c}{\bar{\phi}_2}, \quad F_2(x,y,z) = y\left[c_1\left(\alpha_1(1-\alpha_2 y) - \frac{\theta_1 z}{\eta_2 + z}\right)\right],\\
&G_3 = \frac{c}{\bar{\phi}_3}, \quad F_3(x,y,z) = z\left[c_2\left(\beta_1(1-\beta_2 z) - \frac{\gamma_2 y}{\eta_2 + z} + \frac{\theta_2 y}{\eta_2 + z} - \mu x\right)\right],
\end{aligned}$$

$c_1 = 1/\bar{\phi}_2$, $c_2 = 1/\bar{\phi}_3$, and c is the wave propagation speed.

The factorization of (15) gives

$$\begin{aligned}
&[D - \psi_{11}(x,y,z)][D - \psi_{12}(x,y,z)]x = 0,\\
&[D - \psi_{21}(x,y,z)][D - \psi_{22}(x,y,z)]y = 0,\\
&[D - \psi_{31}(x,y,z)][D - \psi_{32}(x,y,z)]z = 0,
\end{aligned} \tag{16}$$

where $D = \frac{d}{d\xi}$. Comparing (15) and (16), it is easy to deduce that

$$\begin{aligned}
G_1(x,y,z) &= -\left(\psi_{11} + \psi_{12} + \frac{\partial \psi_{12}}{\partial x}x\right),\\
G_2(x,y,z) &= -\left(\psi_{21} + \psi_{22} + \frac{\partial \psi_{22}}{\partial y}y\right),\\
G_3(x,y,z) &= -\left(\psi_{31} + \psi_{32} + \frac{\partial \psi_{32}}{\partial z}z\right),
\end{aligned} \tag{17}$$

and

$$\begin{aligned}
&F_1(x,y,z) = \psi_{11}\psi_{12}x, \quad F_2(x,y,z) = \psi_{21}\psi_{22}y,\\
&F_3(x,y,z) = \psi_{31}\psi_{32}z.
\end{aligned} \tag{18}$$

Choosing ψ_{ij} in such a way that

$$\begin{aligned}
&\psi_{11} = \frac{1}{\kappa_1}\left(\frac{\sigma}{x} - \psi + \frac{\gamma_1 z}{\eta_1 + z} - \nu z\right), \quad \psi_{12} = \kappa_1,\\
&\psi_{21} = \frac{1}{\kappa_2}\left[c_1\left(\alpha_1(1-\alpha_2 y) - \frac{\theta_1 z}{\eta_2 + z}\right)\right], \quad \psi_{22} = \kappa_2,\\
&\psi_{31} = \frac{1}{\kappa_3}\left[c_2\left(\beta_1(1-\beta_2 z) + \frac{\theta_2 y}{\eta_2 + z} - \mu x\right)\right], \quad \psi_{32} = \kappa_3,
\end{aligned}$$

where κ_1, κ_2 and κ_3 are arbitrary constants that can be determined from (18). The system (15) is transformed to eight possible

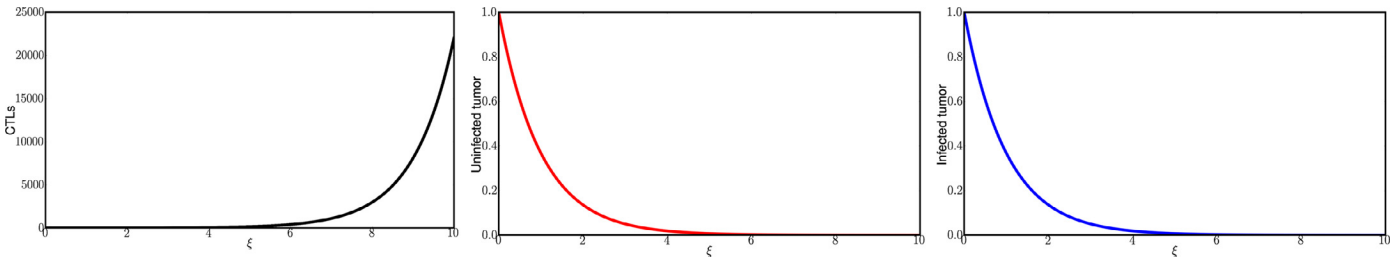

Fig. 6. Traveling wave solutions of the model (12).

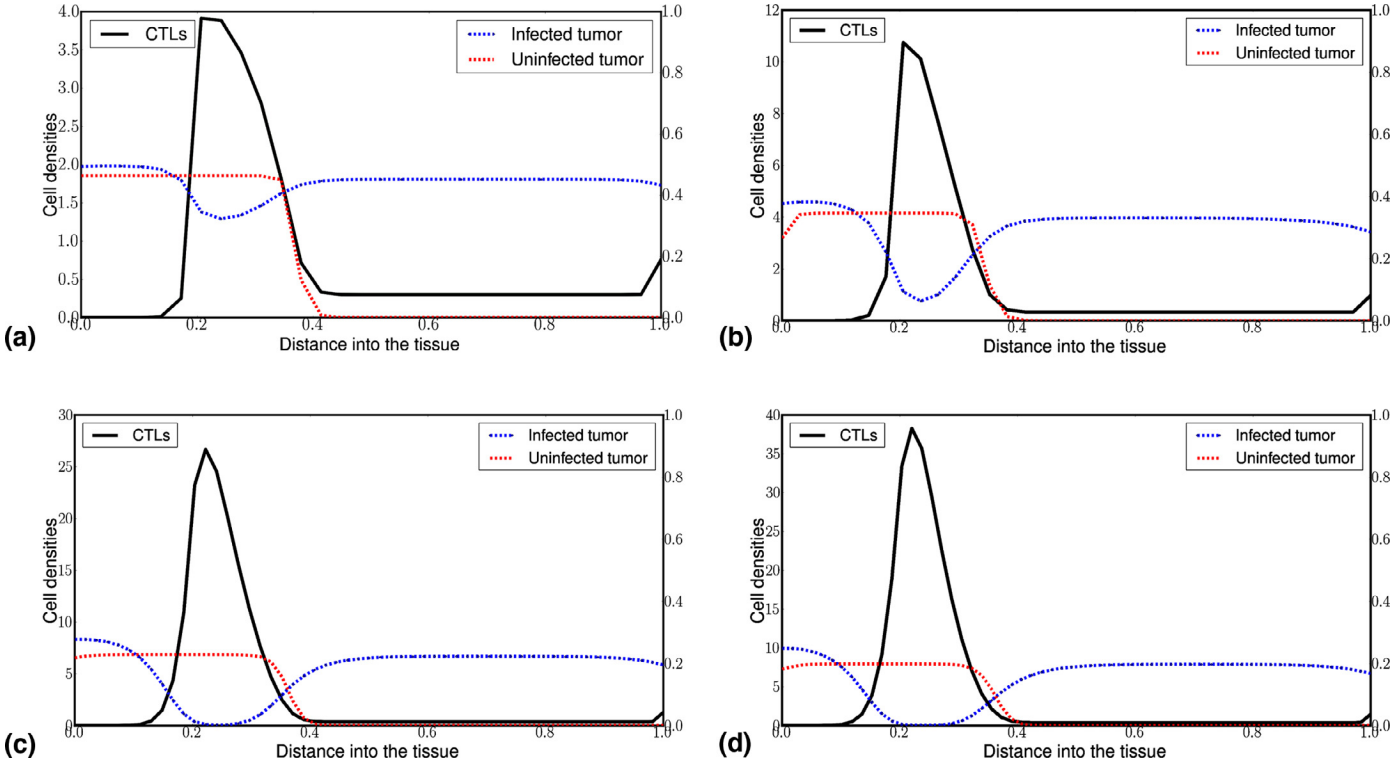

Fig. 7. Spatial distribution of nondimensional CTLs and tumor cell densities for the model (12) in the tissue at times corresponding to (a) 300, (b) 400, (c) 700 and (d) 800 days respectively. The left and right hand scales respectively correspond to CTLs and tumor cell densities.

systems of first order differential equations and we choose to solve the system (19)

$$[D-\psi_{12}(x,y,z)]x=0,\quad [D-\psi_{22}(x,y,z)]y=0,$$
$$[D-\psi_{32}(x,y,z)]z=0, \tag{19}$$

which gives

$$x(\xi)=C\exp[\kappa_1\xi],\quad y(\xi)=C\exp[\kappa_2\xi],\quad z(\xi)=C\exp[\kappa_3\xi], \tag{20}$$

implying that the analytical traveling wave solutions of the system (12) are

$$x(r-c\tau)=C\exp[\kappa_1(r-c\tau)],$$
$$y(r-c\tau)=C\exp[\kappa_2(r-c\tau)],$$
$$z(r-c\tau)=C\exp[\kappa_3(r-c\tau)], \tag{21}$$

where

$$\kappa_1=\frac{-c}{2}\pm\frac{1}{2}\sqrt{c^2+4\psi},\quad \kappa_2=\frac{-c}{\phi_2}\pm\frac{1}{2}\sqrt{(c/\phi_2)^2-4\alpha_1c_1},$$

and $$\kappa_3=\frac{-c}{2\phi_3}\pm\frac{1}{2}\sqrt{(c/2\phi_3)^2-4\beta_1c_2}.$$

It is worth noting that the other systems which can be chosen from (16) are rather not easy to solve because of the many nonlinear terms involved. We therefore focus on one class of solutions.

Fig. 6 shows plots of the traveling wave solutions which we obtained using factorization of differential operators. They show that in the long run, the CTL density exponentially grows while both tumor densities exponentially decrease.

7. Heterogeneous model simulations

Model (12) was simulated using parameter values in Table 1 and $\theta=2$. We assumed that CTLs and tumor cells diffuse at the same rate. We used Crank–Nicholson finite difference schemes to discretize the model equations and solved the resulting system using LU decomposition. We implemented this in PYTHON programming language. Fig. 7(a)–(d) displays the spatial distribution dynamics of CTLs and the infected and uninfected tumor cells in the tissue at times corresponding to 300, 400, 700 and 800 days respectively. In doing these simulations, we set two scales on either sides using twinx in PYTHON software to clearly see the tumor density curves since the scale for the CTLs is high ([0, 40]) and that for the tumor is low ([0, 1]). We notice that the CTLs' density overly keeps increasing with time and the tumor densities are lowered throughout the tissue going by the areas below the curves. We estimated these areas using Riemann sums. The areas under the uninfected tumor curves for 300, 400, 700 and 800 days are respectively 0.17964, 0.1222, 0.08445 and 0.07261 unit squared. The

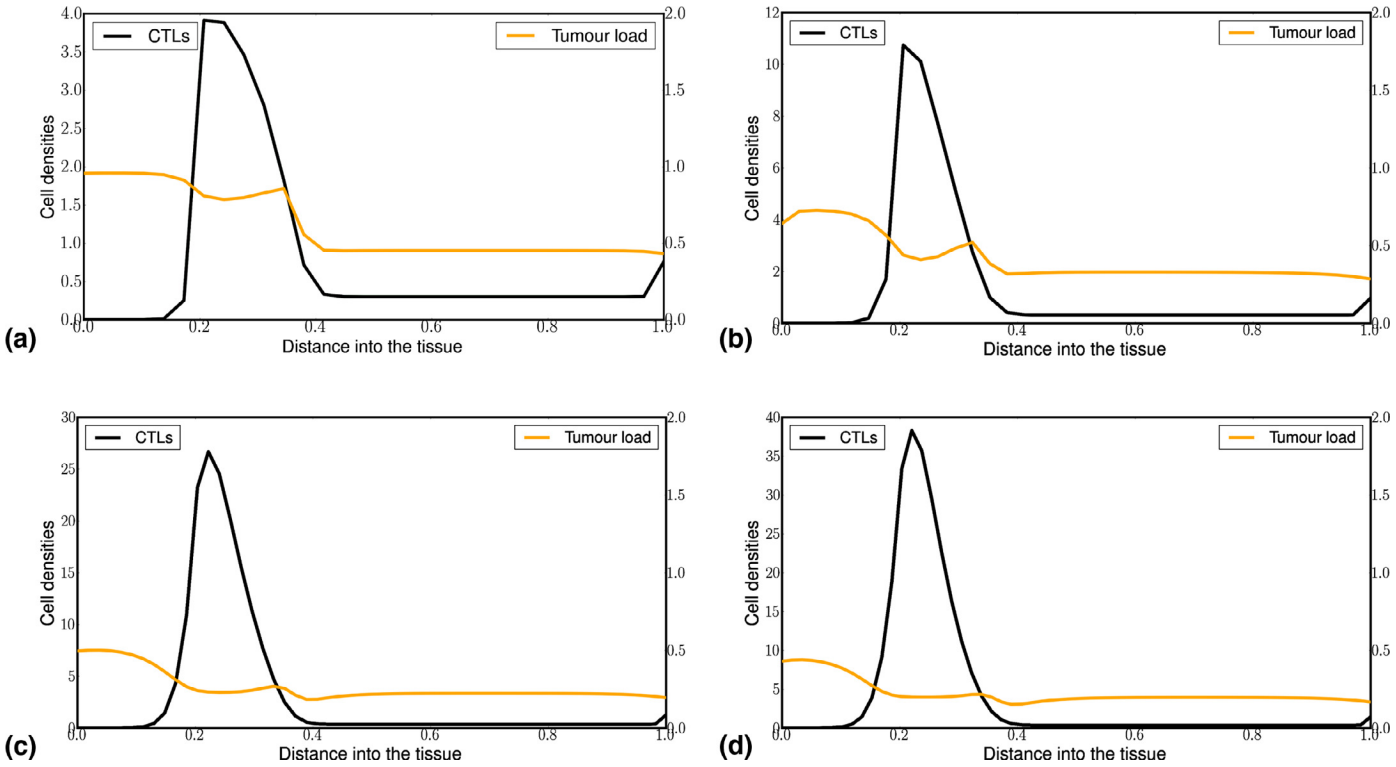

Fig. 8. Nondimensional tumor load and CTLs distribution for the model (12) in the tissue at times corresponding to (a) 300, (b) 400, (c) 700 and (d) 800 days respectively. The left and right hand scales respectively correspond to CTLs and tumor cell densities.

same is observed for the infected tumor cells, which areas are respectively 0.30472, 0.30472, 0.1840 and 0.15715 unit squared. Comparing Fig. 7(a)–(d) with (Fig. 5), we notice that the CTLs occupy more of the domain [0.2, 0.4]. Initially the CTLs lie on [0.2, 1]. As time goes on, the CTLs occupy much of the left hand domain. This shows the attack of the CTLs on predator cells. Fig. 8 shows the total tumor load $(y+z)$ and CTLs spatial distribution. The results are similar to those that we observe in Fig. 7, that is decrease in tumor load, increase in CTLs, and a shift of domains depicting an attack of CTLs on the tumor cells. This can be explained by the response of CTLs to a tumor in body tissue.

8. Conclusions

The advantage of using virotherapy is the fact that it offers less harmful side effects during and after cancer therapy. Several clinical trials for many viruses are currently ongoing and this treatment may soon be available for clinical use. The aim of this study was to examine how virus and immune responses influence the outcome of oncolytic virotherapy. We constructed two deterministic models with the second, an extension considering diffusion and chemotaxis. We determined the homogeneous model's equilibria and investigated their stability. We determined traveling wave solutions for the heterogeneous model and numerical solutions were compared to analytical predictions where possible.

The homogeneous model simulations together with the stability analysis agreed to a fact that virotherapy can reduce the tumor load in body tissue to a very minimum and cancer dormant cell concentration level by killing all the infected cells although a very small number of uninfected tumor cells may remain. Agarwal and Bhadauria [8] in their tumor-oncolytic virus model analysis argue that the tumor load can be reduced to a lower value provided that the net growth of uninfected cells is less than the virus transmission rate, in our case the replication rate. They also conclude that the interior equilibrium point will always be locally asymptotically stable if the growth rate of uninfected cells is higher than that of infected cells. The model parameter values which we used all fulfill the above conditions and the homogeneous numerical results are similar to Agarwal and Bhadauria's. Mukhopadhyay and Bhattacharyya [13] in their analysis of a deterministic model to ascertain the most important parameters that control tumor-immune-virus dynamics stated that the virus replication rate has the ability to stabilize or destabilize the system. Moreover, our homogeneous model simulations clearly indicated that a high virus replication rate can result into a tumor free body tissue. We introduced a space variable to incorporate diffusion and chemotactic movement of cells thus developing a spatial model on a one dimensional domain.

We determined a certain class of analytical solutions to the resulting system of nonlinear hyperbolic partial differential equations. All the spatial model equations, without chemotaxis, are of Lienard type and this gave us an advantage to use the method of factorization of differential operators. The numerical plots of the solutions which we obtained conformed to the fact that in the long run, CTLs density exponentially grows while the tumor cell densities decrease. Malinzi et al. [29] showed that the main tumor invasion properties include tumor growth rate, tumor cells' diffusion rate, and local kinetic interaction terms. The analytical traveling wave solutions we obtained are functions of the wave propagation speed, tumor diffusion rates, and local kinetic interaction terms. Biologically, unchecked exponential increase or decrease in cell population growth is not realistic in comparison to experimental studies (see e.g. Refs. [30–32]). Nevertheless, these solutions point out a decrease in the tumor cell densities and an increase in the CTLs. These solutions are similar to those obtained in the traveling wave analyses done by authors of Refs. [25,33].

The heterogeneous numerical simulations showed the CTLs attacking the tumor. The plots of the total tumor load showed that with time the CTLs maintained the tumor density at a lower dormant level while their density kept on increasing in the body tissue.

In reality, the geometry of human body tissue is intricate and the one dimensional spatial model developed here is not in any way equivalent to body geometry. Nevertheless the results derived from

this model give important insights into tumor-virus-immune interaction dynamics and the model can be extended to a more biologically realistic geometry, perhaps a spherically symmetric one.

Acknowledgments

We are grateful for financial support from the University of KwaZulu-Natal.

References

[1] Australian Institute of Health And Welfare, Authoritative information and statistics to promote better health and well being, 2014. Available from: http://www.aihw.gov.au/cancer/.
[2] World health organization, Cancer report, 2014. Available from: www.bmj.com/content/348/bmj.g1338/.
[3] M.I.S. Costa, J.L. Bolderini, R.C. Bassanezi, Optimal chemotherapy: a case study with drug resistance, saturation effect, and toxicity, J. Math. Med. Biol. 11(1) (1994) 45–59.
[4] E. Kelly, S.J. Russel, History of oncolytic viruses: genesis to genetic engineering, J. Mol. Theory 15(4) (2007) 651–659.
[5] S.J. Russel, K.W. Pengl, J.C. Bell, Oncolytic virotherapy, J. Nat. Biotechnol. 30(7) (2012) 1–13.
[6] H.M. Mambili-Mamboundou, P. Sibanda, J. Malinzi, Effect of immunotherapy on the response of ticls to solid tumor invasion, J. Math. Biosci. 249 (2014) 52–59.
[7] T.C. Liu, E. Galanis, D. Kirn, Clinical trial results with oncolytic virotherapy: a century of promise, a decade of progress, J. Nat. Clin. Pract. Oncol. 4(2) (2007) 101–117.
[8] M. Agarwal, A.S. Bhadauria, Mathematical modeling and analysis of tumor therapy with oncolytic virus, J. Appl. Math. 2(1) (2011) 131–140.
[9] D. Wordaz, Viruses as antitumor weapons defining conditions for tumor remission, J. Cancer Res. 61(8) (2001) 3501–3507.
[10] D. Wordaz, N. Komarova, Computational Biology of Cancer, Lecture Notes and Mathematical Modeling, World Scientific Publishing Company, Singapore, 2005.
[11] A.S. Novozhilov, F.S. Berezovskaya, E.V. Koonin, G.P. Karev, Mathematical modeling of tumor therapy with oncolytic viruses: regimes with complete tumor elimination within the framework of deterministic models, J. Biol. Direct 1(6) (2006) 1–18
[12] J.T. Wu, D.H. Kirn, L.M. Wein, Analysis of a three-way race between tumor growth, a replication-competent virus and an immune response, Bull. Math. Biol. 66(4) (2004) 605–625.
[13] B. Mukhopadhyay, R. Bhattacharyya, A nonlinear mathematical model of a virus-tumor-immune system interaction: deterministic and stochastic analysis, J. Stochas. Anal. Appl. 27(2) (2009) 409–429.
[14] J.G. Wagner, Properties of the Michaelis-menten equation and its integrated form which are useful in pharmacokinetics, J. Pharmacokinet. Biopharm. 1(2) (1973) 103–121.
[15] C. DeLisi, A. Rescigno, Immune surveillance and neoplasia: a minimal mathematical model, Bull. Math. Biol. 39(2) (1977) 201–221.
[16] D. Kirschener, J.C. Panetta, Modelling immunotherapy of the tumor immune interaction, J. Math. Biol. 37(3) (1998) 235–252.
[17] R. Prestwich, K. Harrington, H. Pandha, R. Vile, A. Melcher, F. Errington, Oncolytic viruses: a novel form of immunotherapy, Expert Rev. Anticancer Ther. 8(10) (2008) 1581–1588.
[18] D.A. Lauffenburger, J.J. Linderman, Models for Binding, Trafficking, and Signaling, Oxford University Press, New York, 1993.
[19] V.A. Kuznetsov, I.A. Makalkin, M.A. Taylor, A.S. Perelson, Nonlinear dynamics of immunogenic tumors: parameter estimation and global bifurcation analysis, J. Math. Biol. 56(2) (1994) 295–321.
[20] A. Matzavinos, M.A.J. Chaplain, V.A. Kuznetsov, Mathematical modelling of spatio-temporal response of cytotoxic t-lymphocytes to a solid tumor, J. Math. Med. Biol. 21(1) (2004) 1–34.
[21] H. Siu, E.S. Vitetta, R.D. May, J.W. Uhr, Tumor dormancy: regression of bcl tumor and induction of a dormant tumor state in mice chimeric at the major histocompatibility complex, J. Immunol. 137(1) (1986) 1376–1382.
[22] H.C. Rosu, O. Cornejo, Supersymmetric pairing of kinks for polynomial nonlinearities, J. Phys. Rev. E 71(4) (2005) 46–60.
[23] H.C. Rosu, O. Cornejo, Prog. theor., J. Phys. 114(1) (2005) 553.
[24] H.A. Abdulsalam, E.S. Fahmy, Traveling wave solutions for nonlinear wave equation with dissipation and nonlinear transport term through factorization, J. Appl. Math. Sci. 4(4) (2007) 1–7.
[25] A. Matzavinos, M.A.J. Chaplain, Travelling-wave analysis of a model of the immune response to cancer, C. R. Biol. 327(11) (2004) 995–1008.
[26] E.S. Fahmy, H.A. Abdulsalam, Exact solutions of some reaction diffusion systems with nonlinear reaction polynomial terms, J. Appl. Math. Sci. 3(11) (2009) 533–540.
[27] O. Corneju, H.C. Rosu, Nonlinear second order odes: factorizations and particular solutions, J. Progress Theor. Phys. 114(3) (2005) 533–540.
[28] K. Swapan, P. Debabrata, S. Aparna, T. Benoy, Factorization Method for Nonlinear Evolution Equations, 2013.
[29] J. Malinzi, P. Sibanda, H. Mambili-Mamboundou, Response of immunotherapy to tumour-ticls interactions: a travelling wave analysis, J. Abstr. Appl. Anal. 2014 (2014) 1–10.
[30] J.S. Spratt, T.L. Spratt, Rates of growth of pulmonary metastases and host survival, Ann. Surg. 159(2) (1964) 161–171.
[31] J.D. Stele, P. Buell, Asymptomatic solitary pulmonary nodules. Host survival, tumor size, and growth rate, J. Thorac. Cardiovasc. Surg. 65(1) (1973) 140–151.
[32] V.P. Collins, R.K. Loeffler, H. Tivey, Observations on growth rates of human tumors, Am. J. Roentgenol. Radium Ther. Nucl. Med. 76(5) (1956) 988–1000.
[33] X. Liao, Y. Chenb, S. Zhouc, Traveling wave fronts of a prey-predator diffusion system with stage-structure and harvesting, J. Comput. Appl. Math. 235(8) (2011) 2560–2568.

Chapter 4

Enhancement of chemotherapy using oncolytic virotherapy: A mathematical analysis

We have already studied in Chapter 2 the mechanisms of interaction of immune cells and tumour cells. We have also determined the outcome of oncolytic virotherapy treatment in Chapter 3. From these studies we noticed that tumour cells attack the immune system at full potential and that oncolytic virotherapy may be successful in limiting tumour growth and thereby mitigating cancer development but may not completely eradicate tumour cells from body tissue. In this chapter, we seek to determine the outcome of a combination of treatment types, in this case chemotherapy and virotherapy. The chapter starts by constructing a model of chemovirotherapy. The model's plausibility is shown by proving existence, uniqueness, positivity and boundedness of the model solutions. As with the previous homogeneous models, steady state solutions are determined and their stability is investigated. An efficacy analysis of three drug infusion methods is done to determine how best to infuse cancer drugs in a human body and the outcome of each treatment is investigated. Lastly, the models are numerically simulated and the solutions are compared to analytical results.

Enhancement of chemotherapy using oncolytic virotherapy: A mathematical analysis

Joseph Malinzi, Precious Sibanda, Hermane Mambili-Mamboundou

[a] *School of Mathematics, Statistics, and Computer Science, University of KwaZulu Natal, Pietermritzburg, South Africa*

Abstract

We propose a mathematical model of chemovirotherapy, a recent experimental cancer treatment which combines both chemotherapy and oncolytic virotherapy. We prove existence, uniqueness, and boundedness of the model solutions. Analytical solutions are determined where possible and stability analysis presented. Numerical simulations are obtained using the Runge-Kutta forth order method. We show that chemovirotherapy is capable of reducing the tumor cell density in body tissue in a relatively short time frame.

Keywords: Chemovirotherapy, Oncolytic virotherapy, cancer treatment, Ordinary differential equations

2010 MSC: 049K15, 92B05

1. Introduction

Tumors possess mechanisms that suppress anti-tumor activity such as ligands that block natural killer cells and cytotoxic tumor infiltrating cell functions [1]. Because of this, successful cancer treatment often requires a combination of treatment regimens.

Traditional procedures including chemotherapy, surgery, radiation therapy, and immunotherapy, are not a definite cure for cancer. They are also highly toxic [2]. Chemotherapy, which is the most commonly used regimen,

Email addresses: josephmalinzi@aims.ac.za (Joseph Malinzi), sibandap@ukzn.ac.za (Precious Sibanda), Mambilimamboundou@ukzn.ac.za (Hermane Mambili-Mamboundou)

involves the use of medical drugs to lyse cancer cells. These chemotherapeutic drugs circulate in the body and kill rapidly multiplying cells. Because cancer cells are fast replicating compared to healthy cells, they are more susceptible to the action of these drugs [3]. Damage to healthy tissue is unavoidable and this accounts for the high toxicity of chemotherapy [3].

In the recent past, virotherapy, a less toxic experimental treatment has been identified as a possible cancer treatment (see [4, 5, 6, 7]). Virotherapy involves the use of oncolytic viruses that infect, multiply, and directly lyse cancer cells with less or no toxicity [6]. Their tumor specific properties allow for viral binding, entry, and replication [8]. Oncolytic viruses can greatly enhance the cytotoxic mechanisms of chemotherapeutic drugs [9]. Further, chemotherapeutic drugs lyse fast multiplying cells and, in general, virus infected tumor cells quickly replicate [10].

Nguyen et al. [8] gave an account of the mechanisms through which drugs can successfully be used in a combination with oncolytic viruses. They however note that the success of this combination depends on several factors including the type of oncolytic virus (OV)-drug combination used, the timing, frequency, dosage, and cancer type targeted. This combination of cancer treatment is under clinical trials. There is therefore a need for an investigation into the treatment characteristics which are most important for its success.

The model we construct combines elements from two different existing mathematical models. We briefly review these models. Phino et al. [11] developed a mathematical model of chemotherapy response to tumor growth with stabilized vascularization with the aim of investigating the efficacy of chemotherapy in order to eliminate cancer cells. In their analysis, they showed the region of parameter space in which cancer cells may be eliminated. They also showed the outcome of the cell concentrations with varying infusion rates of the drug. Other chemotherapy mathematical models include [12, 13, 14]. Ursher [15] also gave a summary of some mathematical models for chemotherapy. Tian [16] presented a mathematical model that incorporates burst size for oncolytic virotherapy. His analysis showed that there are two threshold

burst size values and below one of them the tumor always grows to its maximum size, while above the other, there exists one or three families of periodic solutions arising from Hopf bifurcations. His study affirmed that a tumor can be greatly reduced to low undetectable cell counts when the burst size is large enough. Other similar virotherapy mathematical models include [7, 17, 18, 19, 20].

The major aims of this study are; to construct a mathematical model to simulate chemovirotherapy, consider three drug infusion methods and compare their efficacies, use mathematical analysis to predict the outcome of OV-drugs combination treatment, and to compare the efficacy of using each treatment, that is to say, chemotherapy and virotherapy individually. We believe that these issues have not been addressed in literature before. Further, to the best of our knowledge, there has not been a mathematical study on the combination of both chemotherapy and virotherapy, yet theoretical and experimental studies have shown that chemovirotherapy may be a success in cancer treatment.

2. Model construction

We consider time dependent cell concentrations of uninfected tumor cells $U(t)$, infected tumor cells $I(t)$, a free virus population $V(t)$, and a chemotherapeutic drug $C(t)$ in an avascular tumor localization. The uninfected tumor grows logistically at an intrinsic rate α per day and the total tumor carrying capacity is K cells in a tumor nodule. The infected tumor cells die off at a rate δ per day. We model the virus multiplication in the tumor by the function $\beta U(t)V(t)$, where β is the virus replication rate measured per day per 10^6 cells or viruses. The response of the drug to the uninfected and infected tumor is respectively modeled by the functions $\delta_0 U(t)C(t)$ and $\delta_1 I(t)C(t)$ where δ_0 and δ_1 are induced lysis rates caused by the chemotherapeutic drug measured per day per cell. We consider that the virus production is $b\delta I$ where b is the virus burst size, measured in number of viruses per day per cell, and δ is the

infected tumor cells' death rate measured per day. We model the chemotherapeutic drug infusion into the body with a function $g(t)$ and that the drug gets depleted from body tissue at a rate λ per day.

We simulate the drug infusion into the body using (a) a constant rate $g(t) = q$, (b) an exponential $g(t) = q\exp(-at)$ and (c) a sinusoidal function $g(t) = q\sin^2(at)$, where q is the rate of drug infusion. The constant a determines the exponential drug decay and period for the sinusoidal infusion. The constant infusion rate may relate to a situation where a patient is put on an intravenous injection or a protracted venous infusion and the drug is constantly pumped into the body. This form of drug dissemination is used on cancer patients who stay in the hospital for over a week. Higher doses of certain anti-cancer drugs may however lead to hepatic veno-occlusive disease, a condition where the liver is obstructed as a result of using high-dose chemotherapy (see e.g. [21, 22]). The exponential drug infusion simulates a situation where a cancer patient is given a single bolus and the drug exponentially decays in the body tissue. This form of infusion is not common although it is now used for some drugs, for example, a single dose of carbonplatin can be given to patients with testicular germ cell tumors and breast cancer (see [23, 24]). The third scenario is possible when a cancer patient makes several visits to a health facility and is given injections or anti-cancer drugs periodically. This is a more common form of cancer drug infusion (see e.g. [25, 26]).

The assumptions above lead to the following system of non-linear first order differential equations;

$$\begin{aligned}
\dot{U}(t) &= \alpha U(t)\left(1 - \frac{U(t)+I(t)}{K}\right) - \beta U(t)V(t) - \delta_0 U(t)C(t),\\
\dot{I}(t) &= \beta U(t)V(t) - \delta I(t) - \delta_1 I(t)C(t),\\
\dot{V}(t) &= b\delta I(t) - \beta U(t)V(t) - \gamma V(t),\\
\dot{C}(t) &= g(t) - \lambda C(t),
\end{aligned} \tag{1}$$

subject to initial cell concentrations

$$U(0) = U_0,\ I(0) = I_0,\ V(0) = V_0, \text{ and } C(0) = C_0.$$

We re-scale the variables in system (1) by setting $\bar{t} = \delta t$, $U = K\bar{U}$, $I = K\bar{I}$, $V = V_0\bar{V}$, and $C = C_0\bar{C}$. We consider $V_0 = K$. The parameters are renamed to become

$$\bar{\alpha}\frac{\alpha}{\delta},\ \bar{\beta} = \frac{\beta V_0}{\delta},\ \bar{\delta_0} = \frac{\delta_0 C_0}{\delta},\ \bar{\delta_1} = \frac{\delta_1 C_0}{\delta},\ \bar{b} = \frac{bK}{V_0}\ \bar{\gamma} = \frac{\gamma}{\delta},$$

$$\phi = \frac{q}{\delta C_0},\ \psi = \frac{\lambda}{\delta},\ \bar{a} = \frac{a}{\delta}.$$

For simplicity, we drop the bars and equations (1) become

$$\begin{aligned}
\dot{U}(t) &= \alpha U(t)\left(1 - U(t) - I(t)\right) - \beta U(t)V(t) - \delta_0 U(t)C(t),\\
\dot{I}(t) &= \beta U(t)V(t) - I(t) - \delta_1 I(t)C(t),\\
\dot{V}(t) &= bI(t) - \beta U(t)V(t) - \gamma V(t),\\
\dot{C}(t) &= \xi(t) - \psi C(t).
\end{aligned} \tag{2}$$

$\xi(t) = \phi$, $\xi(t) = \phi\exp(-at)$, and $\phi\sin^2(at)$ respectively are the constant, exponential and sinusoidal infusion functions. For this model to be biologically meaningful, its solutions should be positive and bounded because they represent cell concentrations. In the next section, we show that the solutions to the equations (1) exist, are positive and bounded, and the domain in which they lie is positive invariant.

3. Mathematical analysis

3.1. Existence and uniqueness

Theorem 1. *There exists a unique solution to the system of equations (2) in the region* $(U, I, V, C) \in \mathbb{R}^4_+$.

Proof. *We use the Picard-Lindelöf theorem (see [27]) as follows.*
Consider the closed interval $I_T = [t_0 - T, t_0 + T]$ *and the closed ball* $B_d = \{y \in \mathbb{R}^n |\ \|y - x_0\| \leq d\}$ *in* $\mathbb{R}^n$ *where* T *and* d *are positive, real numbers. Suppose that the function*

$$f : I_T \times B_d \to \mathbb{R}^n$$

is continuous and that the partial derivatives in the Jacobian matrix D_f where

$$Df = \begin{pmatrix} \frac{\partial f_1}{\partial x_1} & \frac{\partial f_1}{\partial x_2} & \cdots & \frac{\partial f_1}{\partial x_n} \\ \frac{\partial f_2}{\partial x_1} & \frac{\partial f_2}{\partial x_2} & \cdots & \frac{\partial f_2}{\partial x_n} \\ \vdots & \vdots & \ddots & \vdots \\ \frac{\partial f_n}{\partial x_1} & \frac{\partial f_n}{\partial x_2} & \cdots & \frac{\partial f_n}{\partial x_n} \end{pmatrix}$$

exist and are continuous in $I_T \times B_d$. Then there exists a $\delta > 0$ so that the initial value problem

$$\frac{dx}{dt}(t) = f(t, x),\ x(t_0) = x_0$$

has a unique solution on the interval $I_\delta = [t_0 - \delta, t_0 + \delta]$. It is sufficient to show that

$$f = \begin{pmatrix} f_1 := \alpha U(t)\left(1 - U(t) - I(t)\right) - \beta U(t)V(t) - \delta_0 U(t)C(t) \\ f_2 := \beta U(t)V(t) - \delta I(t) - \delta_1 I(t)C(t) \\ f_3 := bI(t) - \beta U(t)V(t) - \gamma V(t) \\ f_4 := \xi(t) - \psi C(t) \end{pmatrix}, \tag{3}$$

and

$$Df = \begin{pmatrix} \frac{\partial f_1}{\partial U} & \frac{\partial f_1}{\partial I} & \frac{\partial f_1}{\partial V} & \frac{\partial f_1}{\partial C} \\ \frac{\partial f_2}{\partial U} & \frac{\partial f_2}{\partial I} & \frac{\partial f_2}{\partial V} & \frac{\partial f_2}{\partial C} \\ \frac{\partial f_3}{\partial U} & \frac{\partial f_3}{\partial I} & \frac{\partial f_3}{\partial V} & \frac{\partial f_3}{\partial C} \\ \frac{\partial f_4}{\partial U} & \frac{\partial f_4}{\partial I} & \frac{\partial f_4}{\partial V} & \frac{\partial f_4}{\partial C} \end{pmatrix} \tag{4}$$

exist and are continuous on $\mathbb{R}^4_+$. The functions (3) and (4) are polynomials and are therefore continuous on $\mathbb{R}^n$.

3.2. Boundedness and positive invariance

Theorem 2. *if $U(0) \geq 0$, $I(0) \geq 0$, $V(0) \geq 0$, and $C(0) \geq 0$, then $U(t) \geq 0$, $I(t) \geq 0$, $V(t) \geq 0$, and $C(t) \geq 0$ for all $t \geq 0$.*

We use the same idea as in [16] to prove positiveness of the model solutions.

Proof. Assuming that the Theory is not true, then there must be a time t_1 such that atleast one of the solutions becomes zero first. We investigate each

possible case; if $U(t_1) = 0$ first, then $\dot{U}(t_1) = 0$. However, from the first equation in system (2), by the uniqueness of the solution, we know that $U(t) = 0$ for all $t \geq t_1$. The second equation then becomes $\dot{I}(t) = -I(t) - \delta I(t)C(t)$ and its solution is

$$I(t) = I(t_1) \exp\left(- \int_{t_1}^{t} (1 + \delta_1 C(s))ds \right) \text{ and so } I(t) \geq 0.$$

The third equation becomes $\dot{V}(t) = bI(t) - \gamma V(t)$. If you set

$$\dot{V}(t) = bI(t) - \gamma = 0 \geq -\gamma V(t) \text{ so } V(t) \geq R \exp(-\gamma t) \text{ meaning that } V(t) \geq 0.$$

Similarly the fourth equation becomes $\dot{C} = \xi(t) - \psi C(t)$ and its solutions is

$$C(t) = \exp(-\psi t) \left(\int_{t_1}^{t} \phi(s) \exp(\psi s) ds + C(t_1) \right),$$

which implies that $C(t) \geq 0$ for all $t \geq 0$.

If $I(t_1) = 0$ first, then $\dot{I}(t_1) = \beta U(t_1)V(t_1) \geq 0$ implying that when $t > t_1$, $I(t) \geq 0$ since $U(t), V(t), C(t) \geq 0$ as assumed.

If $V(t_1) = 0$ first, $\dot{V}(t_1) = by(t_1) \geq 0$, implying that when $t \geq t_1$, $V(t) \geq 0$ since $U(t), I(t), C(t) \geq 0$ as assumed.

If $C(t_1) = 0$ first, $\dot{C}(t_1) = \phi(t_1) \geq 0$, so when $t \geq t_1$, $C(t) \geq 0$ since $U(t), I(t), C(t) \geq 0$ as assumed.

If two solutions are zero (eg $U(t_1) = 0$ and $I(t_1) = 0$) simultaneously at $t = t_1$, then following the same steps above, it is trivial to check that the other solutions will be non-negative for $t > t_1$.

If three solutions are zero (eg $U(t_1) = 0$, $I(t_1) = 0$, and $V(t_1) = 0$) simultaneously at $t = t_1$, it is trivial to check that the other solution will be non-negative for $t > t_1$.

If the four solutions are zero simultaneously at $t = t_1$, from the uniqueness theorem, $U(t) = I(t) = V(t) = C(t) = 0$ for $t > t_1$.

Theorem 3. *The trajectories evolve in an attracting region* $\mathbb{D} = \{(U, I, V, C) \in \mathbb{R}^4_+ \mid U(t) + I(t) \leq 1,\ V(t) \leq b/\gamma,\ C(t) \leq C(\phi)\}$, *where* $C(\phi)$ *depends on the drug infusion function used.*

PROOF. From equation (1), we know that $U + I \leq K$. This implies that $U + I \leq 1$.

$$\dot{V}(t) \leq bI(t) - \gamma V(t),\ \dot{V}(t) \leq b - \gamma V(t), \quad V(t) \leq \frac{b}{\gamma} - \frac{V_0 \exp(-\gamma t)}{\gamma},$$

$$\lim_{t\to\infty} V(t) \leq \frac{b}{\gamma}.$$

$$\dot{C}(t) + \psi C(t) = \xi(t), \quad C(t) = \exp(-\psi t)\left(\int \xi(t)\exp(\psi t)dt + R\right),$$

where R is an arbitrary constant of integration. For the constant infusion function ϕ, $\lim_{t\to\infty} C(t) = \phi/\psi$. For $\xi(t) = \phi e^{-at}$, $\lim_{t\to\infty} C(t) = 0$, and for $\xi(t) = \phi \sin^2(at)$, $\lim_{t\to\infty} C(t) = \frac{\psi+2a}{4a^2+\psi^2} - \frac{\phi}{\psi}$.

Theorem 4. *The domain* $\mathbb{D}$ *is positive invariant for the model equations (2) and therefore biologically meaningful for the cell concentrations.*

PROOF. The proof directly follows from proofs of Theorems 2 and 3.

3.3. Model solutions

To investigate the efficacy of each treatment and their combination we first study the dynamics of the system without treatment. Without any form of treatment, model (2) is reduced to only one equation

$$\dot{U}(t) = \alpha U(t)\left(1 - U(t)\right),\ U(0) = U_0 \tag{5}$$

whose solution is

$$U(t) = \frac{U_0}{(1 - U_0)\exp(-\alpha t) + U_0},\ \lim_{t\to\infty} U(t) = 1,$$

implying that the tumor exponentially grows to its maximum fractional size. We next analyze the model (2), firstly without virotherapy, without chemotherapy, and then with both treatments incorporated. We firstly obtain, where possible analytical and time invariant solutions which predict the long term dynamics of the model equations (1).

Without virotherapy ($V(t) = 0$), the system (2) is transformed to

$$\begin{aligned} \dot{U}(t) &= \alpha U(t)\left(1 - U(t)\right) - \delta_0 U(t) C(t), \\ \dot{C}(t) &= \xi(t) - \psi C(t), \end{aligned} \tag{6}$$

with $U(0) = U_0$ and $C(0) = C_0$. The second equation in (6) is a first order linear ordinary differential equation which can easily be solved to give

$$C(t) = \exp(-\psi t)\left(\int \xi(t)\exp(\psi t)dt + R\right), \tag{7}$$

where R is a constant of integration. The solution to the first equation in (6) depends on the infusion function $\xi(t)$. For a fixed infusion function ϕ

$$\begin{aligned} U(t) &= \frac{e^{\left(\alpha t - \frac{\delta_0 \phi t}{\psi} + \frac{\delta_0 e^{(-\psi t)}}{\psi}\right)}}{\alpha \int e^{\left(\alpha t - \frac{\delta_0 \phi t}{\psi} + \frac{\delta_0 e^{(-\psi t)}}{\psi}\right)} dt + \frac{e^{\delta_0 \psi}}{U_0}}, \\ C(t) &= \left(C_0 - \frac{\phi}{\psi}\right) e^{-\psi t} + \frac{\phi}{\psi}. \end{aligned} \tag{8}$$

From the solution of $C(t)$ in (8),

$$\lim_{t \to \infty} C(t) = \frac{\phi}{\psi}.$$

Biologically we infer that with a constant drug infusion and without virotherapy, the tumor is not completely cleared and a certain proportion of the drug remains in body tissue. The tumor clearance depends on the drug induced lysis of the tumor and the drug infusion rate which should be maximized, and the tumor growth and drug decay rate which should be minimized.

For $\xi(t) = \phi \exp(-at)$,

$$\begin{aligned} U(t) &= \frac{e^{\left(\frac{a\alpha t}{a-\psi} - \frac{\alpha \psi t}{a-\psi} + \frac{c\delta_0 e^{(-\psi t)}}{a-\psi} - \frac{ac\delta_0 e^{(-\psi t)}}{(a-\psi)\psi} + \frac{\delta_0 \phi e^{(-at)}}{(a-\psi)a}\right)}}{a \int e^{\left(\frac{a\alpha t}{a-\psi} - \frac{\alpha \psi t}{a-\psi} + \frac{c\delta_0 e^{(-\psi t)}}{a-\psi} - \frac{ac\delta_0 e^{(-\psi t)}}{(a-\psi)\psi} + \frac{\delta_0 \phi e^{(-at)}}{(a-\psi)a}\right)} dt + \frac{e^{\frac{c\delta_0}{a-\psi}}}{U_0}}, \\ C(t) &= \left(\frac{C_0\psi - \phi}{\psi} - \frac{\phi e^{(-at+\psi t)}}{a-\psi}\right) e^{(-\psi t)}, \end{aligned} \tag{9}$$

$$\tag{10}$$

$$\text{where } \; c = \frac{C_0\psi - \phi}{\psi}.$$

From (9)

$$\lim_{t\to\infty} C(t) = 0, \text{ and } \lim_{t\to\infty} U(t) = U_*,$$

where U_* is a fractional tumor cell concentration between 0 and 1. This suggests that with a single dosage infusion of the chemotherapeutic drug with exponential decay, and without virotherapy, the tumor cannot be cleared from body tissue. The drug is also completely depleted from the body.

When $\xi(t) = \phi \sin^2(at)$ is substituted in (6), the resulting differential equations are solved to give

$$C(t) = \frac{1}{2}\left(2R - \frac{\left(\psi^2 \cos(2at)\, e^{(\psi t)} + 2a\psi e^{(\psi t)} \sin(2at) - \left(4a^2 + \psi^2\right) e^{(\psi t)}\right)\phi}{4a^2\psi + \psi^3}\right) e^{(-\psi t)}, \tag{11}$$

where

$$R = C_0 + \frac{\psi^2 - \phi(4a^2 + \psi^2)}{2\psi(4a^2 + \psi^2)},$$

and

$$\lim_{t\to\infty} C(t) = C_* = f(a, \phi, \psi).$$

This suggests that with time some drug concentration remains in the body tissue. The analytical solution for $U(t)$ is complicated and difficult undertaking to interpret.

Theorem 5. *The system (6), with constant infusion, has no periodic solutions for positive $U(t)$ and $C(t)$.*

Proof. We use Dulac's criterion (see [30]) as follows.
Suppose $\dot{X} = f(x)$ and $f(x)$ is continuously differentiable on a simply connected domain $\mathbb{D} \subset \mathbb{R}$. If there exists a real valued function $g(x)$ such that $\nabla.(g(\dot{X})) = \nabla.(gf)$ has one sign in $\mathbb{D}$, then there are no closed orbits in $\mathbb{D}$. Using Dulac's criterion, it is sufficient to show that

$$\frac{\partial}{\partial U}\left(g\dot{U}\right) + \frac{\partial}{\partial C}\left(g\dot{C}\right) \neq 0 \quad \forall U, C \in \mathbb{R}^2_+.$$

Consider

$$g(U,C) = \frac{1}{UC},$$

$$\begin{aligned}\nabla.(g\dot{X}) &= \frac{\partial}{\partial U}\left(g\dot{U}\right) + \frac{\partial}{\partial C}\left(g\dot{C}\right), \\ &= -\left(\frac{\alpha}{C} + \frac{\xi(t)}{UC^2}\right) < 0 \;\forall\; U, C \in (\mathbb{R}^+)^2.\end{aligned}$$

Theorem 6. *The system (6) has atleast two steady states for each of the drug infusion functions:*

155

1. *For the constant drug infusion function $\xi(t) = \phi$ there are two steady states of (6); $(U = 0, C = \frac{\phi}{\psi})$ which is locally asymptotically stable provided that $\delta_0\phi > \alpha\psi$ and $(U = 1 - \frac{\delta_0\phi}{\alpha\psi}, C = 0)$ which is locally asymptotically stable provided that $\delta_0\phi + \alpha\psi > 2\delta_0\phi\psi^2$ otherwise it is unstable.*

160

2. *For the exponential drug infusion $\xi(t) = \phi\exp(-at)$, (6) has two steady states; $(U = 0, C = 0, W = 0)$ which is unstable and $(U = 1, C = 0, W = 0)$ which is locally asymptotically stable.*

165 3. *For the sinusoidal infusion function, there are four steady states of (6); $(U = 0, C = 0, W = 0)$, $(U = 1, C = 1, W = 0)$, and $(U = \frac{a\alpha\psi - \delta_0\phi}{a\alpha\psi}, C = \frac{\phi}{a\psi}, W = \frac{\phi}{a})$ which are unstable and $(U = 0, C = \frac{\phi}{a\psi}, W = \frac{\phi}{a})$ which is locally asymptotically stable if $\delta_0\phi > a\alpha\psi$ and $\phi < 1$.*

Proof. 1. It is easy to show that when (6) is equated to zero, one obtains two steady states. The characteristic polynomial of the Jacobian matrix for (6) evaluated at $(0, \frac{\phi}{\psi})$ is

$$\lambda^2 + \left(-\alpha + \frac{\delta_0\phi}{\psi} + \psi\right)\lambda + \delta_0\phi - \alpha\psi,$$

whose roots λ can only be negative if $\delta_0\phi > \alpha\psi$.

The characteristic polynomial evaluated at $(1 - \frac{\delta_0\phi}{\alpha\psi}, 0)$ is

$$\lambda^2 + \left(-2\,\delta_0\phi\psi + \alpha + \frac{\delta_0\phi}{\psi} + \psi\right)\lambda - 2\,\delta_0\phi\psi^2 + \delta_0\phi + \alpha\psi,$$

whose roots are negative provided that $\delta_0\phi + \alpha\psi > 2\delta_0\phi\psi^2$.

2. By letting $W = \phi \exp(-at)$, (6) is turned into an autonomous system

$$\begin{aligned} \dot{U}(t) &= \alpha U(t)\,(1 - U(t)) - \delta_0 U(t)C(t), \\ \dot{C}(t) &= W - \psi C(t), \\ \dot{W}(t) &= -aW. \end{aligned} \tag{12}$$

The eigenvalues of the Jacobian matrix for (12) evaluated at $(0,0,0)$ are $-\psi, \alpha$, and 0 and at $(1,0,0)$ are $-\alpha, -\psi$, and $-a$ are all negative.

3. Similarly, by letting $W = \phi \sin^2 t$, (6) becomes the autonomous system

$$\begin{aligned} \dot{U}(t) &= \alpha U(t)\,(1 - U(t)) - \delta_0 U(t)C(t), \\ \dot{C}(t) &= W - \psi C(t), \\ \dot{W}(t) &= \left[4aW(\phi - W)\right]^{\frac{1}{2}}. \end{aligned} \tag{13}$$

The eigenvalues of the Jacobian matrix for (12) evaluated at $(0,0,0)$ are $-\psi, \alpha$, and 0 and the eigenvalues evaluated at $(1,0,0)$ are $\psi, -\alpha$, and 0. For the third steady state to exist $a\alpha\psi \geq \delta_0\phi$ and the eigenvalues evaluated at this state are $\left(-\frac{a\alpha\psi - \delta_0\phi}{a\psi}, -\frac{4\,a\phi}{\sqrt{4\phi(1-\phi)}}, -\psi\right)$, implying that for it to be locally asymptotically stable, $\delta_0\phi > a\alpha\psi$ yet for this to happen, the steady state will not exist. The eigenvalues evaluated at $(U = 0, C = \frac{\phi}{a\psi}, W = \frac{\phi}{a})$ are $\left(-\frac{a\alpha\psi - \delta_0\phi}{a\psi}, -\frac{4\,a\phi}{\sqrt{4\phi(1-\phi)}}, -\psi\right)$ implying that this steady state is locally asymptotically stable if $\delta_0\phi > a\alpha\psi$ and $\phi < 1$.

Theorems 5 and 6 show that there are no repetitive patterns in the dynamics of (6) and with a constant drug infusion, the tumor can be eliminated from body tissue by chemotherapy provided that the combination of the chemotherapeutic drug induced lysis of the tumor and the drug infusion is greater than the combination of the intrinsic tumor growth rate and the drug deactivation rate. The tumor can also be wiped out with a repetitive type drug infusion provided that the combination of the tumor induced lysis by the drug and the dosage is greater than the intrinsic tumor growth rate and drug decay rate.

With the exponential infusion method, where the chemotherapeutic drug is only infused in the patient once and it exponentially decays, the tumor is not removed from body tissue and may grow to its maximum size.

Without chemotherapy, (2) is reduced to

$$\begin{aligned}\dot{U}(t) &= \alpha U(t)\left(1 - U(t) - I(t)\right) - \beta U(t)V(t),\\ \dot{I}(t) &= \beta U(t)V(t) - I(t),\\ \dot{V}(t) &= bI(t) - \beta U(t)V(t) - \gamma V(t).\end{aligned} \tag{14}$$

The analytical solutions to system (14) are not easy to obtain. We therefore equate (14) to zero to obtain solutions which are time invariant and investigate their stability by linearizing (14) about the steady states.

Theorem 7. 1. *If $\beta + \gamma > b\beta$, the system (14) has two steady states; a tumor free cell state $(0,0,0)$ which is unstable and an infected tumor free state $(1,0,0)$ which is locally asymptotically stable.*

2. *If $b\beta > \beta + \gamma$, the system (14) has three steady states; the tumor free state $(0,0,0)$ and the infected free state $(1,0,0)$ which are unstable and a tumor dormant state*

$$\left(U = \frac{\gamma}{(b-1)\beta}, I = \frac{\alpha\gamma\left(\beta(b-1)-\gamma\right)}{\beta\left(\beta(b-1)^2 + \gamma(b-1)\right)}, V = \frac{\alpha\left(\beta(b-1)-\gamma\right)}{(b-1)^2\beta^2 + \alpha\gamma}\right), \tag{15}$$

$b > 1$ which is locally asymptotically stable if $a_0, a_1, a_2 > 0$ and $a_1 a_2 > a_0$ where a_i are coefficients of the characteristic equation.

Proof. 1. The characteristic equation evaluated at $(0,0,0)$ is

$$\begin{aligned}\lambda^3 + (\gamma - \alpha + 1)\lambda^2 + (\gamma - \alpha\gamma - \alpha)\lambda - \alpha\gamma = 0,\\ (\lambda - \alpha)(\lambda + 1)(\lambda + \gamma) = 0,\end{aligned}$$

from which $\lambda_1 = \alpha$, $\lambda_2 = -1$ and $\lambda_3 = -\gamma$ thus rendering it unstable. The characteristic equation evaluated at $(1,0,0)$ is

$$(\lambda + \alpha)\left(\lambda^2 + \lambda(1 + \beta + \gamma) + \beta + \gamma - b\beta\right) = 0, \tag{16}$$

from which $\lambda_1 = -\alpha$ and $\lambda^2 + \lambda(1 + \beta + \gamma) + \beta + \gamma - b\beta = 0$ which are all negative since $\beta + \gamma > b\beta$.

2. We obtain the same characteristic polynomials as in case 1 and in this case $(1, 0, 0)$ is unstable since $b\beta > \beta + \gamma$, which violates the condition for the roots to all be negative.
3. The characteristic polynomial evaluated at the tumor dormant state is $\lambda^3 + a_2\lambda^2 + a_1\lambda + a_0 = 0$, where

$$a_2 = (2A\alpha + A\beta + C\beta - \alpha + \gamma + 1),$$
$$a_1 = \left(2A^2\alpha\beta - A\alpha\beta + C\alpha\beta - Ab\beta + 2A\alpha\gamma + C\beta\gamma + 2A\alpha + A\beta + C\beta - \alpha\gamma - \alpha + \gamma\right),$$
$$a_0 = -2A^2\alpha b\beta + 2A^2\alpha\beta + A\alpha b\beta + C\alpha\beta\gamma - A\alpha\beta + 2A\alpha\gamma + C\beta\gamma - \alpha\gamma,$$

and A, B, C are the coordinates of the tumor dormant state. Using Routh-Hurwitz stability criterion, this state will only be locally asymptotically stable if $a_0, a_1, a_2 > 0$ and $a_1 a_2 > a_0$.

Since the infected tumor free state is undesirable, the reverse of the condition $\beta + \gamma > b\beta$ is necessary for tumor eradication from body tissue. In other words $b\beta > \beta + \gamma$, that is, the product of the virus replication rate and their burst size should be greater than the sum of the burst size and virus replication rate. We also notice from (15) that

$$\lim_{\beta \to \infty} U = \lim_{b \to \infty} U = 0.$$

It is therefore evident that high virus replication rate β and burst size b lead to lower tumor cell concentrations. The solutions (15) involve many parameters and thereby giving rise to large expressions in the the conditions for its stability. It is therefore a difficult undertaking to infer biological implications from these conditions. Nevertheless we observe that virotherapy can only succeed in eliminating cancer from body tissue when the virus deactivation rate is very small or even zero and the virus replication rate very high.

We next analyze the model with both treatments. For a constant drug infusion rate ϕ, the system (2) has three steady states;

- Tumor free steady state:

$$\left(U = 0, I = 0, V = 0, C = \frac{\phi}{\psi}\right).$$

Here the tumor and viruses are cleared from body tissue by the coupled treatment and a fraction of the chemotherapeutic drug remains in body tissue. The eigenvalues of the Jacobian matrix evaluated at this state are

$$\lambda_1 = -\frac{\delta_0\phi - \alpha\psi}{\psi}, \lambda_2 = -\frac{\delta_1\phi + \psi}{\psi}, \lambda_3 = -\gamma, \lambda_4 = -\psi,$$

implying that this desirable state is locally asymptotically stable if $\delta_0\phi > \alpha\psi$. From this condition, in order to clear a tumor, the combination of the rate at which the drug kills the uninfected tumor cells and the drug infusion must be higher than the tumor growth rate and deactivation of the drug from body tissue.

- Infected tumor free state:

$$\left(U = 1 - \frac{\delta_0\phi}{\alpha\psi}, I = 0, V = 0, C = \frac{\phi}{\psi}\right).$$

In this state, the whole tumor is not cleared as a fraction of uninfected tumor cells remain and all the infected ones are cleared by the treatment combination. The eigenvalues evaluated at this state have huge expressions and the conditions for stability are not trivial. Using well estimated parameter values in Table 3.3 the eigenvalues of the Jacobian matrix evaluated at the infected tumor free state are 0.403, 8.13, and $2.598 \pm 2.418i$, implying that the infected tumor free state is unstable.

- Tumor dormant state:

$$\left(U = \frac{(\delta_1\phi + \psi)\gamma}{b\psi(b-1) - \delta_1\phi\beta}, I = \frac{\Gamma\gamma}{(\delta_1\phi - (b-1)\psi)\beta}, V = \Gamma, C = \frac{\phi}{\psi}\right),$$

where

$$\Gamma = \frac{\left(\beta\delta_0\delta_1\phi^2 - b\beta\delta_0\phi\psi - \alpha\beta\delta_1\phi\psi - \alpha\delta_1\gamma\phi\psi + \alpha b\beta\psi^2 + \beta\delta_0\phi\psi - \alpha\beta\psi^2 - \alpha\gamma\psi^2\right)}{(b-1)\beta^2\psi^2 + \alpha\beta\gamma\psi^2 - \beta^2\delta_1\phi\psi}.$$

It is a difficult undertaking to investigate the stability of this state without substituting parameter values because of the many terms involved.

Using the parameter values in Table 3.3, the eigenvalues are -0.031, -0.025, -1.01, -8.13 implying that this state is stable.

With the consideration of an exponential infusion function $\xi(t) = \phi \exp(-at)$, the equations (2) are first turned into an autonomous system of differential equations by letting $W = \phi \exp(-at)$. This system has three steady states:

- a tumor free state where all cell concentrations diminish to zero

$$(U = 0, I = 0, V = 0, C = 0, W = 0).$$

This state is unstable because the eigenvalues $-\gamma$, $-\psi$, $-a$, -1, and α are not all negative.

- a state where the tumor grows to its maximum size

$$(U = 1, I = 0, V = 0, C = 0, W = 0).$$

The characteristic polynomial evaluated at this state is (16) and this state is locally asymptotically stable if $\beta + \gamma > \beta\gamma$, otherwise it is unstable.

$$\left(U = \frac{\gamma}{(b-1)\beta}, I = \frac{(\alpha b - \alpha)\beta\gamma - \alpha\gamma^2}{(b-1)^2\beta^2 + (\alpha b - \alpha)\beta\gamma}, V = \frac{(\alpha b - \alpha)\beta - \alpha\gamma}{(b-1)\beta^2 + \alpha\beta\gamma}, C = 0, W = 0\right),$$

$b > 1$. The eigenvalues evaluated at this steady state are also big expressions and difficult to analyze analytically and extract conditions for stability. With the set of parameter values in Table (3.3), the eigenvalues are -0.1 , -8.13, 1.054, and $-0.014 \pm 0.085i$ implying that this state is stable.

Similarly, with $\xi(t) = \phi \sin^2(at)$ we change (2) into an autonomous system of equations by letting $W = \phi \sin^2(at)$. The autonomous system has six steady states:

- Tumor free state where all cell concentrations are wiped out of body tissue

$$(U = 0, I = 0, V = 0, C = 0, W = 0).$$

The eigenvalues evaluated at this state are $-\gamma$, $-\psi$, $-a$, -1, and α implying that it is unstable.

- A state where the tumor grows to its maximum size

$$(U = 1, I = 0, V = 0, C = 1, W = 0).$$

The condition for stability of this state are same as with the exponential drug infusion case, that is, the state is locally asymptotically stable if $\beta + \gamma > \beta\gamma$.

- Tumor free state where some concentration of the drug remains

$$\left(U = 0, I = 0, V = 0, C = \frac{\phi}{a\psi}, W = \frac{\phi}{a}\right).$$

This state is locally asymptotically stable if $\delta_0\phi > \alpha\psi$ and $\frac{1}{2} < \phi < 1$ because the eigenvalues evaluated at this state are

$$\frac{\delta_0\phi - \alpha\psi}{\psi}, -\frac{\delta_1\phi + \psi}{\psi}, -\frac{2\,(2\,a\phi(\phi - \phi)}{\sqrt{4\phi(1-\phi)}}, -\gamma, -\psi,$$

250 otherwise it is unstable.

- Infected tumor free state where all infected tumor cells are wiped but a certain proportion of the uninfected remains

$$\left(U = \frac{a\alpha\psi - \delta_0\phi}{a\alpha\psi}, I = 0, V = 0, C = \frac{\phi}{a\psi}, W = \frac{\phi}{a},\right), a\alpha\psi \geq \delta_0\phi.$$

- Drug free state where the chemotherapeutic drug is wiped out of body tissue and proportions of all the other cell concentrations remain

$$\left(U = \frac{\gamma}{(b-1)\beta}, I = \frac{(\alpha b - \alpha)\beta\gamma - \alpha\gamma^2}{(b-1)^2\beta^2 + (\alpha b - \alpha)\beta\gamma}, V = \frac{(\alpha b - \alpha)\beta - \alpha\gamma}{(b-1)\beta^2 + \alpha\beta\gamma}, C = 0, W = 0\right),$$

$b > 1$.

- Tumor dormant state

$$U = \frac{(\delta_1\phi + a\psi)\gamma}{(ab - a)\beta\psi - \beta\delta_1\phi}, I = \frac{\Gamma_2\gamma}{ab\psi - \delta_1\phi - a\psi}, V = \frac{\gamma_2}{a\psi}, C = \frac{\phi}{a\psi}, W = \frac{\phi}{a},$$

where

$$\Gamma_2 = \frac{a^2\alpha b\beta\psi^2 - ab\beta\delta_0\phi\psi - a\alpha\beta\delta_1\phi\psi - a\alpha\delta_1\gamma\phi\psi - a^2\alpha\beta\psi^2 - a^2\alpha\gamma\psi^2 + \beta\delta_0\delta_1\phi^2 + a\beta\delta_0\phi\psi}{(ab\beta\psi + a\alpha\gamma\psi - \beta\delta_1\phi - a\beta\psi)a\beta\psi}.$$

Table 1: **Dimensional parameter values.**

K	α	β	δ	γ	b	q	λ	δ_0	δ_1
10^6	0.206	0.001	0.5115	0.001	10	5	4.16	0.005	0.006
[28]	[28]	[28]	[28]	[28]	[29]	[11]	[11]	estimated	estimated

The conditions for stability for the last three states all depend on huge expressions from which it is hard to extract meaningful biological implications. This analysis however suggests that with both treatments and using a sinusoidal type infusion, the tumor can be eliminated from body tissue provided that the combination of the drug infusion rate and the lysis rate of the tumor is greater than the combination of the tumor growth rate and rate of drug loss.

4. Numerical simulations

4.1. Parameter values

In this section we use estimated parameter values in Table 3.3 to solve model equations (2). These parameter values were obtained from fitted experimental data for untreated tumors and virotherapy in mice [28]. A $1-3$ mm tumor lump contains about 10^5-10^9 tumor cells [31]. Therefore we considered a carrying capacity of 10^6 cells per unit volume. Several invivo experimental tumor growth models estimate the intrinsic rate of growth to be $0.1-0.3$ [32]. We consider the number of viruses produced per day b to be in the range $10-1000$ (see Ref [29]). We consider the rate of drug infusion q to be 5 mg/day and the decay rate λ to be 4.17 mg/day, values which conform to cancer pharmokinetic studies (see eg. Refs[23, 24]). Since infected tumor cells multiplication is enhanced by the oncolytic virus replication, the tumor cells lysis δ_1 is considered to be grater that for uninfected tumor cells δ_0 (see Ref [11]).

4.2. Results

We present numerical simulations firstly with only either treatments and with both treatments implemented. In all our simulations, unless stated oth-

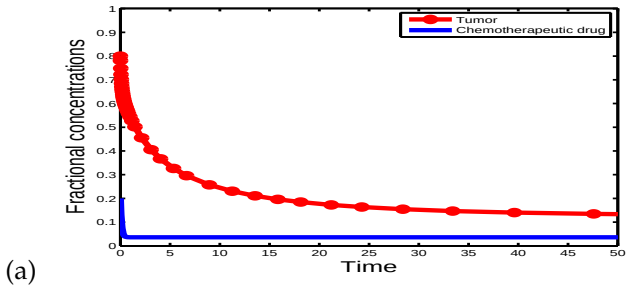

(a)

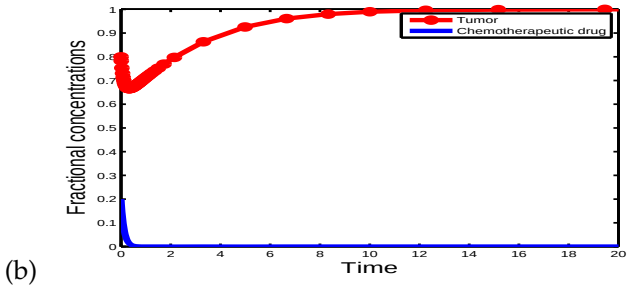

(b)

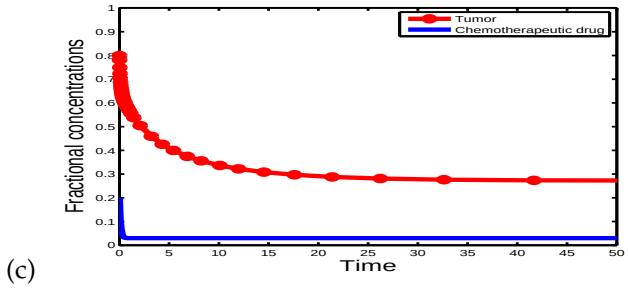

(c)

Figure 1: **Solutions of the model without virotherapy (6) showing a variation of fractional concentrations with time, using (a) a constant , (b) an exponential, and (c) a sinusoidal drug infusion. The intial cell concentrations are $U_0 = 0.8$, and $C_0 = 0.2$.**

erwise, we considered initial concentrations $U_0 = 1$, $I_0 = 0$, $V_0 = 0.1$, and $C_0 = 0.1$ with a high fractional untreated tumor cell count to necessitate clinical intervention. The equations were integrated using a Runge Kutta fourth order scheme and implemented in MATLAB. It is worth noting that the scale for the time and cell concentrations is respectively 1 unit $\approx$ 2 days and 1 unit $= 10^6$ number of cells.

Figure 1 shows numerical solutions of the model (6). The figure shows that a constant and sinusoidal forms of drug infusion are more effective in

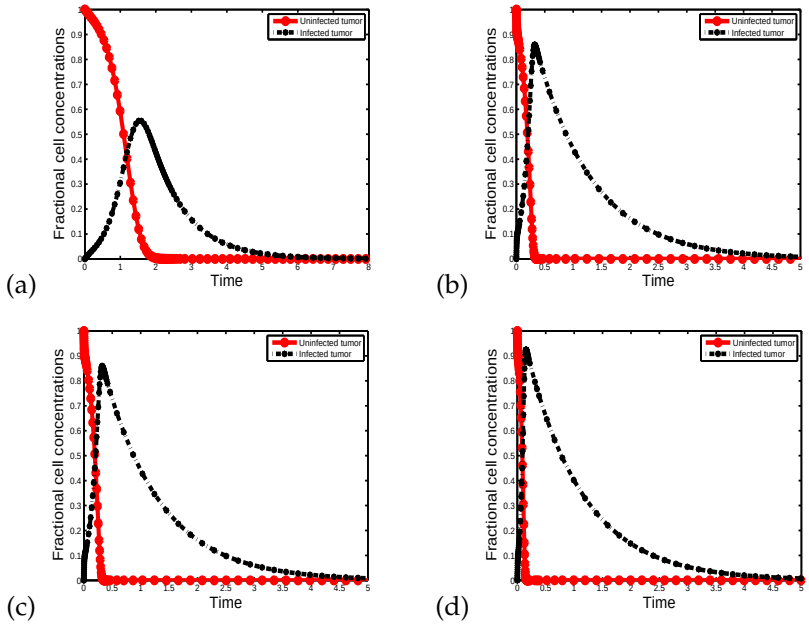

Figure 2: **Solutions of the model (14) without chemotherapy showing a variation of fractional cell concentrations with non-dimensional time using low and high values of the virus replication rate β and burst size b, that is, (a) $\beta = 10^{-6}$, $b = 10$, (b) $\beta = 10^{-3}$, $b = 10$, (c) $b = 10$, $\beta = 10^{-6}$, and (d) $b = 100$, $\beta = 10^{-6}$.**

reducing the tumor concentration as compared to an exponential drug infusion. These numerical solutions agree with the analytical results we earlier obtained in the previous sections; that chemotherapy on its own may not clear all tumor cells in body tissue, the tumor grows to its maximum size and the drug concentration decays to zero with the use of an exponential infusion. We noted in Section 3 that total tumor clearance from body tissue can possibly be achieved if $\delta_0\phi > \alpha\psi$. The parameter values we used however do not conform to this condition.

Figure 2 shows the dynamics of the model without chemotherapy. It is clear from this figure that virotherapy alone could possibly deplete all tumor cells from body tissue provided that the virus replication rate is high. It is worth noting that a high virus burst size also leads to similar results, that is to say, the higher the virus burst rate, the higher the chances of clearing tumor

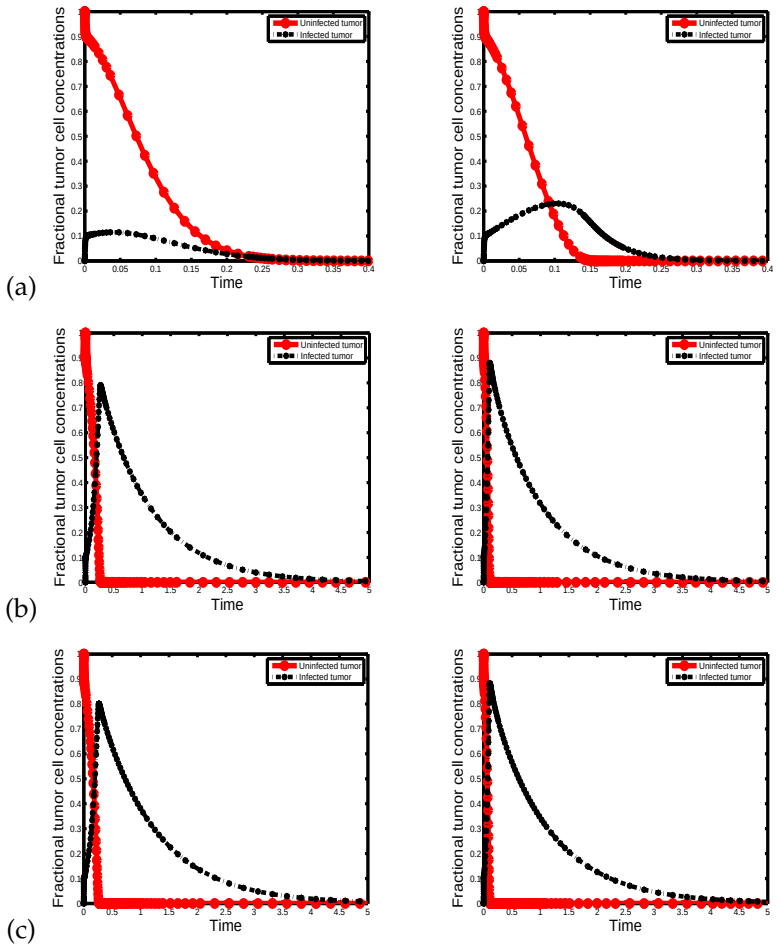

Figure 3: **Solutions of the model (2) with both treatments showing a variation of fractional cell concentrations with time using low and high non-dimensionalized values of the virus burst size, that is,** 15, 25 **and with diferent drug infusion functions, that is, (a) constant, (b) exponential and (c) (sinusoidal).**

cells from body tissue (also see [16]). Figures 2(a) and (b) show a variation of the fractional tumor and virus concentrations against time for different values of the virus replication rate. We notice that with a small virus replication rate for example $\beta = 10^{-6}$, it takes a longer time to clear the tumor cells. Figures 2(b) and (c) show a variation of the fractional concentrations with two different burst sizes. From these figures we notice that when $b = 10$, it takes about

10 days to reduce the whole tumor cell concentrations to zero while it takes only about 5 days with $b = 100$ implying that a high virus burst size yields a quick recovery with virotherapy treatment. These numerical intimations concur with the analytical results we established in Sub-section 3.3.

Figure 3 displays the dynamics of the model (2) with both treatments. The numerical results are similar to those of Figure 2, only that with both treatments it takes a shorter time to bring the tumor cell concentrations to zero. High values of the virus replication rate and burst size lead to tumor clearance in a shorter time period. Both figures 2 and 3 show that an increase in the virus multiplication rate and burst size increase the infected tumor cells concentration. For example comparing figures 3(a) and (b) the number of infected tumor cells were about 0.15×10^6 when $b = 15$ and this increased to 0.35×10^6 when $b = 25$.

5. Conclusion

The aim of this study was to construct a mathematical model to simulate the outcome of using both chemotherapy and virotherapy in treating cancer, to investigate the effect of three different drug infusion methods, and to compare the efficacy of using chemotherapy and virotherapy individually.

We constructed a mathematical model in the form of non-linear and non-autonomous first order ordinary differential equations. We firstly validated the model's plausibility by proving existence, positivity and boundedness of the solutions. We analysed the model with each of the treatments and for each of the infusion functions. We considered the model with both treatments. We found exact solutions where possible and determined the behavior of these solutions. We investigated the stability of time invariant solutions to determine the conditions under which a tumor free situation may be achieved. We simulated the model using a Runge-kutta forth order scheme. The numerical simulations tallied with the analytical predictions. The model analysis suggested the following: A tumor can grow to its maximum size in a case where

there is no treatment and chemotherapy alone is capable of clearing tumor cells in body tissue provided that the combination of the drug induced lysis of the tumor and the drug infusion rate is greater than the combination of drug decay and tumor growth. That a constant and periodic drug infusions are more efficacious than the exponential induction method which biologically suggests that a repeated-dose regimen in which intravenous injections are given at regular intervals or putting a patient on an intravenous injection so that a drug is continuously infused in body tissue is more efficient than giving a bolus infusion. The model analysis also suggested that successful virotherapy is highly dependent on a large virus burst size and a higher virus replication rate and that with the use of both chemotherapy and virotherapy, a tumor may in less than a month be cleared from body tissue. Lastly, successful chemovirotherapy depends on the virus burst size and replication rate, chemotherapeutic drug lysis, infusion and decay rates, and the method of drug infusion.

Biologically, the reduction of a tumor to undetectable levels in less than a week is unrealistic in comparison to existing clinical and research studies (see e.g. [33]). The duration of cancer treatment depends on several factors including the type of cancer being treated and the patient cells' characteristics. This makes it hard to predict the time period to clear a tumor in body tissue. Moreover, a tumor may be reduced to insignificant levels but later reappear [34]. Nevertheless, our study shows that chemovirotherapy is highly likely to bring the tumor to undetectable levels in a short time period.

Conflict of interests

The authors declare that there is no conflict of interests regarding the publication of this manuscript.

Acknowledgments

We are grateful for financial support from the University of KwaZulu-Natal.

[1] V. Groh, J. Wu, C. Yee, and T. Spies, *Tumour-derived soluble MIC ligands impair expression of NKG2D and t-cell activation.*, J. Nature, **409.6908** (2002), 734–738.

[2] M.I.S. Costa, J.L. Bolderini, and R.C. Bassanezi, *Optimal chemotherapy: a case study with drug resistance, saturation effect, and toxicity*, J. Mathematical Medicine and Biology, **11.1** (1994), 45–59.

[3] "World health organization," Cancer report, 2014. Available from: `www.bmj.com/content/348/bmj.g1338/`. Accessed on 14.03.2016.

[4] E. Kelly, and S.J. Russel, *History of oncolytic viruses: genesis to genetic engineering*, J. Molecular Theory, **15.4** (2007), 651–659.

[5] S.J. Russel, K.W. Pengl, and J. C. Bell, *Oncolytic virotherapy*, J. Nature Biotechnology, **30.7** (2012), 1–13.

[6] T.C. Liau, E. Galanis, and D. Kirn, *Clinical trial results with oncolytic virotherapy: a century of promise, a decade of progress*, J. Nature Clinical Practice Oncology, **4.2** (2007), 101–117.

[7] J. Malinzi, P. Sibanda, and H.M. Mambili-Mamoboundou, *Analysis of virotherapy in solid tumor invasion*, J. Mathematical Biosciences, **2**263 (2015), 102–110.

[8] A. Nguyen, L. Ho, and Y. Wan, *Chemotherapy and oncolytic virotherapy: advanced tactics in the war against cancer*, Frontiers in oncology, **4** (2014), 1-10.

[9] P.K. Ottolino, J.S. Diallo, B.D. Lichty, J.C. Bell, and J.A. McCart, *Intelligent design: combination therapy with oncolytic viruses*, J. Molecular therapy, **18.2** (2010), 251–263.

[10] M.J. Bartkowski, et al, (2012) *Chemotherapy of viral infections*. Edited by P.E. Came, and L.A. Caliguiri. Vol. 61. Springer Science & Business Media.

[11] S.T.R. Pinho, D.S. Rodrigues, and P.F.A. Mancera, *A mathematical model of chemotherapy response to tumor growth*, J. Canadian Applied Math Quarterly, **4.19** (2011), 369–384.

[12] L. de Pillis, K. R.Fister, W.Gu, et al. *Mathematical Model Creation for Cancer Chemo-Immunotherapy*, J. Computational and Mathematical Methods in Medicine, **10.3** (2009), 165-184.

[13] W. Liu and H.I. Freedman, *A mathematical model of vascular tumour treatment by chemotherapy*, J. Mathematical and computer modeling, **42.9** (2005), 1089–1112.

[14] S.T.R. Pinho, H.I. Freedman, and F.K. Nani, *A chemotherapy model for the treatment of cancer with metastasis*, J. Mathematical and computer modeling, **36.7** (2002), 773–803.

[15] J. R. Ursher, *Some mathematical models for cancer chemotherapy*, J. Computers and Mathematics with Applications, **28.9** (1994), 73–80.

[16] J.P. Tian, *The replicability of oncolytic virus: defining conditions in tumor virotherapy*, J. Mathematical biosciences and engineering, **8** (2011), 841–860.

[17] Y. Wang, J.P. Tian, and J. Wei *Limit cycle: A defining process in oncolytic virotherapy*, J. Applied Mathematical Modelling, **37.8** (2013), 5962–5978.

[18] D. Wordaz, *Viruses as antitumor weapons defining conditions for tumor remission*, J. Cancer Research, **61.8** (2001), 3501–3507.

[19] A.S. Novozhilov, F.S. Berezovskaya, E.V. Koonin, and G.P . Karev, *Mathematical modeling of tumor therapy with oncolytic viruses: regimes with complete tumor elimination within the framework of deterministic models*, J. Biology Direct, **1.6** (2006), 1–18.

[20] M. Agarwal, and A.S. Bhadauria, *Mathematical modeling and analysis of tumor therapy with oncolytic virus*, J. Applied Mathematics, **2.1** (2011), 131–140.

[21] R. W. Carlson, and B. I. Sikic, *Continuous infusion or bolus injection in cancer chemotherapy*, Annals of internal medicine, **99.6** (1983), 823–833.

[22] M. Yoshimori, H. Ookura, Y. Shimada, T. Yoshida, N. Okazaki, M. Yoshino, and D. Saito, *Continuous infusion of anti-cancer drug with balloon infusor*, [Article in Japanese], **15.11** (1988), 3121–3125.

[23] G.J. Bostol, and S. Patil, *Carboplatin in clinical stage I seminoma: Too much and too little at the same time*, J. Clinical Oncology, **29.8** (2011), 949–952.

[24] R.T.D. Oliver, G.M. Mead, G.J. Rustin, J.K. Roffe, N. Aass, R. Coleman, and S.P. Stenning, *Randomized trial of carboplatin versus radiotherapy for stage I seminoma: mature results on relapse and contralateral testis cancer rates in MRC TE19/EORTC 30982 study (ISRCTN27163214)*, J. Clinical Oncology, **29.8** (2011), 957–962.

[25] M. Bertau, E. Mosekilde, and H.V. Westerhoff, (2008) *Biosimulation in drug development*. John Wiley & Sons.

[26] S.D. Undevia, A.G. Gomez, and M.J. Ratain, *Pharmacokinetic variability of anticancer agents*, J. Nature Reviews Cancer, **5.6** (2005), 447–458.

[27] B.J. Schroers, (2011) *Ordinary differential equations: a practical guide*. Cambridge University Press.

[28] Z. Bajzer, T. Carr, K. Josic, S.J. Russell, D. Dingli, *Modeling of cancer virotherapy with recombinant measles viruses*, J. Journal of Theoretical Biology, **252.1** (2008), 109–122.

[29] T.D. Brock (1990) *The emergence of bacterial genetics*. Cold Spring Harbor, NY: Cold Spring Harbor Laboratory Press.

[30] S. Wiggins, (1990) *Introduction to non-linear dynamical systems and chaos*. New york, NY: Springer-Verlag.

[31] J.S. Spratt, J. S Meyer, and J. A. Spratt *Rates of growth of human solid neoplasms: Part I*, J. Surgical oncology, **60** (1979), 137–146.

[32] S. Benzekry, C. Lamont, A. Beheshti, A. Tracz, and J.M.L. Ebos *"Classical Mathematical Models for Description and Prediction of Experimental Tumor"*, 2014.

[33] S. Pam, Breast cancer treatment and recovery times based on diagnosis, 2015. Available from: `http://breastcancer.about.com/od/whattoexpect/a/Breast-Cancer-Treatment-Recovery-Times_2.htm`.

[34] D. Wordaz, and A.A. Jansen, *A dynamical perspective of CTL cross-priming and regulation:implications for cancer immunology*, J. Immunology, **86** (2003), 213–227.

Chapter 5

Spatiotemporal dynamics of chemovirotherapy

This chapter is an extension of the study in Chapter 4. The model developed to simulate chemovirotherapy is extended to incorporate diffusion and thereby capturing the spatial cell distributions. Steady state solutions for the homogeneous part of the model are obtained and their stability is investigated. Model solutions are obtained numerically using *pdepe* in Matlab and a multi-domain monomial collocation method.

Noname manuscript No.
(will be inserted by the editor)

Spatiotemporal dynamics of chemovirotherapy

Joseph Malinzi · Precious Sibanda · Hermane Mambili-Mamboundou.

Received: date / Accepted: date

Abstract Theoretical and experimental studies have indicated that the combination of chemotherapeutic drugs and oncolytic viruses to eradicate tumours from body tissue is less toxic than traditional cancer treatments. For this reason chemovirotherapy could be an efficacious cancer treatment. Nevertheless, the therapy interaction dynamics and drug-virus combination factors necessary for successful treatment are poorly understood. A spatiotemporal mathematical model, in the form of parabolic nonlinear partial differential equations, is constructed to simulate avascular solid tumour growth, under chemovirotherapy, in a two dimensional spatial domain. The homogeneous model is analyzed by investigating the stability of its time invariant solutions. The heterogeneous model, in one dimension, is solved using factorization of differential operators to obtain analytical traveling wave solutions. Finally, numerical solutions are determined using pdepe, a finite element based method in Matlab, and a multi-domain monomial collocation method. The numerical results show both the chemotherapeutic drug and the virus attacking the tumour from outside the body tissue, and the tumour densities getting depleted from body tissue with time. The traveling wave solutions point out the tumour growth rate, diffusivities, and virus and drug decay rates as the most critical parameters in chemovirotherapy treatment.

Joseph Malinzi
School of Mathematics, Statistics, and Computer Science, University of KwaZulu-Natal, Private Bag X01, Scottsville, Pietermaritzburg, 3209 South Africa
Tel.: +27-033-2606587
E-mail: Malinzij@ukzn.ac.za

Precious Sibanda
School of Mathematics, Statistics, and Computer Science, University of KwaZulu-Natal, Private Bag X01, Scottsville, Pietermaritzburg, 3209 South Africa
Tel.: +27-033-2605626
E-mail: sibandap@ukzn.ac.za

Hermane Mambili-Mamboundou
School of Mathematics, Statistics, and Computer Science, University of KwaZulu-Natal, Private Bag X01, Scottsville, Pietermaritzburg, 3209 South Africa
Tel.: +27-033-2605626
E-mail: Mambilimamboundou@ukzn.ac.za

Keywords Chemotherapy · Virotherapy · Chemovirotherapy · Reaction-diffusion equations · Traveling wave analysis · Numerical simulations

Mathematics Subject Classification (2000) 35Q92 · 35Q92

1 Introduction

Total elimination of a tumour from body tissue using virotherapy requires high dozes of oncolytic viruses which may be lethal to normal tissue cells (Toyoizumi et al, 1999). Using chemotherapeutic agents can counter balance these viral induced toxins thus eliminating the tumour without harm to body tissue (Aghi et al, 2006; Alonso et al, 2007; Siurala et al, 2015).

Chemovirotherapy is a cancer treatment under clinical trials. It combines both chemotherapy and virotherapy treatments. The essence of using this combination is that oncolytic viruses directly lyse tumour cells or deliver genes that make them more susceptible to chemotherapeutic drugs. Some oncolytic viruses used in chemotherapeutic trials have reached phase three out of five of clinical trials and may therefore soon be released to the general public for use, for example, the reovirus for treating head and neck cancer (Binz et al, 2015). Pre-clinical and experimental studies, for example (Binz et al 2015; Ungerechts et al 2007; Bossow et al 2011; Zaoui et al 2012; Tusell Wennier et al 2012; Shafren et al 2004; Kumar et al 2008; Liu et al 2007), have indicated that this type of treatment is capable of eliminating tumour cells with no harm extended to body tissue. Nevertheless, there is a dire need for further studies to describe and characterize the tumour-virus-chemotherapeutic drug interactions.

Mathematical modeling can be an avenue for describing the chemovirotherapy dynamics and determining the drug and virus combination factors, in form of parameters, which are most vital in tumour clearance. The outcome of chemovirotherapy treatment can also be predicted using mathematical modeling. We construct a spatiotemporal model to consider movement and spatial distribution of cells with the aim of investigating the outcome of chemovirotherapy treatment and determining the drug and virus combination factors, in the form of parameters, which are most critical during chemovirotherapy treatment.

2 Model construction

We develop a model that describes an avascular solid tumour growth under chemotherapy and virotherapy treatments in a two dimensional spatial domain. We consider tissue composition with the following variables: densities of uninfected tumour cells $U(r,t)$, infected tumour cells $I(r,t)$, a virus $V(r,t)$, and a chemotherapeutic agent $C(r,t)$, where $r \in [0,L]$ is the radius of the tumour at a time $t \in [0,\infty)$. We consider an avascular tumour, with a necrotic core containing dead cells with a radius L_0, in a radially geometric setting with a fixed radius L. We assume that the tumour has grown to its maximum size and it is just prior to angiogenesis, an assumption to necessitate

clinical intervention. We model the movement of cells using the Kolmogorov equation (see Ma and Fuchssteiner 1996), a linear diffusion model used for simulating cell movement.

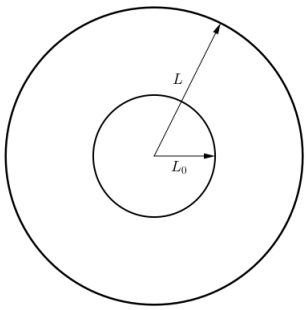

Fig. 1 Representation of the tumour geometry. The tumour radius is L, a size beyond which it mestasizes, with a necrotic core of radius L_0

Figure 1 is a geometrical representation of the tumour with radius L and a necrotic core of size L_0.

Tumour density, $U(r,t)$ and $I(r,t)$

The tumour is considered to grow logistically at an intrinsic rate a per day and its carrying capacity K is taken to be 10^6 cells. The infected tumour density increases as the oncolytic viruses multiply in the uninfected tumour cells and burst. We consider the virus replication into the tumour to be of Michaelis-Menten form (see (Wagner, 1973; Malinzi et al, 2015)). We also assume that the drug kills the tumour cells in a concentration dependent manner (Fornari et al, 1994), that is, the drug cytoxicity increases with increasing drug concentration, asymptotically approaching its maximum. The uninfected and infected tumour cell densities are governed by the reaction-diffusion equations:

$$\frac{\partial U}{\partial t} = D_1 \frac{1}{r^2}\frac{\partial}{\partial r}\left[r^2 \frac{\partial U}{\partial r}\right] + aU\left(1 - \frac{U+I}{K}\right) - \frac{\beta UV}{K_u + U} - \frac{\delta_0 UC}{K_c + C}, \tag{1}$$

$$\frac{\partial I}{\partial t} = D_2 \frac{1}{r^2}\frac{\partial}{\partial r}\left[r^2 \frac{\partial I}{\partial r}\right] + -\frac{\beta UV}{K_u + U} - \frac{\delta_1 IC}{K_c + C} - \delta I, \tag{2}$$

where D_1 and D_2 are diffusion coefficients of the uninfected and infected tumour densities respectively. β is the virus multiplication rate measured per day per cells, $\delta_0 UC/(K_c + C)$ and $\delta_1 IC/(K_c + C)$ are receptively the chemotherapeutic drug responses to the uninfected and infected tumour cells where δ_0 and δ_1 are respectively the lysis induced rates measured per day. k_u and K_c are respectively Michaelis-Menten constants which relate to lysis rates when the virus and the drug are half-maximal.

Virus density, $V(r,t)$

We consider a virus production $b\delta I$ where b is the virus burst size measured per day and δ is the infected tumour cell death rate measured per day. The virus gets deactivated in body tissue at a rate γ per day. We consider that the virus is locally delivered and diffuses into the tumour. The non-linear differential equation (3) describes the virus density:

$$\frac{\partial V}{\partial t} = D_3 \frac{1}{r^2}\frac{\partial}{\partial r}\left[r^2 \frac{\partial V}{\partial r}\right] + b\delta I - \frac{\beta U V}{K_u + U} - \gamma V, \tag{3}$$

where D_3 is the virus diffusion constant.

Drug density, $C(r,t)$

We consider that the chemotherapeutic drug is administered as a single bolus and its concentration in the blood stream exponentially decays just as in (Stamper et al, 2010). We model penetration of the drug into the tumour using reaction diffusion. The drug density is therefore governed by the reaction diffusion equation:

$$\frac{\partial C}{\partial t} = D_4 \frac{1}{r^2}\frac{\partial}{\partial r}\left[r^2 \frac{\partial C}{\partial r}\right] + C_b(t) - \lambda C, \tag{4}$$

where D_3 is the chemotherapeutic drug diffusion coefficient, $C_b(t) := \sigma e^{(-k_c t)}$ is the prescribed drug plasma level in the blood stream, and λ is the natural drug density decay measured per day. The constant σ is the initial drug concentration and k relates to the chemotherapy drug half life $T_{1/2}$, which is roughly one day (Ribba et al, 2005), and is given by

$$k = \frac{\ln 2}{T_{1/2}}.$$

3 Initial and boundary conditions

We assume that the uninfected tumour density in the necrotic core is zero and that it increases towards the outside of the tumour, that is, in the quiescent and proliferating zones (see for example Malinzi et al 2015). We assume that the initial drug and virus densities lie on the sheath of the tumour in small concentrations. We assume that there is no flux at the boundary $r = 0$ for all cell densities because of the geometry considered. At the boundary $r = L$, we assume no flux conditions for the infected and uninfected tumour cells, and the virus density. We consider that the chemotherapeutic drug diffuses into the tumour through the outside tumour boundary $r = L$ whose permeability is denoted ρ and that the virus density at the boundary is determined by the tumour-virus interactions. With these assumptions we close off the system (1-4)

with the following initial and boundary conditions:

$$\left.\begin{aligned} U(r,0) &= \begin{cases} 0, & 0 \le r \le L_0 \\ U_0\left(1-e^{-100(r-L_0)^2}\right), & L_0 \le r \le L, \end{cases} \\ I(r,0) &= 0,\ r \in [0,L] \\ V(r,0) &= \begin{cases} V_0, & r = L \\ 0, & \text{elsewhere}, \end{cases} \\ C(r,0) &= \begin{cases} C_0, & r = L \\ 0, & \text{elsewhere}, \end{cases} \end{aligned}\right\} \tag{5}$$

$$\left.\begin{aligned} &\left.\frac{\partial U}{\partial r}\right|_{r=0} = \left.\frac{\partial I}{\partial r}\right|_{r=0} = \left.\frac{\partial V}{\partial r}\right|_{r=0} = \left.\frac{\partial C}{\partial r}\right|_{r=0} = 0, \\ &\left.\frac{\partial U}{\partial r}\right|_{r=L} = \left.\frac{\partial I}{\partial r}\right|_{r=L} = 0,\ D_3\left.\frac{\partial V}{\partial r}\right|_{r=L} = 0,\ D_4\frac{\partial C}{\partial r} + \rho C\Big|_{r=L} = 0 \end{aligned}\right\} \tag{6}$$

where L_0 is the radius of the necrotic core.

Model re-scaling

The system (1-4) is re-scaled by setting $\bar{U} = U/K$, $\bar{I} = I/K$, $\bar{V} = V/V_0$ and $\bar{C} = C/C_0$ with $\bar{t} = t/t_0$ and $\bar{r} = r/L$ where $L = 1$ mm and $t_0 = r_0/D_1$. The parameters become

$$\phi_i = D_i t_0,\ i = 1,2,3,4,\ \ \alpha = a t_0,\ \bar{\beta} = \frac{\beta V_0 t_0}{U_0},\ \bar{\delta_0} = \delta_0 C_0 t_0,\ \ K_u = \frac{k_u}{U_0},$$

$$K_c = \frac{k_c}{C_0},\ \ \bar{\delta_1} = \delta_1 C_0 t_0,\ \bar{b} = \frac{bK}{V_0},\ \bar{\gamma} = \gamma t_0,\ \bar{\sigma} = \frac{\sigma t_0}{C_0},\ \mu = \lambda t_0,\ \ \phi_5 = \frac{D_4}{r_0}.$$

Dropping the bars for notationality simplicity and taking the necrotic core to be of radius 0.2mm (see Ref García-García et al 2007) gives a re-scaled model defined by the following parabolic system of non-linear reaction diffusion equations:

$$\frac{\partial U}{\partial t} = \phi_1 \frac{1}{r}\frac{\partial}{\partial r}\left[r^2 \frac{\partial U}{\partial r}\right] + \alpha U(1-U-I) - \frac{\beta U V}{K_u + U} - \frac{\delta_0 U C}{k_c + C}, \tag{7}$$

$$\frac{\partial I}{\partial t} = \phi_2 \frac{1}{r^2}\frac{\partial}{\partial r}\left[r^2 \frac{\partial I}{\partial r}\right] + \frac{\beta U V}{K_u + U} - \frac{\delta_1 I C}{k_c + C} - \delta I, \tag{8}$$

$$\frac{\partial V}{\partial t} = \phi_3 \frac{1}{r^2}\frac{\partial}{\partial r}\left[r^2 \frac{\partial V}{\partial r}\right] + bI - \frac{\beta U V}{K_u + U} - \gamma V, \tag{9}$$

$$\frac{\partial C}{\partial t} = \phi_4 \frac{1}{r^2}\frac{\partial}{\partial r}\left[r^2 \frac{\partial C}{\partial r}\right] + C_b(t) - \mu C, \tag{10}$$

with the initial and boundary conditions (11) & (12).

$$\left.\begin{aligned} U(r,0) &= \begin{cases} 0, & 0 \le r \le 0.2 \\ 1 - e^{(-100r - L_0)^2}, & 0.2 \le r \le 1, \end{cases} \\ I(r,0) &= 0,\ r \in [0,1], \\ V(r,0) &= \begin{cases} 1, & r = 1 \\ 0, & \text{elsewhere}, \end{cases} \\ C(r,0) &= \begin{cases} 1, & r = 1 \\ 0, & \text{elsewhere}, \end{cases} \end{aligned}\right\} \tag{11}$$

and

$$\left.\begin{aligned} &\left.\frac{\partial U}{\partial r}\right|_{r=0} = \left.\frac{\partial I}{\partial r}\right|_{r=0} = \left.\frac{\partial V}{\partial r}\right|_{r=0} = \left.\frac{\partial C}{\partial r}\right|_{r=0} = 0, \\ &\left.\frac{\partial U}{\partial r}\right|_{r=1} = \left.\frac{\partial I}{\partial r}\right|_{r=1} = 0,\ \phi_3 \left.\frac{\partial V}{\partial r} + \rho V\right|_{r=1} = 0,\ \phi_5 \left.\frac{\partial C}{\partial r} + \rho C\right|_{r=1} = 0. \end{aligned}\right\} \tag{12}$$

Results

Homogeneous model analysis

Firstly, we present results for the model analysis without spatial dynamics, that is, model predictions of the cell densities at different time periods without the consideration of space. Without spatial effects the model equations (7-10) become

$$\dot{U}(t) = \alpha U(1 - U - I) - \frac{\beta UV}{K_u + U} - \frac{\delta_0 UC}{k_c + C}, \tag{13}$$

$$\dot{I}(t) = \frac{\beta UV}{K_u + U} - \frac{\delta_1 IC}{k_c + C} - \delta I, \tag{14}$$

$$\dot{V}(t) = bI - \frac{\beta UV}{K_u + U} - \gamma V, \tag{15}$$

$$\dot{C}(t) = C_b(t) - \mu C. \tag{16}$$

The Equations (13-15) are highly non-linear and difficult to solve. Equation (16) is a first order linear differential equation and can be solved using a suitable integrating factor to get

$$C(t) = Re^{-(\mu t)} - \left(\frac{\sigma}{\mu - k_c}\right) e^{-(k_c t)},\ R = C_0 + \frac{\sigma}{k_c - \mu},\quad \lim_{t \to \infty} C(t) = 0. \tag{17}$$

Equation (17) shows that with time the drug concentration is depleted from body tissue. By equating (13-16) to zero we obtain the following steady states to which the cell concentrations may converge after a long time period; the tumour can be eradicated from body tissue, namely, $U = 0, I = 0, V = 0, C = 0$ or it can grow to its

maximum size, that is, $U=1, I=0, V=0, C=0$ or it may co-exist with the virus, that is,

$$\left.\begin{aligned} U &= \frac{\delta\gamma k_u}{\beta(b-\delta)-\delta\gamma}, \\ I &= \frac{(\delta\gamma k_u - b\beta + \beta\delta + \delta\gamma)\alpha\gamma k_u}{(\alpha\gamma k_u + b\beta - \beta\delta - \delta\gamma)(\beta\delta + \delta\gamma - b\beta)}, \\ V &= \frac{(\delta\gamma k_u - b\beta + \beta\delta + \delta\gamma)\alpha(b-\delta)k_u}{(\alpha\gamma k_u + b\beta - \beta\delta - \delta\gamma)(\beta\delta - \delta\gamma - b\beta)}. \end{aligned}\right\} \tag{18}$$

The characteristic polynomial of the Jacobian matrix evaluated at the tumour free steady state has both positive and negative real roots, that is, $-\gamma, -\mu, -k, \alpha, -1$. This shows that the tumour free state is unstable and therefore unattainable. The other states are stable or unstable depending on the parameter values, mostly K_u, K_c, and β. This implies that without the consideration of space, the homogeneous model predicts that, the tumour may either co-exist with the virus or it may grow to its maximum size depending on several conditions as defined by the parameters in (18). Equation (18) shows that with time, except for the chemotherapeutic drug, all tumour densities co-exist in body tissue. It also shows that high values of the virus burst size b and the virus replication β lead to lower tumor densities.

3.1 Traveling wave solutions

In this section we employ the factorization of differential operators method (Malinzi et al, 2015; Rosu and Cornejo-Pérez, 2005; Cornejo-Pérez, 2008) to determine traveling wave solutions to the system (7-10) in one dimension. This method leads to particular solutions of Lienard type equations (Rosu and Cornejo-Pérez, 2005; Cornejo-Pérez, 2008). Using the transformation $\zeta = r - ct$, where c is the propagation speed, the equations (7-10), in one dimension, are transformed to

$$\frac{d^2U}{d\zeta^2} + G_1(U,I,V,C)\frac{dU}{d\zeta} + F_1(U,I,V,C) = 0, \tag{19}$$

$$\frac{d^2I}{d\zeta^2} + G_2(U,I,V,C)\frac{dI}{d\zeta} + F_2(U,I,V,C) = 0, \tag{20}$$

$$\frac{d^2V}{d\zeta^2} + G_3(U,I,V,C)\frac{dV}{d\zeta} + F_3(U,I,V,C) = 0, \tag{21}$$

$$\frac{d^2C}{d\zeta^2} + G_4(U,I,V,C)\frac{dC}{d\zeta} + F_4(U,I,V,C) = 0, \tag{22}$$

where

$$
\begin{aligned}
G_1 &= \frac{c}{\phi_1}, \quad F_1 = c_1 U\left(\alpha(1-U-I) - \frac{\beta V}{K_u+U} - \frac{\delta_0 C}{k_c+C}\right),\\
G_2 &= \frac{c}{\phi_2}, \quad F_2(x,y,z) = c_2 I\left(\frac{\beta U V}{I(K_u+U)} - \frac{\delta_1 C}{k_c+C} - \delta\right),\\
G_3 &= \frac{c}{\phi_3}, \quad F_3(x,y,z) = c_3 V\left(\frac{bI}{V} - \frac{\beta U}{K_u+U} - \gamma\right),\\
G_4 &= \frac{c}{\phi_4}, \quad F_3(x,y,z) = c_4 C\left(\frac{C_b(t)}{C} - \mu\right),
\end{aligned}
$$

where $c_i = 1/\bar{\phi_i}$, $i = 1,2,3,4$.

The factorization of Equations (19-22) gives sixteen possible systems of first order differential equations

$$[D-\psi_{11}(U,I,V,C)][D-\psi_{12}(U,I,V,C)]U = 0, \tag{23}$$
$$[D-\psi_{21}(U,I,V,C)][D-\psi_{22}(U,I,V,C)]I = 0, \tag{24}$$
$$[D-\psi_{31}(U,I,V,C)][D-\psi_{32}(U,I,V,C)]V = 0, \tag{25}$$
$$[D-\psi_{41}(U,I,V,C)[D-\psi_{44}(U,I,V,C)]C = 0, \tag{26}$$

where $D = \frac{d}{d\zeta}$. Comparing (19-22) and (23-26) implies that

$$G_1 = -\left(\psi_{11}+\psi_{12}+\frac{\partial\psi_{12}}{\partial U}U\right), \tag{27}$$
$$G_2 = -\left(\psi_{21}+\psi_{22}+\frac{\partial\psi_{22}}{\partial I}I\right), \tag{28}$$
$$G_3 = -\left(\psi_{31}+\psi_{32}+\frac{\partial\psi_{32}}{\partial V}V\right), \tag{29}$$
$$G_4 = -\left(\psi_{41}+\psi_{32}+\frac{\partial\psi_{42}}{\partial C}C\right), \tag{30}$$

and

$$F_1 = \psi_{11}\psi_{12}U,\ F_2 = \psi_{21}\psi_{22}I,\ F_3 = \psi_{31}\psi_{32}I,\ F_4 = \psi_{41}\psi_{42}C. \tag{31}$$

Choosing ψ_{ij} in such a way that

$$
\begin{aligned}
\psi_{11} &= \frac{1}{\gamma_1}\left(\alpha(1-U-I) - \frac{\beta V}{K_u+U} - \frac{\delta_0 C}{k_c+C}\right), \quad \psi_{12} = \gamma_1,\\
\psi_{21} &= \frac{1}{\gamma_2}\left(\frac{\beta U V}{I(K_u+U)} - \frac{\delta_1 C}{k_c+C} - \delta\right), \quad \psi_{22} = \gamma_2,\\
\psi_{31} &= \frac{1}{\gamma_3}\left(\frac{bI}{V} - \frac{\beta U}{K_u+U} - \gamma\right), \quad \psi_{32} = \gamma_3,\\
\psi_{41} &= \frac{1}{\gamma_4}\left(\frac{C_b(t)}{C} - \mu\right), \quad \psi_{42} = \gamma_4,
\end{aligned}
$$

where γ_i, $i = 1,2,3,4$ are constants that can be determined from the equation (27-30). We choose to solve the differential equations

$$[D-\psi_{12}]U = 0, \quad [D-\psi_{22}]I = 0, \quad [D-\psi_{32}]V = 0 \quad [D-\psi_{42}]C = 0, \tag{32}$$

which gives

$$U(\zeta) = \kappa_1 e^{[\gamma_1\zeta]}, I(\zeta) = \kappa_1 e^{[\gamma_2\zeta]}, V(\zeta) = \kappa_1 e^{[\gamma_3\zeta]}, C(\zeta) = \kappa_1 e^{[\gamma_4\zeta]} \tag{33}$$

$$U(\zeta) = \kappa_1 e^{(\gamma_1\zeta)} = \kappa_1 e^{(\gamma_1(r-ct))}, \tag{34}$$

$$I(\zeta) = \kappa_2 e^{(\gamma_2\zeta)} = \kappa_1 e^{(\gamma_2(r-ct))}, \tag{35}$$

$$V(\zeta) = \kappa_3 e^{(\gamma_3\zeta)} = \kappa_1 e^{(\gamma_3(r-ct))}, \tag{36}$$

$$C(\zeta) = \kappa_4 e^{(\gamma_4\zeta)} = \kappa_1 e^{(\gamma_4(r-ct))}, \tag{37}$$

From equations (27-30) the constants are determined to be

$$\gamma_1 = -\frac{c}{2\phi_1} \pm \frac{1}{2}\sqrt{\left(\frac{c}{\phi_1}\right)^2 + 4\alpha}, \tag{38}$$

$$\gamma_2 = -\frac{c}{2\phi_2} \pm \frac{1}{2}\sqrt{\left(\frac{c}{\phi_2}\right)^2 + 4\delta}, \tag{39}$$

$$\gamma_3 = -\frac{c}{2\phi_1} \pm \frac{1}{2}\sqrt{\left(\frac{c}{\phi_3}\right)^2 + 4\gamma}, \tag{40}$$

$$\gamma_4 = -\frac{c}{2\phi_1} \pm \frac{1}{2}\sqrt{\left(\frac{c}{\phi_4}\right)^2 + 4\mu}. \tag{41}$$

Equations (34-37) are cell traveling wave solutions which we determined from the choice of differential equation which we made. These solutions are all of exponential form and they all suggest that γ_i should be less than zero, that is, $\gamma_i < 0$ for all the cell densities U, I, V, C to decay to zero as ζ, the traveling wave co-ordinate tends to infinity. It is worth noting that the other sets of differential equations in (23-26) arising from different choices are rather difficult to solve due to their non-linearities and the many terms involved. The equations (38-41) highlight the parameters which are critical in chemovirotherapy treatment. These parameters include the cell diffusion constants, tumour growth rate, infected tumour death rate, and the virus and drug decay rates.

3.2 Heterogenous Model simulations

In this section we present results from numerical simulations of the models (7-10) which describes the spatiotemporal dynamics of an avascular tumour under chemovirotherapy treatment. It is not an easy undertaking to find analytical solutions to the

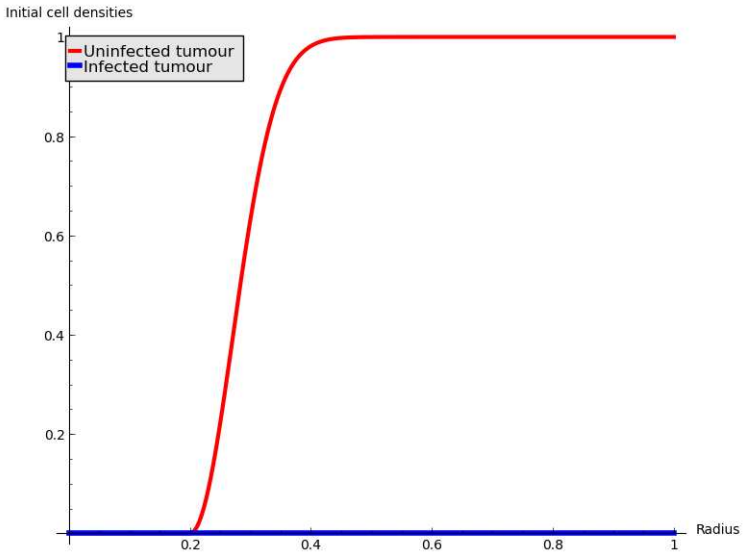

Fig. 2 Fractional tumour cell densities at $t = 0$ with the necrotic core lying in the region $0 \leq r \leq 0.2$.

equations (7-10) because it is highly coupled and involves many terms. In this section we use a multidomain monomial based collocation method (Motsa, 2015) and pdepe (Skeel and Berzins, 1990), a finite element based method in Matlab, to determine numerical solutions to the system (7-10).

The parameter values we used were obtained from fitted experimental data for untreated tumors and virotherapy in mice (Bajzer et al, 2008). We considered the carrying capacity of the tumour to be 10^6 cells per unit volume because a tumour nodule contains about 10^5 to 10^9 tumour cells (Spratt et al, 1996). The tumour growth rate was taken to be 0.26 per day because several experimental tumour growth models estimate it to be in the range 0.1 to 0.3 (Benzekry et al, 2014). The number of viruses produced in a day is considered to be in the range 10 to 1000 (see Ref Brock 1990). The rate of drug infusion into body tissue is taken to be 20 mg/day since most cancers require high dozes of treatment and the drug decay rate is estimated to be 4.17 mg/day, values which concur with cancer pharmokinetic studies (see for example Refs Bosl and Patil 2011; Oliver et al 2011). Since infected tumor cells multiplication is enhanced by the oncolytic virus replication, the tumor cells lysis is considered to be grater that for uninfected tumor cells.

Figure 2 shows the initial tumour distributions. It shows that the tumour density is zero in the necrotic core and increases towards the sheath of the tumour. The infected tumor density is zero throughout the tissue. We firstly simulate the equation (7) which models tumour growth without any form of treatment ($C = V = I = 0$) to investigate the efficacy of each treatment and their combination.

Figure 3 shows the distribution of tumour cells in the tissue without any form of treatment. The tumour density is zero at the center and it increases towards the outside of the tissue. The figure shows that with time the tumour density increases.

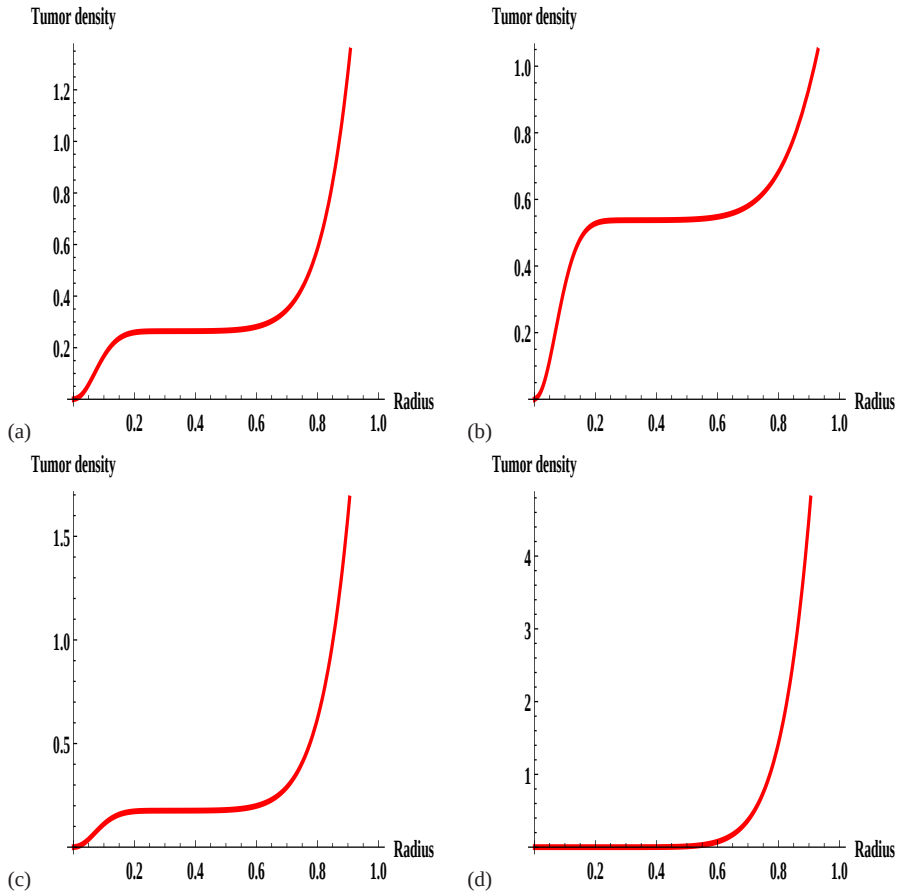

Fig. 3 Spatial distribution of fractional untreated tumour density in the tissue at times corresponding to (a) 200, (b) 400 (c)600, and d) 1000 days respectively.

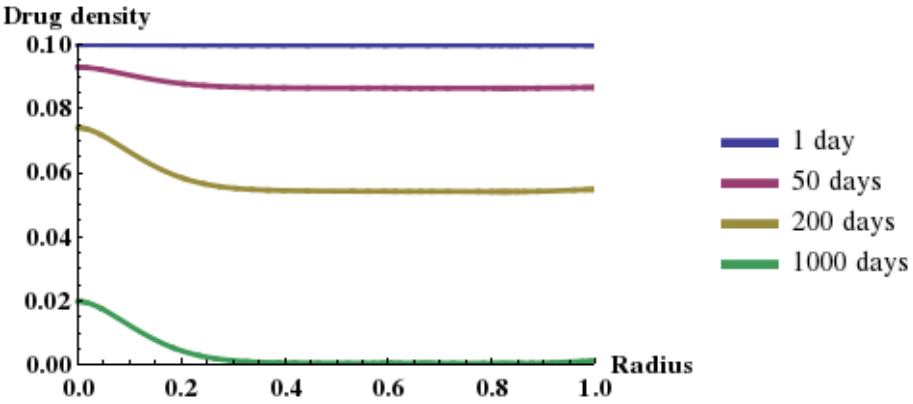

Fig. 4 Fractional drug density distributions for different time periods.

This can be seen from Figure 3 (a)-(d), where even after 1000 days the fractional tumour density rose to 4×10^6 cells per unit volume from 1.2×10^6 cells per unit volume. Figure 4 shows the fractional distribution of the chemotherapeutic drug in body tissue. It shows that the drug density is highest inside the tissue. It also shows that the density is reduced with time. Initially the fractional drug density is maximum outside the tumour and with time it circulates in the tumour and redistributes to have a higher density inside the tissue, that it, maximum concentration is near the core than outside where $r \geq 0.2$.

We have determined numerical solutions of a tumour without any form of treatment and a chemotherapeutic drug in body tissue. We next simulate chemotherapy and virotherapy treatments to determine how the drug and virus treatment affects the tumour density and spatiotemporal distribution. Later we combine both treatments to simulate chmovirotherapy. Figure 5 shows numerical solutions of Equation (7) which simulates the tumour with chemotherapy treatment. The tumour density in the tissue is reduced with time. Comparing the results in Figures 3 to 5, we note that the tumour density was reduced to 0.04×10^6 - 0.065×10^6 cells per unit volume in 2000 days whereas with the case with no treatment, even after 1000 days the fractional tumour density only reduced to 0.193×10^6 - 0.196×10^6 cells per unit volume.

Figure 6 is a numerical representation of tumour treatment with virotherapy several days after administration of the treatment. We note that with time the virus reduces the uninfected tumour density and the infected tumor density first increases and then decreases, going by the areas below the curves. These areas were estimated using Riemann sums. Initially we assume that there are no infected tumour cells in the tissue and that the tumour has grown to its maximum size. After a period of 10 days, Figure 6(a) shows that the uninfected tumour density begins to reduce and the infected tumour density begins to increase from the right boundary, that is, from outside the tissue. After 100 days, and comparing to Figure 6(a) to 6(d), the uninfected tumour density was reduced from 0.792 to 0.098 square units. The infected tumour density solutions are inform of a traveling wave front propagating from the right to the left.

Figure 7 displays the spatiotemporal dynamics of the tumour with both chemotherapy and virotherapy treatments combined. The figure shows that with time the tumour density is reduced from both ends of the tissue, that is, from inside and outside the tissue. We notice that with time the infected tumour density, just like with the virotherapy treatment, first increases and then decreases. Comparing Figures 6 and 7 we discover that the tumour is attacked by both the virus and the drug from outside the tissue. The areas under the uninfected tumour curves for the 10, 25, 50, and 100 days are respectively 0.41, 0.35, 0.12, and 0.09 square units.

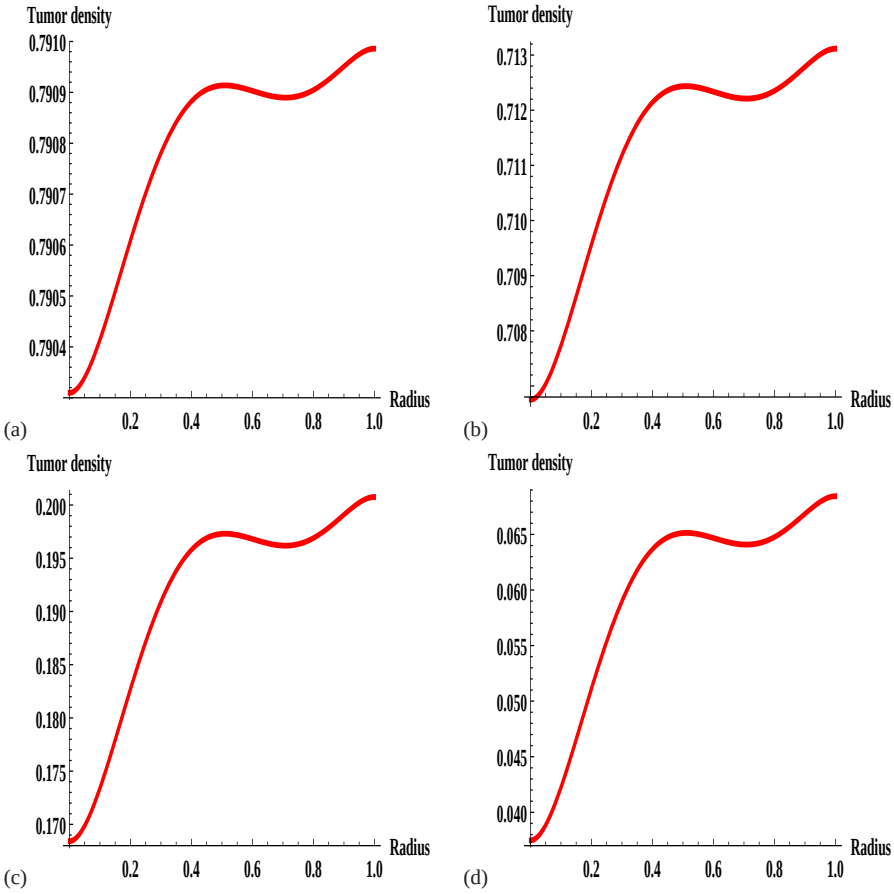

Fig. 5 Spatial distribution of fractional tumour density in the tissue after incorporating chemotherapy at times corresponding to (a) 10, (b) 100 (c)1000, and d) 2000 days respectively.

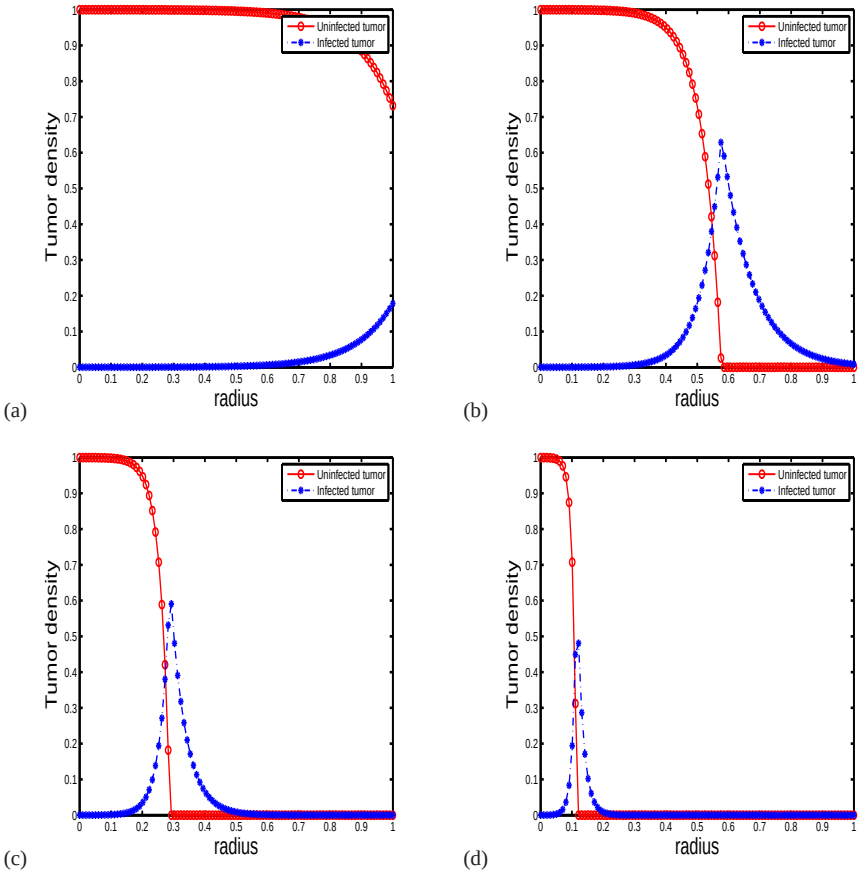

Fig. 6 Spatial distribution of fractional uninfected and infected tumour densities with virotherapy treatment for times corresponding to (a) 10, (b) 25 (c)50, and d) 100 days respectively.

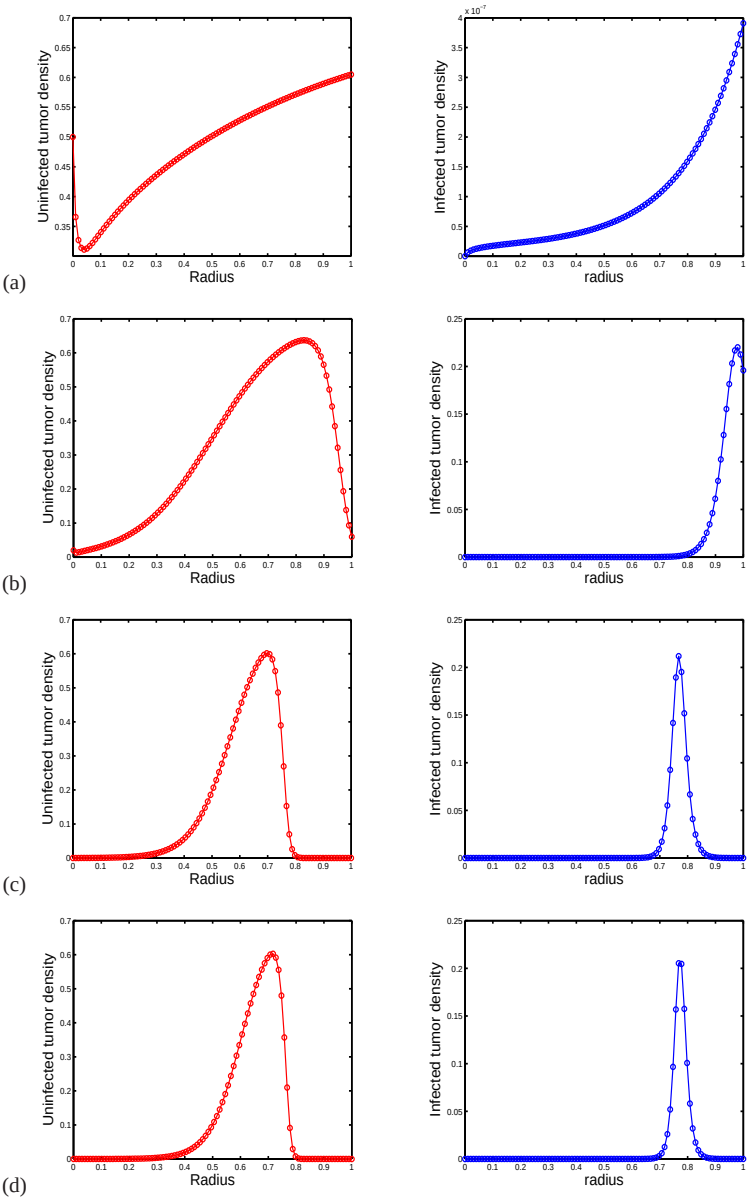

Fig. 7 Spatial distribution of fractional uninfected and infected tumour densities with both treatments for times corresponding to (a) 10, (b) 25 (c) 50, and (d) 100 days respectively.

4 Discussion

The main purpose of this study was to propose a spatiotemporal model to simulate avascular tumour growth under chemovirotherapy treatment with the aim of determining the outcome of combining drugs with oncolytic viruses in order to eliminate tumours from body tissue and also to determine the parameters which are most critical during chemovirotherapy treatment. We constructed a mathematical model of an avascular tumour which has grown to its maximum size and under chemovirotherapy treatment. The resulting mathematical model equations were solved using pdepe and a multi-domain monomial based collocation method. Analytical traveling wave solutions of the heterogeneous model, in one dimension, were also determined. The traveling wave solutions depicted that the most critical parameters during chemovirotherapy treatment are ; cell diffusion constants, tumour growth rate, infected tumour death rate, and the virus and drug decay rates. The numerical simulations revealed that chemotherapy or virotherapy alone may not be capable of depleting tumour cells in body tissue but a combination of the two is capable of eradicating tumour cells and in a relatively short time period. The numerical solutions also showed the virus and the drug lysing the tumour from outside the tissue.

Tumour cell propagation and progression may take several months or years. Nevertheless, one may not live for many years with cancer, and without treatment unless if it is in a dormant situation. The 1000 days for which we simulated a tumour without any form of treatment may not be plaussible but we can infer that even after several years, without any clinical intervention, cancer may result to death and that chemovirotherapy treatment is capable of attenuating it.

Conflict of interests

The authors declare that there is no conflict of interests regarding the publication of this manuscript.

Acknowledgments

We acknowledge the financial support of the university of KwaZulu-Natal.

References

References

Aghi M, Rabkin S, Martuza RL (2006) Effect of chemotherapy-induced dna repair on oncolytic herpes simplex viral replication. Journal of the National Cancer Institute 98(1):38–50

Alonso M, Gomez-Manzano C, Jiang H, Bekele N, Piao Y, Yung W, Alemany R, Fueyo J (2007) Combination of the oncolytic adenovirus icovir-5 with chemotherapy provides enhanced anti-glioma effect in vivo. Journal of Cancer Gene Therapy 14(8):756–761

Bajzer Ž, Carr T, Josić K, Russell SJ, Dingli D (2008) Modeling of cancer virotherapy with recombinant measles viruses. Journal of Theoretical Biology 252(1):109–122

Benzekry S, Lamont C, Beheshti A, Tracz A, Ebos JM, Hlatky L, Hahnfeldt P (2014) Classical mathematical models for description and prediction of experimental tumor growth

Binz E, Lauer U, Binz E, Lauer UM (2015) Chemovirotherapy: combining chemotherapeutic treatment with oncolytic virotherapy. Journal of Drug Design, Development and Therapy 9:1209–1216

Bosl GJ, Patil S (2011) Carboplatin in clinical stage i seminoma: too much and too little at the same time. Journal of Clinical Oncology 29(8):949–952

Bossow S, Grossardt C, Temme A, Leber M, Sawall S, Rieber E, Cattaneo R, von Kalle C, Ungerechts G (2011) Armed and targeted measles virus for chemovirotherapy of pancreatic cancer. Journal of Cancer Gene Therapy 18(8):598–608

Brock TD (1990) The emergence of bacterial genetics. Cold Spring Harbor Laboratory Press Cold Spring Harbor, NY

Cornejo-Pérez O (2008) Traveling wave solutions for some factorized nonlinear pdes. Journal of Physics A: Mathematical and Theoretical 42(3):035,204

Fornari FA, Randolph JK, Yalowich JC, Ritke MK, Gewirtz DA (1994) Interference by doxorubicin with dna unwinding in mcf-7 breast tumor cells. Journal of Molecular Pharmacology 45(4):649–656

García-García HM, Goedhart D, Serruys PW (2007) Relation of plaque size to necrotic core in the three major coronary arteries in patients with acute coronary syndrome as determined by intravascular ultrasonic imaging radiofrequency. The American Journal of Cardiology 99(6):790–792

Kumar S, Gao L, Yeagy B, Reid T (2008) Virus combinations and chemotherapy for the treatment of human cancers. Current Opinion in Molecular Therapeutics 10(4):371–379

Liu TC, Galanis E, Kirn D (2007) Clinical trial results with oncolytic virotherapy: a century of promise, a decade of progress. Journal of Nature Clinical Practice Oncology 4(2):101–117

Ma WX, Fuchssteiner B (1996) Explicit and exact solutions to a kolmogorov-petrovskii-piskunov equation. International Journal of Non-Linear Mechanics 31(3):329–338

Malinzi J, Sibanda P, Mambili-Mamboundou H (2015) Analysis of virotherapy in solid tumor invasion. Journal of Mathematical Biosciences 263:102–110

Motsa S (2015) On a multi-domain bivariate lagrange polynomial based spectral collocation method for solving non-linear evolution partial differential equations. In: South African Symposium on Numerical and Applied Mathematics

Oliver RTD, Mead GM, Rustin GJ, Joffe JK, Aass N, Coleman R, Gabe R, Pollock P, Stenning SP (2011) Randomized trial of carboplatin versus radiotherapy for stage i seminoma: mature results on relapse and contralateral testis cancer rates in mrc te19/eortc 30982 study (isrctn27163214). Journal of Clinical Oncology 29(8):957–962

Ribba B, Marron K, Agur Z, Alarcón T, Maini P (2005) A mathematical model of doxorubicin treatment efficacy for non-hodgkinâĂŹs lymphoma: investigation of the current protocol through theoretical modelling results. Bulletin of Mathematical Biology 67(1):79–99

Rosu H, Cornejo-Pérez O (2005) Supersymmetric pairing of kinks for polynomial nonlinearities. Physical Review E 71(4):046,607

Shafren DR, Au GG, Nguyen T, Newcombe NG, Haley ES, Beagley L, Johansson ES, Hersey P, Barry RD (2004) Systemic therapy of malignant human melanoma tumors by a common cold-producing enterovirus, coxsackievirus a21. Journal of Clinical Cancer Research 10(1):53–60

Siurala M, Bramante S, Vassilev L, Hirvinen M, Parviainen S, Tähtinen S, Guse K, Cerullo V, Kanerva A, Kipar A, et al (2015) Oncolytic adenovirus and doxorubicin-based chemotherapy results in synergistic antitumor activity against soft-tissue sarcoma. International Journal of Cancer 136(4):945–954

Skeel RD, Berzins M (1990) A method for the spatial discretization of parabolic equations in one space variable. SIAM Journal on Scientific and Statistical Computing 11(1):1–32

Spratt JS, Meyer JS, Spratt JA (1996) Rates of growth of human neoplasms: Part ii. Journal of Surgical Oncology 61(1):68–83

Stamper I, Owen M, Maini P, Byrne H (2010) Oscillatory dynamics in a model of vascular tumour growth-implications for chemotherapy. Biology Direct 5(1):27

Toyoizumi T, Mick R, Abbas AE, Kang EH, Kaiser LR, Molnar-Kimber KL (1999) Combined therapy with chemotherapeutic agents and herpes simplex virus type 1 icp34. 5 mutant (hsv-1716) in human non-small cell lung cancer. Journal of Human Gene Therapy 10(18):3013–3029

Tusell Wennier S, Liu J, McFadden G (2012) Bugs and drugs: oncolytic virotherapy in combination with chemotherapy. Journal of Current Pharmaceutical Biotechnology 13(9):1817–1833

Ungerechts G, Springfeld C, Frenzke ME, Lampe J, Johnston PB, Parker WB, Sorscher EJ, Cattaneo R (2007) Lymphoma chemovirotherapy: Cd20-targeted and convertase-armed measles virus can synergize with fludarabine. Journal of Cancer Research 67(22):10,939–10,947

Wagner JG (1973) Properties of the michaelis-menten equation and its integrated form which are useful in pharmacokinetics. Journal of Pharmacokinetics and Biopharmaceutics 1(2):103–121

Zaoui K, Bossow S, Grossardt C, Leber M, Springfeld C, Plinkert P, von Kalle C, Ungerechts G (2012) Chemovirotherapy for head and neck squamous cell carcinoma with egfr-targeted and cd/uprt-armed oncolytic measles virus. Journal of Cancer

Chapter 6

Conclusion

This thesis was primarily concerned with modeling the role of the immune system response to tumour invasion and investigating the outcome of some new forms of cancer treatment. We used mathematical modeling techniques, which are described herein. The mathematical models which we constructed are in the form of ODEs and PDEs which allow for future predictions and investigation of spatial density distributions.

In Chapter 2, we investigated the presence of traveling wave solutions in a tumour-immune interaction model with immuotherapy, and calculated the minimum wave speed. The purpose of this chapter was to measure the strength with which a tumour attacks immune cells and to determine the most important factors, in the form of parameters, which should be targeted to mitigate tumour growth. The presence of traveling wave solutions was investigated using the method employed by Bellomo et al. [76]. We established the presence of a heteroclinic orbit joining two different equilibrium points in the phase space in which the solutions were defined. The model was shown to exhibit traveling wave solutions and this confirmed that a tumour attacks immune cells at full potential. The numerical solitons depicted periodic cell densities with a low tumour level, oscillating about a stable equilibrium state. These solutions depict cancer dormancy which has previously been observed in several cancers, for example ostoegenic sarcomas,

basel-cell carcinomas, and breast cancers. The parameters which we noted as the pivotal ones during tumour invasion are; tumour growth rate, resting immune cell growth rate, carrying capacity of the resting TICLs, resting cell supply, diffusion rate of the tumour cells, and the local kinetic interaction parameters, namely, tumour cell death and inactivation of TICLs.

In Chapter 3, two deterministic models to simulate virotherapy were developed and analyzed. We noted earlier, in Chapter 1, that there is a need to investigate the outcome of the new forms of cancer therapy and also determine which conditions are necessary in order to mitigate tumour growth. The stability analysis of the homogeneous model, together with the numerical solutions, confirmed that virotherapy can reduce the tumour load in body tissue to a very minimum and cancer dormant cell concentration level, by killing all the infected cells. A small number of uninfected tumour cells may remain, depending on the virus characteristics, mostly the virus replication rate. We showed that oncolytic virotherapy as a cancer therapy is most effective if the virus used in the treatment rapidly replicates, that is, if the virus replication rate is very high. The stability analysis of the homogeneous model's steady states revealed the existence of an unstable tumour free state, implying that achieving a cancer free state in body tissue could be practically impossible. Nevertheless, the same analysis showed the existence of a tumour dormant state where the tumour in very small concentrations can co-exist with immune cells. We determined a certain class of solutions to the heterogeneous model using the factorization of differential operators. All the spatial model equations, without chemotaxis, are of Lienard type. These traveling wave solutions showed that in the long run the immune cell density grows exponentially while the tumour cell densities decay exponentially. These solutions are all functions of the wave propagation speed, tumour diffusion rates, and local kinetic interaction terms; parameters which were determined in Chapter 2 as being

central to the process of tumour invasion. The heterogeneous numerical simulations showed an attack on the tumour by the immune cells. The plots of the total tumour load showed that with time the immune cells maintained the tumour density at very low dormant levels while their spatial distribution kept on increasing in the body tissue.

In Chapter 4, we constructed a simple model to simulate chemovirotherapy treatment with the aim of investigating the effect of three different drug infusion methods, and individually comparing the efficacy of chemotherapy and virotherapy. We showed the plausibility of the model by proving existence, positivity and boundedness of the solutions. The model was analysed by determining analytic solutions where possible, and stability analysis of its steady states. The model was also numerically simulated and the solutions matched with the analytical results. The model analysis showed that a tumour can grow to its maximum size in case there is no treatment. Chemotherapy alone is capable of clearing tumour cells in body tissue provided that the combination of the drug induced lysis of the tumour and the drug infusion rate is greater than the combination of drug decay and tumour growth. We noted that constant and periodic drug infusions are more efficacious than the exponential induction method. This biologically suggests that a repeated-dose regimen in which intravenous injections are given at regular intervals, or putting a patient on an intravenous injection so that a drug is continuously infused in body tissue, is more efficient than giving a bolus infusion. We discovered that virotherapy as a treatment form is highly effective provided that a large virus burst size is ensured for the viruses used during treatment. The analysis of the combined drug-virotherapy treatment revealed that chemovirotherapy may be a definite cancer treatment provided that the drug used is infused at a high rate, decays at a very low rate, and has a high rate of lysis of tumour cells. Further, the virus used should have a large burst size probably each with the capacity to produce about one hundred viruses per day.

This specific result tallies with the results obtained in Chapter 2 where we noted that successful virotherapy is dependent on the virus replication rate which, in this case, is a combination of the burst size and infected tumour cell death rate.

Ben-Jacob et al. [77] noted that the three major challenges in cancer modeling studies are concerned with understanding cancer dormancy and relapse, multidrug therapy and immune resistance, and metastatic colonization. This thesis sought to address two of these issues, namely, cancer dormancy and cancer therapy combinations. Nonetheless, it is impractical to incorporate all the natural processes involving the dynamics of a tumour in mathematical modeling. The mathematical models considered in this thesis therefore leave out certain aspects which when considered could give more insights concerning tumour dynamics and cancer therapy. Human body tissue geometry is highly complex and therefore a possible extension of this study would be to consider a higher dimensional tumour spatial domain, such as 3-dimensional (3D) rather than the 1D and 2D considered in this thesis. The interaction of the tumour with its macro environment, rather than just considering its interior domain, would also be a good aspect to consider in extending the models in this thesis. This would also give insights into the dynamics of the cells in the surrounding tissue. Other analytic techniques, for example, lie-symmetries could be employed in determining solutions to the complex sets of ODEs and PDEs in this thesis. Multistage modeling to consider all the tumour growth stages, rather than just the avascular stage, is also a plausible extension of this study to investigate when a certain cancer treatment would be feasible to give to a cancer patient. Lastly, fitting these models to real data would make this study more deductive as it would determine how realistic the models are and ascertain the parameter values that may be required for a complete cancer treatment. This work may be of use to physicians, clinicians, and cancer drug developers.

Appendix 1- Errata on chapter 2 and 3

In chapter 2:

- $fC/(g_1 + T)$ simulates immune cells proliferation. f and g_1 are Michaelis Menten kinetic parameters derived from experimental results. f in this case relates to the maximum immune cell concentration reached and g_1 may relate to the concentration at which the immune cells proliferation is half maximal.
- $fC/(g_3 + T)$ simulates the chemokine production term. Similarly, f and g_3 are Michaelis Menten kinetic parameters derived from experiments. f in this case may relate to the maximum chemokine concentration reached and g_3 relates to the concentration at which the chemokine production is half maximal.
- The term $\omega IL_2.R$ simulates resting cells activation where ω is the rate of stimulation of resting cells.
- There is a typo in equation (5). The boundary conditions on E and R should be
$$\frac{\partial E(0,t)}{\partial x} = ... = \frac{\partial R(0,t)}{\partial t}.$$
- $\eta_1 = g_1/T_0$ and $\eta_2 = g_2/IL_{2_0}$.
- The term $\theta_1/(\eta_1 + T)$ comes from the assumption that the formation of cellular conjugates C occurs on a time scale of several minutes to a few hours, that is, $dC/dt \approx 0$. This reduces the system to the terms in the model (See references [11] and [70]).

In chapter 3:

- The model (4) is not non-dimensionalized but rather a re-scaled one because some terms like η_2, β_2 and θ_2 are still dimenaional. This does not however in any way change any part of the analysis and results.
- The dimesnions of k_1 are day^{-1}cells^{-1}cm.

References

[1] R.N. Anderson. Deaths: leading causes for 2001. *National Vital Statistics Reports*, 52(9):1–88, 2003.

[2] R. Siegel, D. Naishadham, and A. Jemal. Cancer statistics. *CA: Journal for Clinicians*, 63(1):11–30, 2013.

[3] R. Siegel, J. Ma, Z. Zou, and A. Jemal. Cancer statistics. *CA: Journal for Clinicians*, 64(1):9–29, 2014.

[4] World Health Organization. 2014 Cancer Report, Accessed on 01.09.2015. URL http://www.who.int/cancer/en/.

[5] World Health Organization. WHO handbook for reporting results of cancer treatment, Accessed on 14.03.2016. URL http://apps.who.int/iris/handle/10665/37200.

[6] M.R. Stratton, P.J. Campbell, and P.A. Futreal. The cancer genome. *Journal of Nature*, 458(7239):719–724, 2009.

[7] R. Weinberg. *The biology of cancer*. Garland Science, 2013.

[8] M.A.J.Chaplain. Avascular growth, angiogenesis and vascular growth in solid tumours: The mathematical modelling of the stages of tumour development. *Journal of Mathematical and Computer Modelling*, 23(6):47–87, 1996.

[9] J.A. Aguirre-Ghiso. Models, mechanisms and clinical evidence for cancer dormancy. *Journal of Cancer Nature Reviews*, 7(11):834–846, 2007.

[10] S.J. Russell, K.W. Peng, and J.C. Bell. Oncolytic virotherapy. *Journal of Nature Biotechnology*, 30(7):658–670, 2012.

[11] H. Mambili-Mamboundou, P. Sibanda, and J. Malinzi. Effect of immunotherapy on the response of TICLs to solid tumour invasion. *Journal of Mathematical Biosciences*, 249:52–59, 2014.

[12] X. Yan, R.J. Orentas, and B.D. Johnson. Tumor-derived macrophage migration inhibitory factor (MIF) inhibits T lymphocyte activation. *Cytokine*, 33(4): 188–198, 2006.

[13] E. Alici. *Therapeutic potential of natural killer cells in multiple myeloma*. Institutionen för medicin, Huddinge Sjukhus/Department of Medicine at Huddinge University Hospital, 2006.

[14] K. Mitsui, S. Tanaka, H. Yamamoto, Akihito K.E. Tsuyoshi, T. Yano, H. Goto, H. Nakase, S. Tanaka, T.Matsui, et al. Role of double-balloon endoscopy in the diagnosis of small-bowel tumours: the first Japanese multicenter study. *Journal of Gastrointestinal Endoscopy*, 70(3):498–504, 2009.

[15] E. Frei and G.P Canellos. Dose: a critical factor in cancer chemotherapy. *The American Journal of Medicine*, 69(4):585–594, 1980.

[16] A. Yagoda and D. Petrylak. Cytotoxic chemotherapy for advanced hormone-resistant prostate cancer. *Journal of Cancer*, 71(S3):1098–1109, 1993.

[17] A. Yagoda, D. Petrylak, and S. Thompson. Cytotoxic chemotherapy for advanced renal cell carcinoma. *The Urologic Clinics of North America*, 20(2):303–321, 1993.

[18] S.H. Kaufmann and W.C. Earnshaw. Induction of apoptosis by cancer chemotherapy. *Journal of Experimental Cell Research*, 256(1):42–49, 2000.

[19] G.P Corrie. Cytotoxic chemotherapy: clinical aspects. *Journal of Medicine*, 36 (1):24–28, 2008.

[20] A.J.J. Wood and C.G. Moertel. Chemotherapy for colorectal cancer. *New England Journal of Medicine*, 330(16):1136–1142, 1994.

[21] I.S. Cooper. Cryogenic surgery for cancer. In *Federation proceedings*, volume 24, page S237, 1965.

[22] J. Lumley, R. Stitz, A. Stevenson, G. Fielding, and A. Luck. Laparoscopic colorectal surgery for cancer. *Journal of Diseases of the Colon & Rectum*, 45(7): 867–872, 2002.

[23] J.G. Fortner, B.J. Maclean, D.K. Kim, W.S. Howland, A.D. Turnbull, P. Goldiner, G. Carlon, and E.J. Beattie. The seventies evolution in liver surgery for cancer. *Journal of Cancer*, 47(9):2162–2166, 1981.

[24] J. Werner, S.E. Combs, C. Springfeld, W. Hartwig, T. Hackert, and M.W. Büchler. Advanced-stage pancreatic cancer: therapy options. *Journal of Nature Reviews Clinical oncology*, 10(6):323–333, 2013.

[25] C.C. Wang, P.H. Blitzer, and H.D. Suit. Twice-a-day radiation therapy for cancer of the head and neck. *Journal of Cancer*, 55(S9):2100–2104, 1985.

[26] H.D. Thames, S.M. Bentzen, I. Turesson, M. Overgaard, and W. Van den Bogaert. Time-dose factors in radiotherapy: a review of the human data. *Journal of Radiotherapy and Oncology*, 19(3):219–235, 1990.

[27] D.M. Shepard, M.C. Ferris, G.H. Olivera, and T.R. Mackie. Optimizing the delivery of radiation therapy to cancer patients. *Journal of SIAM Review*, 41 (4):721–744, 1999.

[28] I. Mellman, G. Coukos, and G. Dranoff. Cancer immunotherapy comes of age. *Journal of Nature*, 480(7378):480–489, 2011.

[29] J.N. Blattman and P.D. Greenberg. Cancer immunotherapy: a treatment for the masses. *Journal of Science*, 305(5681):200–205, 2004.

[30] S.A. Rosenberg, J.C. Yang, and N.P Restifo. Cancer immunotherapy: moving beyond current vaccines. *Journal of Nature medicine*, 10(9):909–915, 2004.

[31] M.J. Scanlan, A.O. Gure, A.A. Jungbluth, L.J. Old, and Y.T. Chen. Cancer/testis antigens: an expanding family of targets for cancer immunotherapy. *Journal of Immunological Reviews*, 188:22–32, 2002.

[32] Y. Sato. [anti-angiogenic drugs]. *Journal of Cancer & Chemotherapy*, 36(7): 1072–1075, 2009.

[33] A.R. Quesada, Ramón Muñoz-Chápuli, and M.A. Medina. Anti-angiogenic drugs: from bench to clinical trials. *Jornal of Medicinal Research Reviews*, 26(4): 483–530, 2006.

[34] J.E. Markus M.J. Vähä-Koskela, E. Jari Heikkilä, and A.E. Hinkkanen. Oncolytic viruses in cancer therapy. *Cancer Letters*, 254(2):178–216, 2007.

[35] S.J. Russell. RNA viruses as virotherapy agents. *Journal of Cancer Gene Therapy*, 9(12):961–966, 2002.

[36] J. Davis and B. Fang. Oncolytic virotherapy for cancer treatment: challenges and solutions. *Journal of Gene Medicine*, 7(11):1380–1389, 2005.

[37] G. Motalleb. Virotherapy in cancer. *Journal of Cancer Prevention*, 6(2):101, 2013.

[38] A. Does, T. Thiel, and N. Johnson. Rediscovering biology: molecular to global perspectives. *Annenberg Learner*, 2003.

[39] A.B. Holder. *Mathematical models for tumour invasion*. PhD thesis, University of Wollongong, August .

[40] American society of clinical oncology. Understanding immunotherapy, Accessed on 20.08.2015. URL http://www.cancer.net/navigating-cancer-care/how-cancer-treated/immunotherapy-and-vaccines/understanding-immunotherapy.

[41] E. Kelly and S.J. Russell. History of oncolytic viruses: genesis to genetic engineering. *Journal of Molecular Therapy*, 15(4):651–659, 2007.

[42] J.W. Choi, J.S. Lee, S.W. Kim, and C.O. Yun. Evolution of oncolytic adenovirus for cancer treatment. *Journal of Advanced Drug Delivery Reviews*, 64(8): 720–729, 2012.

[43] K.W. Reichard, R.M. Lorence, C.J. Cascino, E.M. Peeples, R.J. Walter, M.B. Fernando, H.M. Reyes, and J.A. Greager. Newcastle disease virus selectively kills human tumor cells. *Journal of Surgical Research*, 52(5):448–453, 1992.

[44] V. Groh, J. Wu, C. Yee, and T. Spies. Tumour-derived soluble MIC ligands impair expression of NKG2D and t-cell activation. *Journal of Nature*, 419 (6908):734–738, 2002.

[45] N.V. Stepanova. Course of the immune reaction during the development of a malignant tumour. *Journal of Biophysics*, 24(1):220–235, 1980.

[46] A. d'Onofrio, U. Ledzewicz, and H. Schättler. On the dynamics of tumour-immune system interactions and combined chemo-and immunotherapy. In *New Challenges for Cancer Systems Biomedicine*, pages 249–266. Springer Milan, 2012.

[47] A. Matzavinos, M.A.J Chaplain, and V.A.Kuznetsov. Mathematical modelling of the spatio-temporal response of cytotoxic t-lymphocytes to a solid tumour. *Journal of Mathematical Medicine and Biology*, 21(1):1–34, 2004.

[48] J.R. Usher. Some mathematical models for cancer chemotherapy. *Journal of Computers & Mathematics with Applications*, 28(9):73–80, 1994.

[49] D. Wodarz and V.A.A Jansen. A dynamical perspective of ctl cross-priming and regulation: implications for cancer immunology. *Immunology letters*, 86 (3):213–227, 2003.

[50] D. Kirschner and J.C. Panetta. Modeling immunotherapy of the tumor–immune interaction. *Journal of Mathematical Biology*, 37(3):235–252, 1998.

[51] A. dâĂŹOnofrio. A general framework for modeling tumor-immune system competition and immunotherapy: Mathematical analysis and biomedical inferences. *Journal of Physica D: Nonlinear Phenomena*, 208(3):220–235, 2005.

[52] H.P. de Vladar and J.A. González. Dynamic response of cancer under the influence of immunological activity and therapy. *Journal of Theoretical Biology*, 227(3):335–348, 2004.

[53] V.A. Kuznetsov, I.A. Makalkin, M.A. Taylor, and A.S. Perelson. Nonlinear dynamics of immunogenic tumours: parameter estimation and global bifurcation analysis. *Bulletin of Mathematical Biology*, 56(2):295–321, 1994.

[54] A. d'Onofrio. tumour-immune system interaction: modeling the tumour-stimulated proliferation of effectors and immunotherapy. *Journal of Mathematical Models and Methods in Applied Sciences*, 16(08):1375–1401, 2006.

[55] S.T.R. Pinho, H.I. Freedman, and F. Nani. A chemotherapy model for the treatment of cancer with metastasis. *Journal of Mathematical and Computer Modelling*, 36(7):773–803, 2002.

[56] L. de Pillis, R.K. Fister, W. Gu, C. Collins, M. Daub, D. Gross, J. Moore, and B. Preskill. Mathematical model creation for cancer chemo-immunotherapy. *Journal of Computational and Mathematical Methods in Medicine*, 10(3):165–184, 2009.

[57] W. Liu and H.I. Freedman. A mathematical model of vascular tumour treatment by chemotherapy. *Journal of Mathematical and Computer Modelling*, 42(9): 1089–1112, 2005.

[58] A.G. López, J.M. Seoane, and A.F. Miguel Sanjuán. A validated mathematical model of tumour growth including tumour–host interaction, cell-mediated immune response and chemotherapy. *Bulletin of mathematical biology*, 76(11): 2884–2906, 2014.

[59] J.P. Tian. The replicability of oncolytic virus: defining conditions in tumour virotherapy. *Journal of Mathematical Biosciences*, 8:841–860, 2011.

[60] D. Wodarz. Viruses as antitumour weapons defining conditions for tumour remission. *Journal of Cancer Research*, 61(8):3501–3507, 2001.

[61] A.S. Novozhilov, F.S. Berezovskaya, E.V. Koonin, and G.P Karev. Mathematical modeling of tumour therapy with oncolytic viruses: regimes with complete tumour elimination within the framework of deterministic models. *Biology Direct*, 1(6):1–18, 2006.

[62] M. Agarwal, A.S. Bhadauria, et al. Mathematical modeling and analysis of tumour therapy with oncolytic virus. *Journal of Applied Mathematics*, 2(01): 131, 2011.

[63] D. Dingli, M.D. Cascino, K. Josić, S.J. Russell, and Z. Bajzer. Mathematical modeling of cancer radiovirotherapy. *Journal of Mathematical Biosciences*, 199 (1):55–78, 2006.

[64] Y. Tao and Q. Guo. A free boundary problem modelling cancer radiovirotherapy. *Journal of Mathematical Models and Methods in Applied Sciences*, 17 (08):1241–1259, 2007.

[65] A. Nguyen, L. Ho, and Y. Wan. Chemotherapy and oncolytic virotherapy: advanced tactics in the war against cancer. *Frontiers in Oncology*, 4(145):1–10, 2014.

[66] J.D. Murray. *Mathematical Biology I: An Introduction, vol. 17 of Interdisciplinary Applied Mathematics*. Springer, New York, NY, USA,, 2002.

[67] A. Boondirek, Y. Lenbury, J. Wong-Ekkabut, W. Triampo, I.M. Tang, and P. Picha. A stochastic model of cancer growth with immune response. *Journal of Physical Society*, 49(4):1652, 2006.

[68] A.S. Qi, X. Zheng, C.Y. Du, and B.S. An. A cellular automaton model of cancerous growth. *Journal of Theoretical Biology*, 161(1):1–12, 1993.

[69] E.A. Reis, L.B.L. Santos, and S.T.R. Pinho. A cellular automata model for avascular solid tumor growth under the effect of therapy. *Journal of Physica A: Statistical Mechanics and its Applications*, 388(7):1303–1314, 2009.

[70] J. Smolle and H. Stettner. Computer simulation of tumour cell invasion by a stochastic growth model. *Journal of Theoretical Biology*, 160(1):63–72, 1993.

[71] J. Malinzi. Modelling the response of cytotoxic t-lymphocytes in controlling solid tumour invasion. Master's thesis, University of KwaZulu-Natal, Pietermaritzburg, 2013.

[72] P. Ashwin, M.V. Bartuccelli, T.J. Bridges, and S.A. Gourley. Travelling fronts for the kpp equation with spatio-temporal delay. *Journal of Physik*, 53(1):103–122, 2002.

[73] E. Konukoglu, O. Clatz, B.H. Menze, B. Stieltjes, M. Weber, E. Mandonnet, H. Delingette, and N. Ayache. Image guided personalization of reaction-diffusion type tumor growth models using modified anisotropic eikonal equations. *Journal of Medical Imaging*, 29(1):77–95, 2010.

[74] B. Perthame. Pde models for chemotactic movements: parabolic, hyperbolic and kinetic. *Journal of Applications of Mathematics*, 49(6):539–564, 2004.

[75] T.C. Liu, E. Galanis, and D Kirn. Clinical trial results with oncolytic virotherapy: a century of promise, a decade of progress. *Nature Clinical Practice Oncology*, 4(2):101–117, 2007.

[76] N. Bellomo and E. de Angelis. *Selected topics in cancer modeling: genesis, evolution, immune competition, and therapy*. Springer Science & Business Media, 2008.

[77] E. Ben-Jacob, D.S. Coffey, and H. Levine. Bacterial survival strategies suggest rethinking cancer cooperativity. *Trends in Microbiology*, 20(9):403–410, 2012.